
Louisiana Transportation Research Center

Final Report 422

**Optimization of Asphalt Mixture Design for the
Louisiana ALF Test Sections**

by

Louay N. Mohammad, Ph.D., P.E.
Khalid Alshamsi
Shadi Saadeh, Ph.D., P.E.

LSU/LTRC



4101 Gourrier Avenue | Baton Rouge, Louisiana 70808
(225) 767-9131 | (225) 767-9108 fax | www.ltrc.lsu.edu

TECHNICAL REPORT STANDARD PAGE

1. Report No. FHWA/LA.07/422		2. Government Accession No.	3. Recipient's Catalog No.
4. Title and Subtitle Optimization of Asphalt Mixture Design for Louisiana ALF Test Sections		5. Report Date May 2018	
		6. Performing Organization Code LTRC Project Number: 03-3B State Project Number: 736991104	
7. Author(s) Louay N. Mohammad, Ph.D., P.E., Khalid Alshamsi, Ph.D., Shadi Saadeh, Ph.D., P.E.		8. Performing Organization Report No. 422	
9. Performing Organization Name and Address Louisiana Transportation Research Center 4101 Gourrier Avenue Baton Rouge, LA 70808		10. Work Unit No. 03-3B	
		11. Contract or Grant No. 763991104	
12. Sponsoring Agency Name and Address Louisiana Department of Transportation and Development P.O. Box 94245 Baton Rouge, LA 70804-9245		13. Type of Report and Period Covered Final Report January 2004-December 2006	
		14. Sponsoring Agency Code	
15. Supplementary Notes			
16. Abstract This research presents an extensive study on the design and characterization of asphalt mixtures used in road pavements. Both mixture volumetrics and physical properties obtained from several laboratory tests were considered in optimizing the mixture design. The research was divided into two phases. Phase 1 included the design and detailed analysis of compaction and performance characteristics of asphalt concrete mixtures, where aggregate structures were designed using an analytical aggregate blending method. In this study, Bailey Method which is a comprehensive gradation based mixture design method was selected. Three types of aggregate (i.e., limestone, sandstone, and granite) were considered and three different aggregate structures for each aggregate type were designed using this Bailey Method. All the aggregates were crushed aggregates. Sandstone and granite mixtures had a nominal maximum aggregate size (NMAS) of 12.5 mm and were designed for high traffic level, while two types of limestone mixtures were designed (25.0-mm and 12.5-mm NMAS) for two traffic levels (high-and low-traffic volumes). For the heavy traffic mixtures, the asphalt binder type selected was PG 76-22M while PG70-22M was used for low-volume mixtures. In Phase 2, further evaluation of the mixtures selected in Phase 1 was conducted with the consideration of specific attributes. The concept of locking point was adopted in modifying the current Superpave mixture design method, in order to improve the durability of the mixtures without compromising the stability. The outcome of this research suggests that suitable mixes with dense aggregate structures can be developed using the Bailey Method of aggregate gradation, providing good resistance to permanent deformation while still maintaining adequate levels of durability. A systematic and simplified design approach in which asphalt mixtures were designed based on the locking point concept, analytical aggregate gradation method, and fundamental mechanistic properties is also recommended.			
17. Key Words Bailey Method, Mix Design, Superpave, Asphalt, Mixtures, Performance, Rutting Susceptibility, Gradation		18. Distribution Statement Unrestricted. This document is available through the National Technical Information Service, Springfield, VA 21161.	
19. Security Classif. (of this report) Unclassified	20. Security Classif. (of this page) Unclassified	21. No. of Pages	22. Price N/A

Project Review Committee

Each research project will have an advisory committee appointed by the LTRC Director. The Project Review Committee is responsible for assisting the LTRC Administrator or Manager in the development of acceptable research problem statements, requests for proposals, review of research proposals, oversight of approved research projects, and implementation of findings.

LTRC appreciates the dedication of the following Project Review Committee Members in guiding this research study to fruition.

LTRC Administrator

Samuel B. Cooper, III., Ph.D., P.E.
Materials Research Administrator

Members

Mr. Philip Arena
Mr. Mike Boudreaux
Mr. Gary Fitts
Ms. Luanna Cambas
Mr. Jay Collins
Mr. Mark Kelly

Directorate Implementation Sponsor

Janice P. Williams, P.E.
DOTD Chief Engineer

Optimization of Asphalt Mixture Design for the Louisiana ALF Test Sections

by

Louay N. Mohammad, Ph.D., P.E.
Professor of Civil and Environmental Engineering
Department of Civil and Environmental Engineering
Director, Engineering Materials Characterization Research Facility
Louisiana Transportation Research Center
Louisiana State University

Khalid Alshamsi
Former Graduate Student
Louisiana State University

Shadi Saadeh, Ph.D., P.E.
Former Materials Research Associate
Engineering Materials Characterization Research Facility
Louisiana Transportation Research Center

LTRC Project No. 03-3B
State Project No. 736991104

conducted for

Louisiana Department of Transportation and Development
Louisiana Transportation Research Center

The contents of this report reflect the views of the authors, who are responsible for the facts and the accuracy of the data presented herein. The contents do not necessarily reflect the official views or policies of the Louisiana Department of Transportation and Development, or the Louisiana Transportation Research Center. This report does not constitute a standard, specification, or regulation.

May 2018

ABSTRACT

This research presents an extensive study on the design and characterization of asphalt mixtures used in road pavements. Both mixture volumetrics and physical properties obtained from several laboratory tests were considered in optimizing the mixture design. The research was divided into two phases. Phase 1 included the design and detailed analysis of compaction and performance characteristics of asphalt concrete mixtures, where aggregate structures were designed using an analytical aggregate blending method. In this study, Bailey Method which is a comprehensive gradation based mixture design method was selected. Three types of aggregate (i.e., limestone, sandstone, and granite) were considered and three different aggregate structures for each aggregate type were designed using this Bailey Method. All the aggregates were crushed aggregates. Sandstone and granite mixtures had a nominal maximum aggregate size (NMAS) of 12.5 mm and were designed for high traffic level, while two types of limestone mixtures were designed (25.0-mm and 12.5-mm NMAS) for two traffic levels (high-and low-traffic volumes). For the heavy traffic mixtures, the asphalt binder type selected was PG 76-22M while PG70-22M was used for low-volume mixtures. In Phase 2, further evaluation of the mixtures selected in Phase 1 was conducted with the consideration of specific attributes. The concept of locking point was adopted in modifying the current Superpave mixture design method, in order to improve the durability of the mixtures without compromising the stability. The outcome of this research suggests that suitable mixes with dense aggregate structures can be developed using the Bailey Method of aggregate gradation, providing good resistance to permanent deformation while still maintaining adequate levels of durability. A systematic and simplified design approach in which asphalt mixtures were designed based on the locking point concept, analytical aggregate gradation method, and fundamental mechanistic properties is also recommended.

ACKNOWLEDGMENTS

This research was supported by the Louisiana Transportation Research Center (LTRC) and the Louisiana Department of Transportation and Development (DOTD) as Project No. 03-3B. The authors would like to express thanks to all the people involved in the Engineering Materials Characterization Research Facility for all their help in conducting this research.

IMPLEMENTATION STATEMENT

The results of the laboratory performance tests conducted during this study support the implementation of the Bailey method during the asphalt mixture design process. Significant information on the relationship between aggregate characteristics such as gradation and type, and asphalt mixture performance was discussed.

TABLE OF CONTENTS

ABSTRACT	iii
ACKNOWLEDGMENTS	v
IMPLEMENTATION STATEMENT	vii
TABLE OF CONTENTS	ix
LIST OF TABLES	xiii
LIST OF FIGURES	xv
INTRODUCTION	1
OBJECTIVE	5
SCOPE	7
METHODOLOGY	11
Aggregates	11
Compactability of Asphalt Mixture	11
Preparation of Test Specimens.....	14
Laboratory Test Procedures	16
Permeability	16
Wheel Tracking Test (LWT)	16
Semi-Circular Fracture Energy Test	16
Indirect Tensile Strength Test (ITS)	18
Dissipated Creep Strain Energy (DCSE)	18
Dynamic Modulus Test.....	19
PHASE 1: MIXTURE DESIGN AND PERFORMANCE EVALUATION.....	21
Aggregate Structure Design.....	21
Mixture Design	26
Permeability	30
Asphalt Mixtures Compactability	31
SGC Locking Point	32
PDA Locking Point.....	33
SGC Compaction Densification Index (CDI).....	34
SGC Traffic Densification Index (TDI).....	34
PDA Compaction Force Index (CFI).....	34
PDA Traffic Force Index (TFI).....	34
Estimating Locking Point	41
Gradation Analysis.....	44
Gradation Parameters and Mixture Design.....	45
Gradation Parameters and Mixture Compactability	51

Mixture Performance	52
Hamburg Loaded Wheel Tracking Test.....	52
Indirect Tensile Strength (ITS) Test	58
Semi-Circular Bend Fracture Energy Test.....	67
PHASE 2: VERIFICATION OF PROPOSED MIXTURE DESIGN APPROACH	71
Mixture Selection for Phase 2	71
Analysis of Results and Discussion	76
Mixtures Physical Properties	76
Performance Tests Results	79
Stiffness Characteristics.....	83
Dissipated Creep Strain Energy	86
Performance of Low Volume Mixtures	89
CONCLUSIONS.....	95
RECOMMENDATIONS	97
ACRONYMS, ABBREVIATIONS, AND SYMBOLS	99
REFERENCES	101
APPENDIX A.....	104
List of Laboratory Tests for Aggregate Stockpiles.....	105
Individual Aggregate Stockpiles Properties.....	106
Binder Laboratory Test Results	109
APPENDIX B	111
The Bailey Method	111
Basic Principles.....	111
Aggregate Packing	111
Coarse and Fine Aggregate.....	112
Combining Aggregates by Volume	114
Loose Unit Weight of Coarse Aggregate.....	114
Rodded Unit Weight of Coarse Aggregate	115
Chosen Unit Weight of Coarse Aggregate.....	116
Rodded Unit Weight of Fine Aggregate	118
Determining a Design Blend.....	118
Analysis of the Design Blend	119
CA Ratio	120
Coarse Portion of Fine Aggregate.....	121
Fine Portion of Fine Aggregate.....	122
Summary of Ratios	122
Example Bailey Method Design Calculations	123

APPENDIX C	131
Sample Calculations.....	131
SGC Locking Point.....	131
SGC Compaction Densification Index (CDI).....	134
SGC Traffic Densification Index (TDI).....	134
PDA Compaction Force Index (CFI).....	135
PDA Traffic Force Index (TFI).....	135
Indirect Tensile Strength.....	136
Semi-Circular Fracture Energy Test.....	137
Dissipated Creep Strain Energy (DCSE).....	137
APPENDIX D.....	142
Recommended Design Approach	143

LIST OF TABLES

Table 1 Summary of test specimens dimensions	16
Table 2 Bailey gradation properties for high-volume mixtures.....	25
Table 3 Bailey gradation properties for low-volume mixtures.....	25
Table 4 Power law gradation parameters for high volume mixtures	26
Table 5 Power law gradation parameters for low-volume mixtures.....	26
Table 6 Job mix formula- 12.5-mm mixes- $N_{des} = 125$ gyrations.....	28
Table 7 Job mix formula- 25.0-mm mixes- $N_{des} = 125$ gyrations.....	30
Table 8 Permeability data	31
Table 9 Example data set for SCG locking point determination	32
Table 10 Example data set for PDA locking point determination	33
Table 11 Linear regression analysis to estimate locking point.....	43
Table 12 Summary of the statistical analysis on LWT data	55
Table 13 Effect = GRA Method = Tukey-Kramer ($P < .05$)	55
Table 14 Effect = TYPE Method = Tukey-Kramer($P < .05$).....	56
Table 15 Statistical analysis of gradation parameters and LWT test data	56
Table 16 Summary of the statistical analysis on IT strength data	61
Table 17 Effect = GRADATION Method = Tukey-Kramer ($P < .05$).....	61
Table 18 Effect = TYPE Method = Tukey-Kramer($P < .05$).....	61
Table 19 Summary of the statistical analysis on IT strain data	62
Table 20 Effect = GRA Method = Tukey-Kramer ($P < .05$)	62
Table 21 Effect = TYPE Method = Tukey-Kramer ($P < .05$).....	62
Table 22 Statistical analyses on the effect of aging on IT strain	63
Table 23 Statistical analysis of gradation parameters and IT strength	65
Table 24 Statistical analysis of gradation parameters and J_c test data.....	70
Table 25 Mixture attributes used in the selection procedure	72
Table 26 Selection procedure for ½-in. mixtures	73
Table 27 Overall ranking of the mixtures	75
Table 28 Calculations of the dissipated creep strain energy.....	88
Table 29 Bailey gradation properties for low volume mixtures	90
Table 30 Mix design properties for low volume mixes	90

LIST OF FIGURES

Figure 1 Phase 1 of the research	8
Figure 2 Phase 2 of the research	9
Figure 3 Pressure distribution analyzer: (a) the PDA device (b) analysis of forces (c) inserting the PDA in the compaction mold (d) typical results.....	13
Figure 4 Sample preparation for the SCB test	15
Figure 5 Specimen preparation for the dynamic modulus test	15
Figure 6 Semi-circular test setup	17
Figure 7 Typical output from the J_c test.....	17
Figure 8 Dissipated creep strain energy determination.....	19
Figure 9 Aggregate structures for ½ in. granite mixtures	21
Figure 10 Aggregate structures for ½ in. limestone mixtures.....	22
Figure 11 Aggregate structures for ½ in. sandstone mixtures	23
Figure 12 Aggregate structures for 1 in. limestone mixtures.....	23
Figure 13 Aggregate structure for ½ in. low volume mixtures.....	24
Figure 14 Aggregate structure for 1 in. low-volume mixtures	24
Figure 15 Rate of change of height during SCG compaction.....	32
Figure 16 Rate of change of frictional resistance during SCG compaction	33
Figure 17 SCG compaction indices definition.....	34
Figure 18 PDA compaction indices definition.....	35
Figure 19 SCG locking point results.....	36
Figure 20 PDA locking point results	36
Figure 21 SCG and PDA locking points correlation	37
Figure 22 SCG densification indices	38
Figure 23 PDA densification indices	38
Figure 24 Correlation between PDA and SCG compaction indices.....	39
Figure 25 Comparison of traffic indices from SCG and PDA.....	40
Figure 26 Frictional resistance of asphalt mixtures	41
Figure 27 Accuracy of the locking point estimation model.....	43
Figure 28 Relationship of the coarse gradation parameters from the Bailey and the power law methods (a) aCA vs. CA ration (b) nCA vs. CA ration.....	44
Figure 29 Fine gradation parameters from the Bailey Method and the power law method (a) aFA vs. F_{AC} ratio (b) aFA vs. F_{AC} ratio	45
Figure 30 Bailey coarse gradation parameter; CA ratio and mixture physical properties: (a) CA ratio vs. VMA (b) CA ratio vs. VFA (c) CA ratio vs. effective film thickness.....	47
Figure 31 Bailey fine gradation parameter; F_{AC} ratio and mixture physical properties: (a) F_{AC}	

ratio vs. VMA; (b) F_{AC} ratio vs. VFA; (c) F_{AC} ratio vs. effective film thickness.....	48
Figure 32 Power-law coarse gradation parameter aCA and mixture physical properties.....	49
Figure 33 Power-law coarse gradation parameter nCA and mixture physical properties	50
Figure 34 Power-law fine gradation parameter aFA and mixture volumetrics	50
Figure 35 Power-law fine gradation parameter nFA and mixture volumetrics	50
Figure 36 Power-law fine gradation parameters and effective film thickness.....	51
Figure 37 Relationship of the Bailey gradation parameters with mixture compactability	51
Figure 38 Relationship of power-law coarse gradation parameters and mixture compactability.....	52
Figure 39 Relationship of power-law fine gradation parameters and mixture compactability.....	52
Figure 40 Rut profile from the LWT test.....	53
Figure 41 Results of the LWT test.....	54
Figure 42 Gradation analysis on LWT test results (a) aCA vs. LWT (b) aFA vs. LWT.....	57
Figure 43 Relationship between the energy indices and LWT results (a) TDI vs. LWT rut depth. (b) TFI vs. LWT rut depth.....	58
Figure 44 Effect of VMA on rutting from LWT test.....	58
Figure 45 Indirect tensile strength results.....	59
Figure 46 Indirect tensile strain results.....	60
Figure 47 Aging index from the ITS test.....	63
Figure 48 Relationship between effective film thickness and IT strain at failure	64
Figure 49 Film thickness and aging index using IT strain at failure	64
Figure 50 Gradation analysis on IT strength test results: (a) aCA vs. ITS (b) aFA vs. ITS ...	65
Figure 51 Traffic densification index (TDI) and IT strength.....	66
Figure 52 Traffic force index (TFI) and IT strength.....	66
Figure 53 Fracture energy from the semi-circular fracture test.....	67
Figure 54 Effect of aging on J_c (a) aging index data and (b) Comparison of aged and unaged J_c	68
Figure 55 Effect of film thickness on J_c aging index.....	68
Figure 56 Effect of the gradation parameter CA ration on J_c	69
Figure 57 Effect of the gradation parameter nCA on J_c	69
Figure 58 Design asphalt content.....	76
Figure 59 Voids in the mineral aggregate data	77
Figure 60 Voids filled with asphalt data.....	77
Figure 61 Dust/ P_{beff} results	78
Figure 62 Effective film thickness.....	78
Figure 63 Loaded wheel tracking results	79

Figure 64 IT strength comparison.....	80
Figure 65 IT strain comparison.....	81
Figure 66 Unaged toughness index.....	82
Figure 67 Aged toughness index.....	82
Figure 68 Fracture energy J_c results.....	83
Figure 69 E^* data at 10HZ, 54.4°C.....	84
Figure 70 E^* data at 0.5HZ, 54.4°C.....	85
Figure 71 E^* data at 10HZ, 21.1°C.....	85
Figure 72 Calculations of the dissipated creep strain energy	87
Figure 73 Dissipated creep strain energy of the designed mixtures	88
Figure 74 Relationship between DCSE and the fatigue parameter from the dynamic modulus test.....	89
Figure 75 Comparison of rutting parameter of both high and low volume limestone mixtures.....	91
Figure 76 Comparison of fatigue parameter of both high and low volume limestone mixtures.....	92
Figure 77 DCSE results for low volume mixtures.....	92
Figure 78 Performance of 1 in. limestone low volume mixtures in LWT test	93
Figure 79 Performance of ½ in. limestone low volume mixture in LWT test.....	93
Figure 80 Performance comparison of low volume mixes in LWT test.....	94

INTRODUCTION

Asphalt concrete mixtures have been used on pavements for more than a century. Asphalt mixture combines bituminous binder and aggregate to give pavements a structure that is flexible over a wide range of climatic conditions. Since the discovery of the petroleum asphalt refining process and the growth of the interstate system, asphalt mixtures have seen increasing their use in pavement applications in the United States (e.g., asphalt binder usage increased from less than 3 million tons in 1920 to more than 30 million tons in 2000 [1]). Currently, more than 93% of all the road surfaces in the U.S. are paved with asphalt mixtures [2].

The design of asphalt mixtures evolved with increase in their use. In the early 1900s, engineers designed asphalt mixtures based totally on their personal experiences. Historically speaking, there were three major asphalt mixture design methods developed in the United States in the first half of the 20th century: the Hubbard-Field method, the Hveem mix design method, and the Marshall mix design method [1]. The Hubbard-Field method was originally developed in the 1920s for sheet asphalt mixtures with 100% passing the 4.75-mm sieve, and later modified to cover the design of coarser asphalt mixtures. The Hubbard-Field Stability test is a laboratory test that measures the strength of the asphalt mixture with a punching-type shear load. The Hveem mix design method was developed by the California Department of Highways Materials and Design Engineer in the 1930s [3]. The Hveem stabilometer measures an asphalt mixture's ability to resist lateral movement under a vertical load. The Hveem mix design is still used in California and other western states. The Marshall mix design was originally developed by a Mississippi State Highway Department Engineer and later refined in the 1940s by the Corps of Engineers for designing asphalt mixtures for airfield pavements. The primary features of the Marshall mix design are a density/voids analysis and a stability test. The optimum asphalt content is determined by the ability of a mix to satisfy stability, flow, and volumetric properties. According to survey in 1984, approximately 75% of the State Highway Departments used some variation of the Marshall method while the remaining 25% used some variation of Hveem method [4].

The Marshall and Hveem mix design methods have played important roles in the traditional asphalt mix design; however, both of them are based on empirical relationships and do not produce fundamental engineering properties of the compacted asphalt mixture that are related to pavement design and performance [5]. Marshall mix design has been used in Louisiana and much of the eastern states where fine mixtures are preferred due to their tendency to be relatively impermeable. Hveem method has been typically used in the western states where

coarse gradations are more typical and permeability is of less concern. It should be noted that the availability of sands may have made a difference in each of these states choices of mix design methods, as well. Superpave built around Texas gyratory mimicked the Hveem in the fact that coarse mixes were more likely to meet the gradations suggest by its design.

It is also difficult to establish uniform specifications for different areas. Despite the best efforts using these existing mix design methods, it is common to see severe rutting and cracking in asphalt pavements due to abruptly increased traffic loads in terms of increased vehicle-miles and higher tire pressure and broad environmental conditions (from very cold to hot regions). Recognizing the declining performance and durability in pavements (including both asphalt and Portland concrete), the Strategic Highway Research Program (SHRP) was approved by Congress in 1987 as a five year research program to improve the performance and durability of United States roads and to make those roads safer for both motorists and highway workers [1].

Hot mix asphalt (HMA) is the most common material used for paving applications in the United States. It primarily consists of asphalt binder and mineral aggregates. The binder acts as a gluing agent that binds aggregate particles into a cohesive mass. When bound by an asphalt binder, mineral aggregate acts as a stone framework that provides strength and toughness to the system. The behavior of HMA depends on the properties of the individual components and how they react with each other in the system.

Several mixture design methods have been developed, the purpose of which is developing a mixture that is capable of providing acceptable performance based on certain predefined set of criteria. This is normally achieved by selecting an optimum design asphalt content that will achieve a balance among all the desired properties. The desired properties may include, durability, impermeability, strength, stability, stiffness, flexibility, fatigue resistance, and workability. It should be emphasized however, that there is no single asphalt content that will maximize all of these properties. Instead, the design asphalt content is selected on the basis of optimizing the properties necessary for a specific condition [6].

Usually, the mixture design consists of two main parts: the volumetric design portion and either empirical or fundamental mechanical testing to verify the design. In addition, the design method may include other requirements that the mixture must meet in order to satisfy the overall specification standard. Such requirements may include certain aggregate qualities like minimum percent of crushed aggregate, maximum amount of rounded sand materials and specific aggregate gradation requirements [6].

The most recently developed mixture design method is the Superpave method, the final product of the \$50 million Strategic Highway Research Program (SHRP). It represents an improved system for specifying asphalt binders and aggregates, developing asphalt mixture design, and analyzing the designed mixtures for their expected performance. Several new requirements were proposed as means to improve mixtures performance by taking into account the critical factors affecting the behavior of individual mixture components as well as the compacted mixtures. The Superpave mixture design includes several processes and decision points. In summary, the design compaction levels are established and materials are selected and characterized. Then, mixture specimens are prepared and laboratory test results are compared to criteria.

The Superpave system is a great leap towards a better approach for designing asphalt mixture. It was hoped that such a sophisticated system may resolve some inherent problems in the previous asphalt mixture design systems. The system, however, still suffers from certain shortcomings that need to be addressed and improved.

One of the main shortcomings of the Superpave mixture design method is the fact that the whole process is purely volumetric and solely relies on certain volumetric requirements that are supposed to ensure acceptable performance. The criteria were derived based either on experience of panels of experts or on some research studies that were conducted on certain Superpave mixtures under limited conditions. Mixtures are accepted or rejected based on those criteria at an early stage in the design process without any validation of their expected performance. An example of such criteria is the percentage of voids in the mineral aggregate (VMA). VMA is the total void space between the aggregate particles in compacted asphalt concrete, including air voids and asphalt not absorbed by the aggregates. It was reported by several researchers and highway agencies that there exist difficulties in meeting the minimum voids in VMA requirements [7-12]. Studies have also shown that the current defined VMA criterion was seen to be insufficient by itself to correctly differentiate well performing mixtures from poor ones. In other words, the design process in the Superpave system does not properly address the expected performance of the designed mixtures in terms of major pavement distresses like permanent deformation and fatigue cracking through laboratory performance testing.

Although aggregate constitutes approximately 95% by weight of asphalt mixtures, the aggregate specifications in the Superpave system were developed based on experience from a number of experts in the field who formulated what is called the Aggregate Expert Task

Group (ETG). The ETG did no research on aggregates. They did build on the studies and recommendations of researchers who came before them and the expertise of many practitioners. From this previous research they developed rules and recommendations for the Superpave System.

As a result of the lack of research conducted in developing such aggregate specifications, there are still open windows for improvement on those specifications and requirements especially designing the aggregate structure to improve mixture stability. For example, in the current Superpave system, guidance is lacking in the selection of the design aggregate structure and understanding the interaction of the aggregate structure with mixture design and performance. Furthermore, the trial and error nature of the actual conventional process of formulating the gradation curve, and the use of weight instead of volume when blending aggregates, offer alternatives to evaluate more rational approaches to design an aggregate structure based on sound principles of aggregate packing concepts.

A key to a successful mixture design is the balance between the volumetric composition and the properties of the raw materials used (binder and aggregates). The interaction between these components and properties. From the above discussion, there is clearly a need to address the issues of concern in the current Superpave mix design system by introducing more rational, systematic steps to the current system for better design and evaluation of asphalt mixtures

OBJECTIVE

The primary objective of this study was to develop an optimum asphalt mixture design (i.e., a mixture with an optimum aggregate structure (gradation) and asphalt content), as determined by an analytical aggregate gradation design method and mixture mechanistic performance tests. The selected mixture design will be recommended for field performance verifications at the Louisiana Accelerated Loading Facility.

A secondary objective of this research was to understand the effect of identifiable variables on mixture mechanical responses. Nominal maximum particle size, gradation and type of aggregate, temperature, compaction level, film thickness, and quality and amount of fines in the mixture were considered in conducting mechanical tests. The limitations of Superpave mixture design criterion were critically examined in order to include wider range of mixes that have potentials of providing superior laboratory performances.

SCOPE

To achieve the objectives mentioned above, the proposed test factorial was developed by considering the following controlled parameters:

- Aggregate Type: Three aggregate types were used in this study, that are commonly used by (DOTD):
 - Hard aggregates (Crushed granite),
 - High friction aggregate (Sandstone), and
 - Low friction, low water absorption aggregate (Limestone aggregate).
- Aggregate Structure: Two mix types were designed; 12.5 mm (1/2 in.) Nominal Maximum Aggregate Size (NMAS) and 25 mm (1 in.) NMAS. The 12.5-mm mix was designed for all the three aggregate types mentioned above. The 25-mm mix was designed using only limestone aggregates. Within the same NMAS, three aggregate structures (coarse, medium, and fine) were designed using the Bailey Method of aggregate gradation evaluation. The coarse aggregate structure has the highest volume of coarse particles. This volume decreases as the structure becomes finer.
- Binder Type: Two asphalt cement types were used. PG 76-22M was used with the high volume mixture type while PG70-22M was used with mixtures designed for low volume traffic.
- Compaction Level: Two compaction levels were used to fabricate test specimens using the Superpave Gyrotory Compactor (SGC). These levels were 125 and 75 Gyration. These two compaction levels correspond to high and low traffic levels respectively in the Superpave system.

The study was divided into two phases. As illustrated in Figure 1, the first phase (i.e., Phase 1) involved designing the aggregate structures and performing Superpave mixture design to determine the design asphalt content providing four percent air void that is an acceptable design parameter for dense graded mixtures in the Superpave system. Following that, the first suite of mixture evaluation tests was conducted in order to determine the best performing aggregate structure for each aggregate type and size combination. This evaluation included the following:

- Determining compaction properties and frictional resistance of the mixtures.
- Measuring the permeability of each mixture as an important physical parameter for a successful performance of asphalt mixture.
- Performing simulative test (Hamburg Loaded Wheel Tracking Test) on the mixtures to determine their stability under harsh environment of moisture and high temperature.
- Conducting fundamental mechanistic tests to evaluate the performance of the designed mixtures. These tests include Indirect Tensile Strength Test (ITS) and

Fracture Energy Test. Those tests were conducted at 25°C on both aged and unaged specimens as part of the durability evaluation of the mixtures.

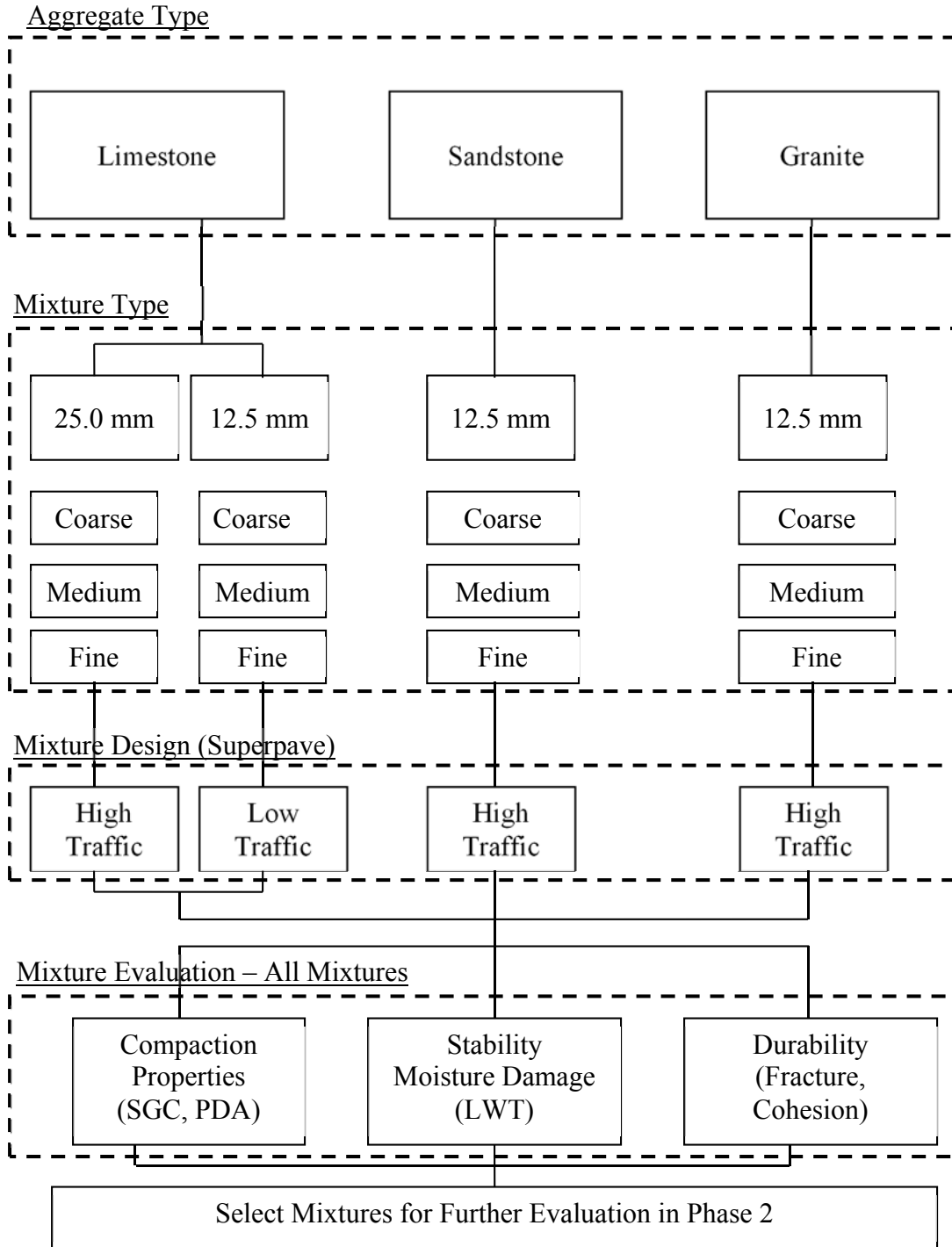


Figure 1
Phase 1 of the research

Phase 2 involved utilizing the data from Phase 1 in selecting mixtures with specific attributes for further evaluation. The locking point concept was introduced in this phase and used in modifying the current Superpave mixture design methodology in order to improve the durability of the mixtures without compromising the stability. It also included conducting other fundamental engineering tests in order to include performance related parameter(s) that can be added to the current volumetric mixture design process. Figure 2 illustrates the main tasks of Phase 2 for this research.

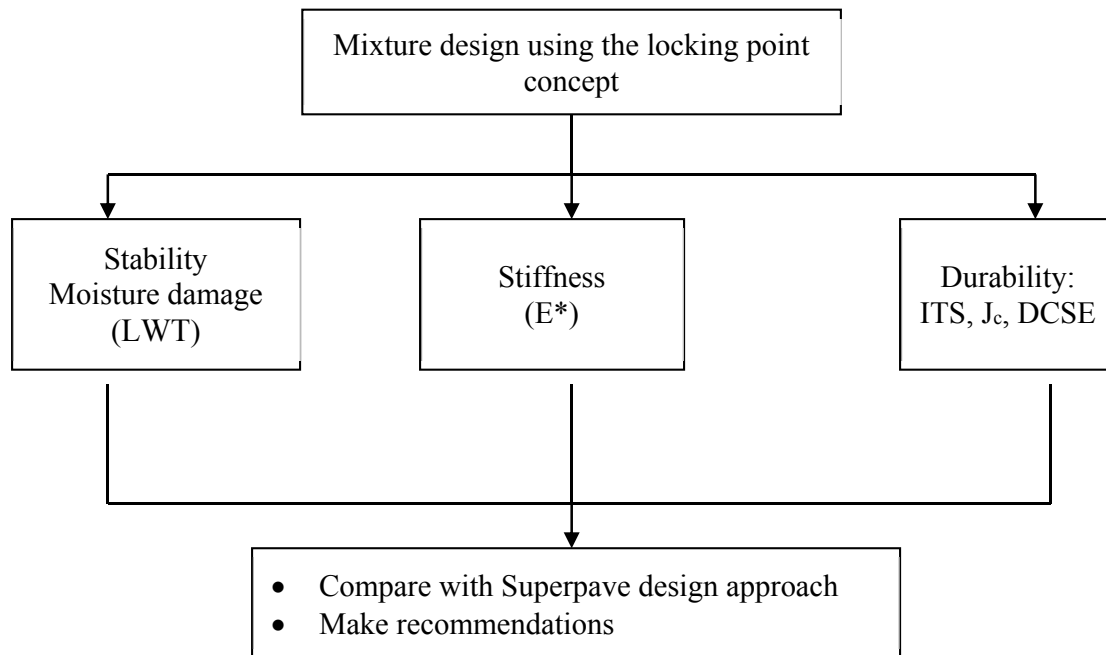


Figure 2
Phase 2 of the research

The following terms were used in the flow charts in Figures 1 and 2:

- SGC: Superpave Gyrotory Compactor,
- PDA: Pressure Distribution Analyzer,
- LWT: Hamburg Loaded Wheel Tracking,
- E*: Dynamic Modulus,
- ITS: Indirect Tensile Strength,
- J_c: Critical J-integral, and
- DCSE: Dynamic Creep Strain Energy.

METHODOLOGY

Asphalt mixture is a composite material that is largely made of two main components: aggregate and asphalt cement. This section provides detailed information on the materials used and their properties. It also highlights the laboratory procedures for the tests performed.

Aggregates

Sources of aggregate were selected to encompass a wide range of aggregates typically used in Louisiana. Three types of aggregates were used:

- Crushed granite for hard aggregates,
- Sandstone for high friction aggregate, and
- Limestone for low friction, low water absorption aggregate.

Different stockpiles from each type of aggregates were acquired. Natural coarse sand was used whenever necessary in the final design blends. Aggregates were acquired in 50-gallon barrels and kept properly sealed from any moisture intrusion. Detailed laboratory evaluation procedures of individual stockpiles were conducted to determine the basic aggregate properties such as specific gravity, gradation, and other Superpave consensus properties. The laboratory tests conducted on each aggregate stockpile and the results from all of these tests are presented in Appendix A.

Asphalt Binders

Two binder types were used in this study: SB polymer-modified asphalt binders meeting Louisiana PG specifications of PG76-22M for high-volume traffic mixtures (greater than 30 million equivalent single axle load; ESALs) and PG70-22M for low volume category (less than 0.3 million equivalent single axle load; ESALs). The laboratory test results on the selected binders are summarized in Appendix A.

Compactability of Asphalt Mixture

The densification curve obtained from the SGC was used to evaluate mixture resistance to the compaction energy applied by the SGC. The behavior of the mixtures during compaction was also captured using the Pressure Distribution Analyzer (PDA). This is a simple accessory that measures the force applied to the mixtures using three load cells equally spaced at an angle of 120°. The load-cells allow measuring the variation of forces during gyration such that the position or eccentricity of the resultant force from the gyratory compactor can be determined in real time. The two dimensional distributions of the eccentricity of the resultant force can be used to calculate the effective moment required to overcome the internal shear

frictional resistance of mixtures when tilting the mold to conform to the 1.25° angle. Based on the data from the load-cells, the two components of the eccentricity of the total load relative to the center of the plate (e_x and e_y) can be calculated. The calculations are simply done with general moment equilibrium equations along two perpendicular axes passing through the center of one of the load-cells as shown in Figure 3 using the following equation:

$$\sum M_x = 0 \Rightarrow e_y; \quad \sum M_y = 0 \Rightarrow e_x; \quad e = \sqrt{e_x^2 + (r_y - e_y)^2} \quad (1)$$

where,

e_x and e_y are x- and y-components of the eccentricity, e , and r_y is location of the plate center point with respect to the x-axis.

The frictional shear resistance of the asphalt mixture can be calculated using the following relationship:

$$FR = Re/AH \quad (2)$$

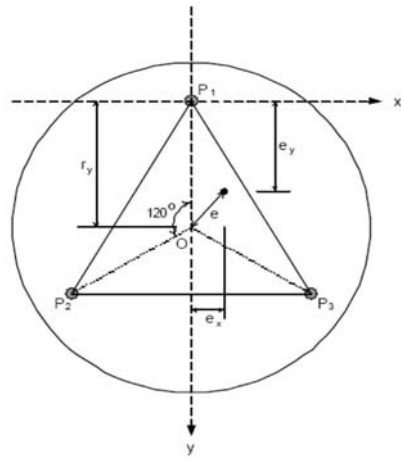
where,

FR = the frictional resistance,
 R = resultant force,
 e = eccentricity,
 A = cross-section area, and
 H = sample height at any gyration cycle.

Two specimens per mixture were tested for compactability in both SGC and PDA devices.



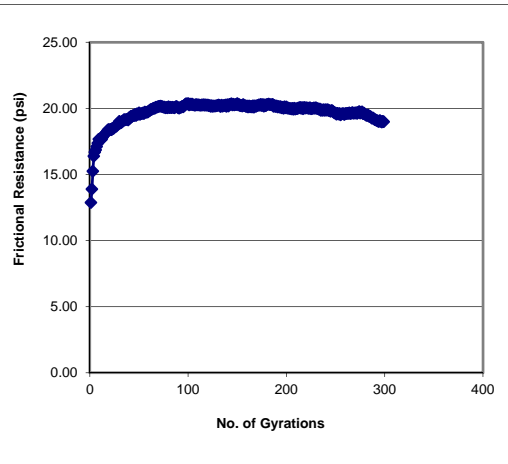
(a)



(b)



(a)



(b)

Figure 3

Pressure distribution analyzer: (a) the PDA device (b) analysis of forces (c) inserting the PDA in the compaction mold (d) typical results

Preparation of Test Specimens

The mixtures were compacted to $7\% \pm 0.5\%$ air voids for testing. Two specimen categories were produced: rectangular slabs and cylindrical specimens. Asphalt concrete slabs with 260.8 mm wide and 320.3 mm long and either 40 mm thick for 12.5-mm ($\frac{1}{2}$ -in.) NMAS mixes or 80 mm thick for 25.0-mm (1-in.) NMAS mixes were fabricated for the Hamburg Loaded Wheel Tracking Test (LWT) using a linear kneading compactor.

For other tests such as ITS test, SCB fracture test, Dynamic Modulus test, and resilient modulus test, the cylindrical specimens were prepared. For the ITS test, the diameter and height of SGC samples were 101.6 mm and 63.5 mm, respectively, while the samples with 150 mm in diameter were fabricated for the SCB fracture test, Dynamic Modulus test, and resilient modulus tests.

For the SCB fracture test, SGC specimens were then sliced perpendicular to the central axis to obtain the semi-circular test specimens. Two test specimens were then cut from each SGC sample. Air void measurements were made again on the cut specimens to ensure that the level of air voids was still within the targeted range. A vertical notch was introduced along the symmetrical axis of the test specimen using a special saw blade of 3.0 mm thickness. Three notch depths were used; 25.4 mm, 31.8 mm, and 38.0 mm. Two specimens per notch depth were fabricated. Figure 4 presents a graphical description of the process of preparing the SCB fracture test specimens.

The test specimens for the Dynamic Modulus test were fabricate to have 100 mm in diameter by coring SGC samples of 150 mm diameter and 156 mm height using a diamond-tipped coring barrel. The specimens were then ground on both ends to obtain the desired thickness of 150 mm. Air void measurements were made on the finished specimens to ensure that the level of air voids was still within the targeted range of $7.0 \pm 0.5\%$. Figure 5 shows the process of preparing test specimens for dynamic modulus testing.

For the resilient modulus test, test specimens with 150 mm diameter were prepared. A similar approach to the dynamic modulus test specimen preparation was followed except that the SGC specimens were compacted to 56 mm height and then ground to the desired thickness of 50 mm. Table 1 summarizes the dimensions of the specimens for the various types of test conducted.

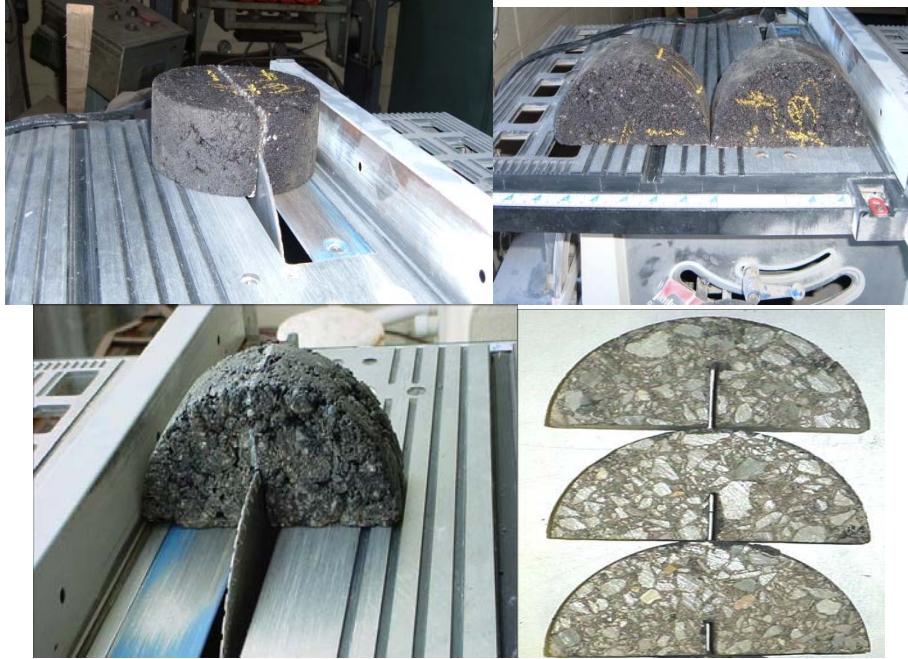


Figure 4
Sample preparation for the SCB test



Figure 5
Specimen preparation for the dynamic modulus test

Table 1
Summary of test specimens dimensions

Test	ITS ¹ (25°C)	J _c ² (25°C)	LWT ³ (50°C)	IT Mr ⁴ (10°C)	ITS (10°C)	E* ⁵
Sample type	SGC	SGC	SGC	SGC	SGC	SGC
Sample diameter (mm)	101.6	150	320.3 x 260.8 ⁶	150	150	100
Sample height (mm)	63.5	57	40.0, 80.0 ⁷	50	50	150

¹ ITS = Indirect Tensile Strength

² J_c = SCB Fracture Test

³ LWT = Loaded Wheel Test

⁴ IT Mr = Indirect Tensile Resilient Modulus Test

⁵ E* = Dynamic Modulus Test

⁶ Slab Length = 320.3 mm and slab width = 260.8 mm

⁷ Slab thickness is 40.0 mm for 12.5 mm mixes and 80.0 mm for 25.0 mm mixes

Laboratory Test Procedures

A comprehensive laboratory evaluation was conducted on the designed mixtures. A suite of mechanistic and simulative tests were performed to study the behavior of asphalt mixtures under various loading and environmental conditions. This section provides a description of the test methods and procedures used for evaluating asphalt mixtures.

Permeability

A falling head permeability test was performed, according to ASTM PS 129-01, *Standard Provisional Test Method for Measurement of Permeability of Bituminous Paving Mixtures using a Flexible Wall Permeameter*, to determine the rate of flow of water through a saturated compacted specimen. Water from a graduated standpipe was allowed to flow through a saturated compacted asphalt mixture specimen. Time interval to reach a known change in head was recorded and used to compute the coefficient of permeability.

Wheel Tracking Test (LWT)

A Hamburg type of Loaded Wheel Tracking (LWT) tester manufactured by PMW, Inc. of Salina, Kansas was used in this study. This test is considered a torture test that produces damage by rolling a 703 N (158-lb) steel wheel across the surface of a slab that is submerged in 50°C water for 20,000 passes at 56 passes a minute. A maximum allowable rut depth of 6 mm at 20,000 passes is used in DOTD specifications.

Semi-Circular Fracture Energy Test

In this study, the fracture resistance of the designed mixtures was characterized using SCB fracture test with notched semi-circular specimens [13, 14]. This approach is gaining popularity for characterizing heterogeneous materials such as asphalt mixtures. The method accounts for the flaws as represented by a notch, which in turn, reveals the material's

resistance to crack propagation or what is called fracture resistance. During the test, the specimen was loaded monotonically to failure at a constant cross-head deformation rate of 0.5 mm/min in a three-point bend load configuration, as shown in Figure 6. The load and deformation were continuously recorded determined and as follows:

$$J_c = - \left(\frac{1}{b} \right) \frac{dU}{da} \quad (3)$$

where, b is the specimen thickness, a is the notch depth, and U is the total strain energy to failure, i.e. the area up to fracture under the load-deflection plot (see Figure 7).

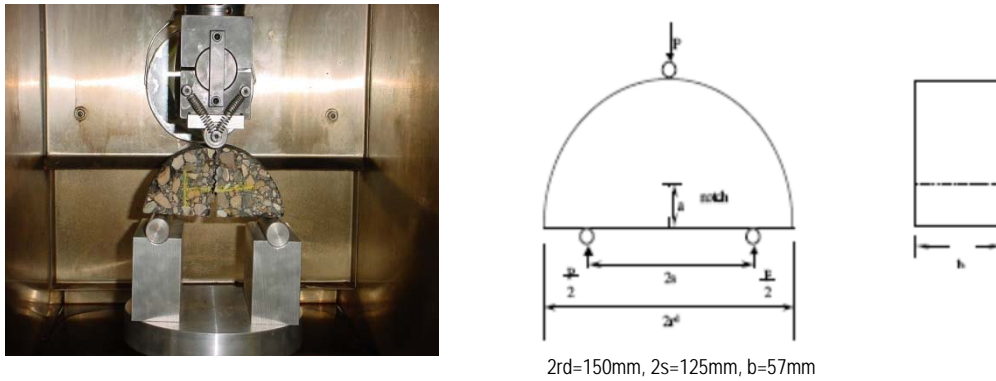


Figure 6
Semi-circular test setup

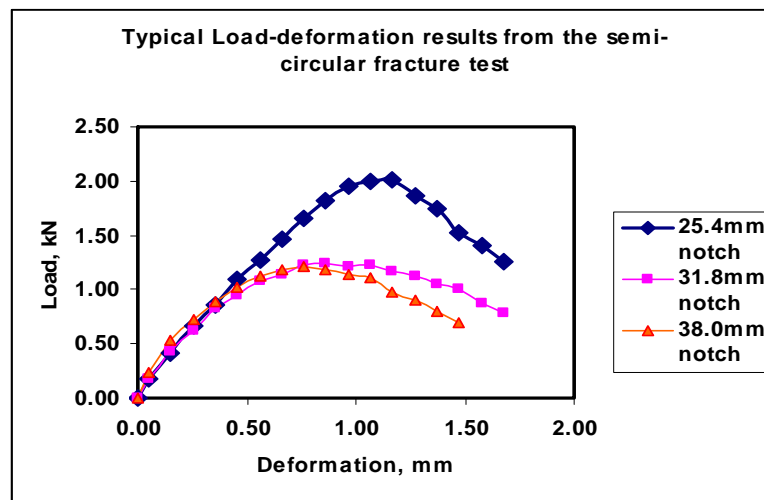


Figure 7
Typical output from the J_c test

To determine the critical value of J- integral, semi-circular specimens with at least two different notch depths (parameter “ a ” in Figure 6) need to be tested for one mixture. In this study, three notch depths of 25.4 mm, 31.8 mm, and 38 mm were selected based on an a/r_a

ratio (the notch depth to the radius of the specimen) of between 0.34 and 0.51 [6]. For each notch depth three duplicates were tested at a temperature of 25° C. This test was conducted on two groups of specimens: unaged and oven aged.

Indirect Tensile Strength Test (ITS)

According to the ASTM D6931, the Indirect Tensile Strength Test was conducted at 25°C. A cylindrical specimen was loaded until its failure at a deformation rate of 50 mm/min (2 in/min) using a MTS machine. The indirect tensile strength (ITS) was used in the analysis. In this study, one SGC sample and one field core from each test section were tested.

Dissipated Creep Strain Energy (DCSE)

The dissipated creep strain energy (DCSE) is determined using two types of laboratory tests: indirect resilient modulus test and the indirect tensile strength test. Both tests were conducted at 10°C on 150-mm diameter and 50-mm thick specimens. DCSE is defined as the fracture energy (FE), minus the elastic energy (EE) (see Figure 8). The fracture energy is defined as the area under the stress-strain curve up to the point where the specimen begins to fracture. The elastic energy is the energy recovered after unloading the specimen. The failure strain (ϵ_f), tensile strength (S_t) and fracture energy were determined from the indirect tensile strength test. From the resilient modulus test, the resilient modulus (M_R) was obtained. The calculation of the DCSE was then determined as follows:

$$\epsilon_0 = (M_R * \epsilon_f - S_t) / M_R \quad (4)$$

$$EE = \frac{1}{2} S_t (\epsilon_f - \epsilon_0) \quad (5)$$

$$DCSE = FE - EE \quad (6)$$

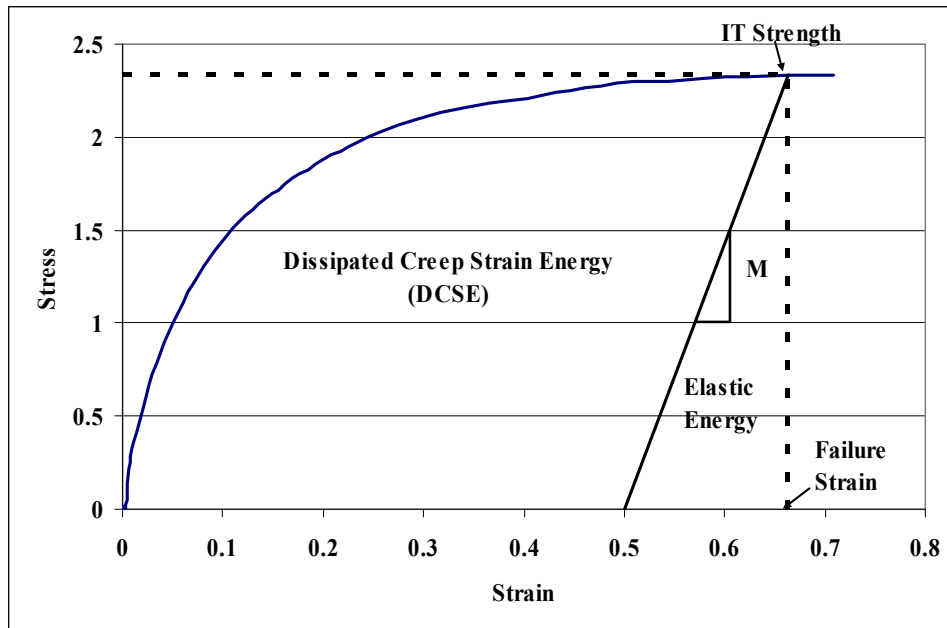


Figure 8
Dissipated creep strain energy determination

Because of the relatively low test temperature and the dynamic nature of the M_R test, the researchers used sample instrumentation in order to accurately capture the small deformations resulting from the repeated load applied. Brass gage points were attached to the test specimens with a strong adhesive [Devcon plastic steel 5-minute epoxy putty_(SF) 10240] using a special template. Four gage points were installed on each face of the specimen along the vertical and horizontal axis. Two units of single integral, bi-axial extensometers (Model 3910 from Epsilon Technology) that can measure both lateral and vertical deformations were clipped onto gage points mounted on each face of the specimen. The tests were performed using an MTS hydraulic loading system with the Teststar II data acquisition system. An environmental chamber kept the temperature constant $\pm 0.1^\circ\text{C}$.

Dynamic Modulus Test

For the dynamic modulus test, a uniaxial sinusoidal (i.e., haversine) compressive stress was applied to an unconfined or confined HMA cylindrical test specimen. The stress-to-strain relationship under a continuous sinusoidal loading for linear viscoelastic materials was defined by a complex number called the “complex modulus” (E^*). The absolute value of the complex modulus, $|E^*|$, was defined as the dynamic modulus. The dynamic modulus is mathematically defined as the maximum (i.e., peak) dynamic stress (σ_0) divided by the peak recoverable axial strain (ϵ_0) as follows:

$$|E^*| = \frac{\sigma_0}{\epsilon_0} \quad (7)$$

The dynamic modulus test consists of a series of tests conducted at different temperatures including -10 , 4.4 , 21.1 , 37.8 , and 54.4°C (14 , 40 , 70 , 100 , and 130°F) and various loading frequencies of 0.1 , 0.5 , 1.0 , 5 , 10 , and 25 Hz for the development of master curves for use in pavement response and performance analysis. The haversine compressive stress was applied on each sample to achieve a target vertical strain level of 100 microns in an unconfined test mode.

PHASE 1: MIXTURE DESIGN AND PERFORMANCE EVALUATION

Aggregate Structure Design

An analytical aggregate gradation evaluation method, Bailey Method was selected to design the aggregate structures. Details of the Bailey Material test procedures maybe found in Appendix B. This method produced a rational applied to blending different sizes of aggregate to achieve a densely packed aggregate skeleton with a minimized binder content and maximized volume filled by mineral aggregates for stiffness and bearing capacity purposes. Three aggregate structures were designed for each aggregate gradation (i.e., coarse, medium, and fine). The structures for the heavy traffic category mixtures were designed to meet the recommended ranges of the Bailey Method parameters. Low volume mixtures were designed using limestone aggregates only and had higher amounts of natural sand (>20%). Figures 9 to 14 are the design gradations for all the mixtures in this study. The Bailey gradation parameters for all the mixtures are summarized in Tables 2 and 3 for high and low volume, respectively.

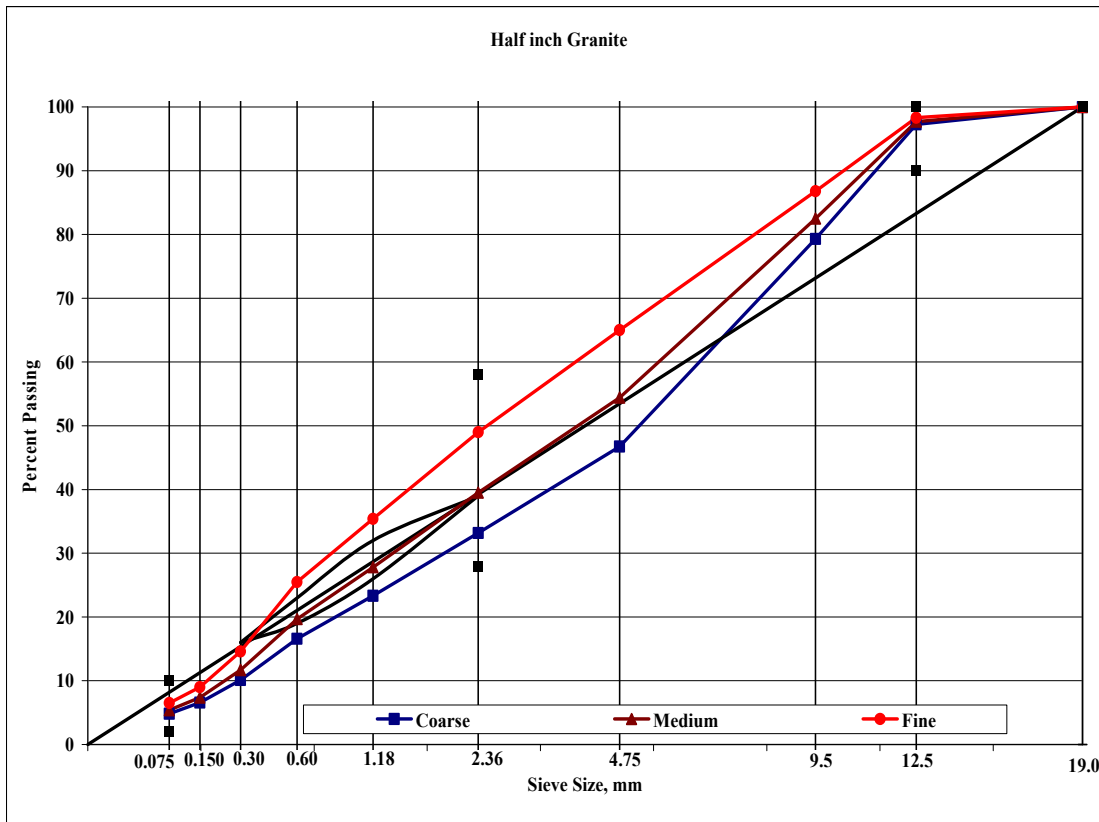


Figure 9
Aggregate structures for 1/2 in. granite mixtures

Reasonable separation was maintained between the aggregate gradations within each type of aggregate in order to capture the variation in performance (if any) within the same NMAS for each type of aggregate. This separation was quantified by the decrease in the volume of coarse aggregate in the structure when moving from coarse to fine gradation. A great effort was made to maintain a practical number of stockpiles for each aggregate blend. A maximum of four different stockpiles of readily available and commonly used aggregates in Louisiana were used.

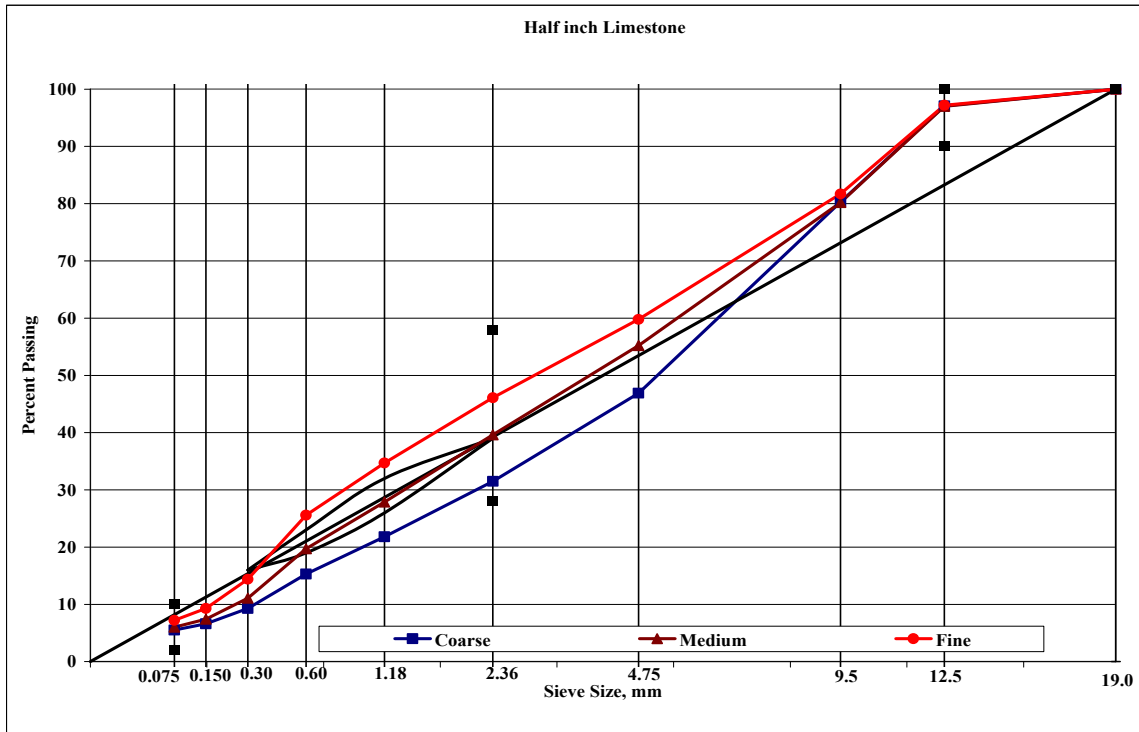


Figure 10
Aggregate structures for ½ in. limestone mixtures

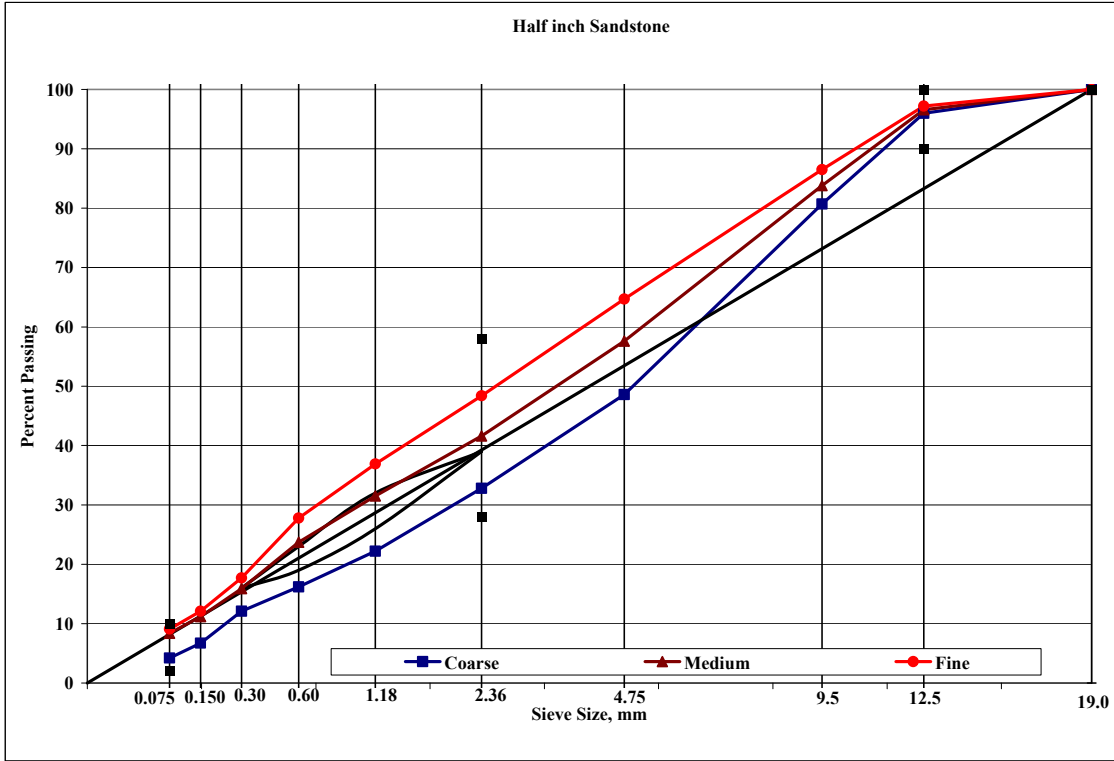


Figure 11
Aggregate structures for 1/2 in. sandstone mixtures

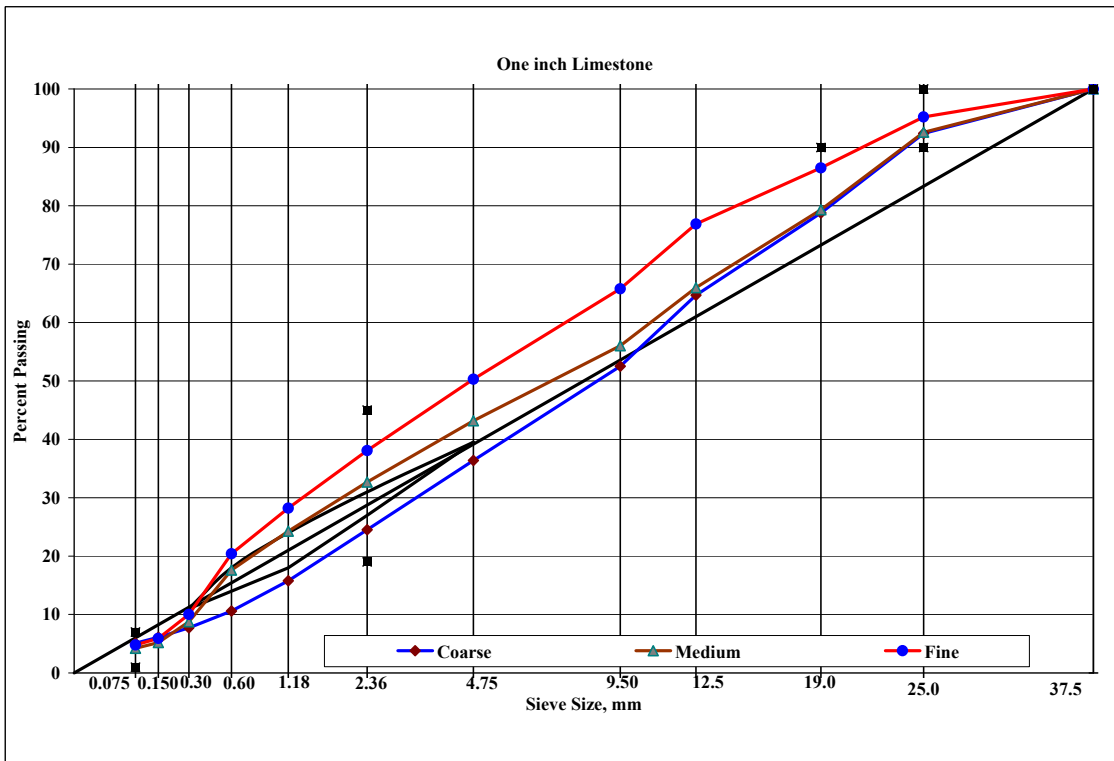


Figure 12
Aggregate structures for 1 in. limestone mixtures

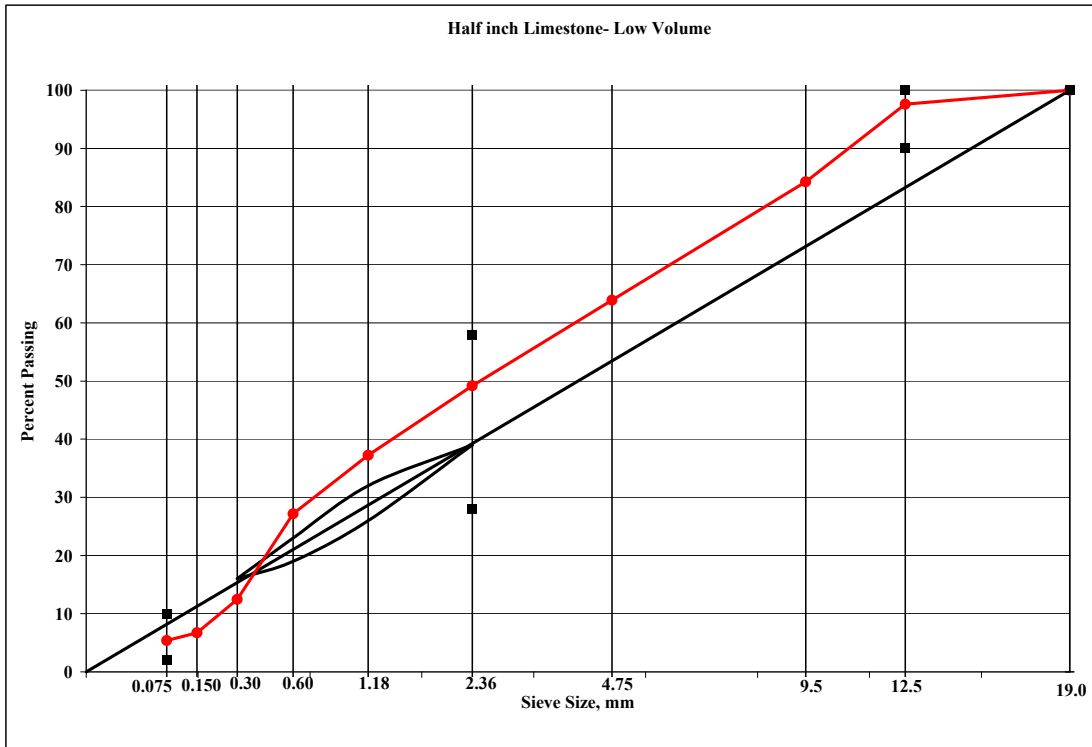


Figure 13
Aggregate structure for ½ in. low volume mixtures

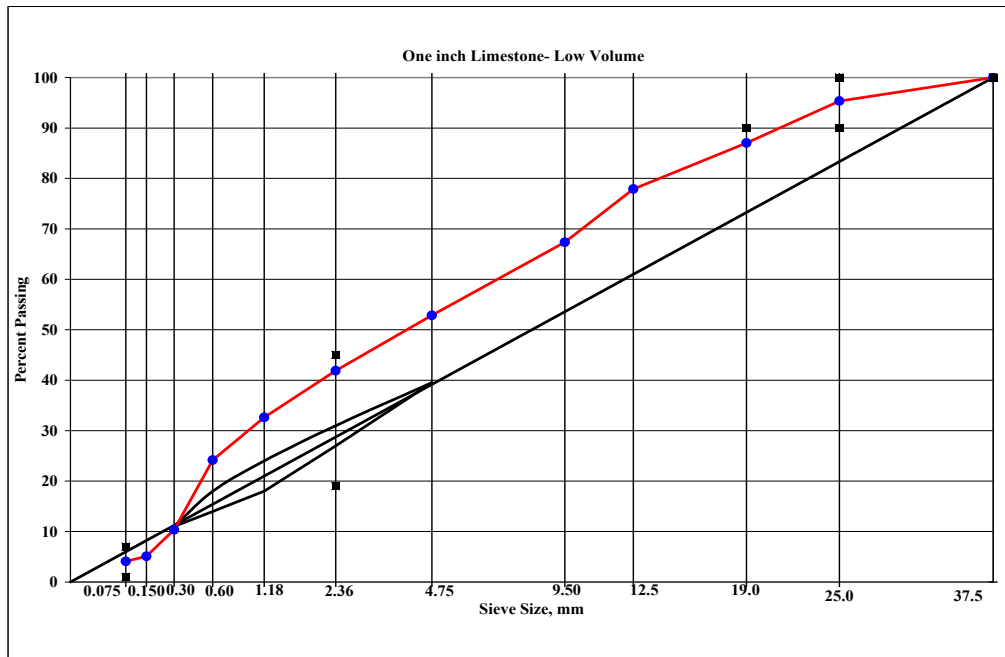


Figure 14
Aggregate structure for 1 in. low-volume mixtures

Table 2
Bailey gradation properties for high-volume mixtures

Aggregate Type	Gradation	NMAS	Designation	CA ¹ Volume	FA ² Volume	CUW ³	%PCS ⁴	CA ⁵ Ratio	F _{AC} ⁶ Ratio	F _{AF} ⁷ Ratio
Granite	Fine	½ in.	GRF-1/2 in.	38.3	61.7	70	49	0.728	0.352	N/A*
Granite	Medium	½ in.	GRM-1/2 in.	48.1	51.9	88	39.5	0.694	0.377	N/A
Granite	Course	½ in.	GRC-1/2 in.	55.2	44.8	101	33.2	0.686	0.396	N/A
Limestone	Fine	½ in.	LSF-1/2 in.	41.0	59.0	75	46.1	0.797	0.361	N/A
Limestone	Medium	½ in.	LSM-1/2 in.	46.4	53.6	85	39.6	0.706	0.374	N/A
Limestone	Course	½ in.	LSC-1/2 in.	56.0	44.0	103	31.5	0.612	0.487	N/A
Sandstone	Fine	½ in.	SSF-1/2 in.	40.8	59.2	75	48.4	0.792	0.435	N/A
Sandstone	Medium	½ in.	SSM-1/2 in.	47.8	52.2	88	41.6	0.765	0.471	N/A
Sandstone	Course	½ in.	SSC-1/2 in.	56.0	44.0	103	32.8	0.627	0.493	N/A
Limestone	Course	1 in.	LSC-1 in.	54.7	45.3	103	36.4	0.802	0.434	0.49
Limestone	Medium	1 in.	LSM-1 in.	47.1	52.9	89	43.2	0.803	0.36	0.482
Limestone	Fine	1 in.	LSF-1 in.	40.0	60.0	75	50.3	0.801	0.356	0.475

¹ CA = Coarse Aggregate Volume

² FA = Fine Aggregate Volume

³ CUW = Chosen Unit Weight

⁴ %PCS = Percent Passing Primary Control Sieve

⁵ CA Ratio = Coarse Aggregate Ratio

⁶ F_{AC} Ratio = Coarse Ratio of Fine Aggregate

⁷ F_{AF} Ratio = Fine Ratio of Fine Aggregate. This ratio is not calculated for 1/2 in. mixtures.

Table 3
Bailey gradation properties for low-volume mixtures

Aggregate Type	Gradation	NMAS	Designation	CA ¹ Volume	FA ² Volume	CUW ³	%PCS ⁴	CA ⁵ Ratio	F _{AC} ⁶ Ratio	F _{AF} ⁷ Ratio
Limestone	Fine	1 in.	LSF-1 in.,	37.3	62.7	70	52.9	1.134	0.617	0.317
Limestone	Fine	½ in.	LSF-1/2 in.	37.1	62.9	68	49.2	0.842	0.246	N/A

The designed gradations were further evaluated using the power-law method suggested by Ruth et al. [15]. Tables 4 and 5 present the power law gradation parameters for all the aggregate structures in this study. The divider sieve between the coarse and fine aggregate used in the power law analysis was chosen as the primary control sieve as determined from the Bailey Method analyses. This was the 2.36-mm (No 8) sieve for the 12.5-mm (½-in.) NMAS mixtures and the 4.75-mm (No. 4) for the 25.0-mm (1-in.) NMAS mixtures.

Table 4
Power law gradation parameters for high volume mixtures

Mixture	a _{CA}	n _{CA}	a _{FA}	n _{FA}
GRF-1/2 in.	34.15	0.42	31.07	0.61
GRM-1/2 in.	24.15	0.55	24.65	0.60
GRC-1/2 in.	18.20	0.66	20.90	0.58
LSF-1/2 in.	30.93	0.44	30.24	0.57
LSM-1/2 in.	24.66	0.53	24.50	0.58
LSC-1/2 in.	17.01	0.68	19.53	0.53
SSF-1/2 in.	33.77	0.42	33.10	0.50
SSM-1/2 in.	26.60	0.51	28.61	0.48
SSC-1/2 in.	18.31	0.65	20.93	0.59
LSC-1 in.	15.20	0.56	15.40	0.50
LSM-1 in.	20.80	0.50	19.40	0.60
LSF-1 in.	28.00	0.38	22.40	0.61

Table 5
Power law gradation parameters for low-volume mixtures

Mixture	a _{CA}	n _{CA}	a _{FA}	n _{FA}
LSF-1 in.	30.60	0.36	23.80	0.68
LSF-1/2 in.	34.40	0.41	30.80	0.70

Mixture Design

Mixture design was performed on all the aggregate structures that were formulated using the Bailey Method. The Superpave mixture design method was followed except for the VMA requirement. All the mixtures were designed for high-volume traffic ($N_{des} = 125$ gyrations at 1.25° angle of gyration). The optimum asphalt content was determined as the asphalt content required to achieve 4.0% air voids at N_{des} . Tables 6 and 7 summarize the results of the mixture design conducted on all the mixtures considered in Phase 1 of this study. The optimum asphalt contents ranged from 3.0% to 5.1%. The coarse mixtures had higher optimum asphalt contents for all the aggregate types considered. These mixtures have higher VMA values compared to the other ones, which created more inter-granular void space for the asphalt cement to occupy and hence increased the optimum asphalt content. The VMA

values in mineral aggregates ranged from 8.4% to 13.5%. Sandstone medium and fine mixtures had the lowest VMA values. The VMA values for all the mixtures were below the minimum requirement of the current Superpave system. It is noted that coarse and fine mixtures with similar NMAAS had different VMA values. This observation supports the concern on the validity of the current Superpave VMA requirement based on the NMAAS. It is evident that VMA is sensitive to aggregate gradation within the same NMAAS. All the mixtures met the Superpave requirements for %G_{mm} at N_{ini} and %G_{mm} at N_{max}. The average effective binder film thicknesses ranged from 8.8 microns for limestone and sandstone coarse mixtures to as low as 2.5 microns for medium and fine sandstone mixtures. For most medium and fine mixtures, the calculated film thickness was below the generally reported range of 6.0 – 8.0 microns. It was found that film thickness was strongly affected by the amount of dust (passing #200 sieve) in relation to asphalt content or what is called *Dust/P_{beff}* ratio. Medium and fine sandstone mixtures with the lowest film thickness values had the highest *Dust/P_{beff}* ratio of 4.7.

Table 6
Job mix formula- 12.5-mm mixes- $N_{des} = 125$ gyrations

Mixture name	LS Coarse	LS Medium	LS Fine	SST Coarse	SST Medium	SST Fine	GR Coarse	GR Medium	GR Fine
Mix type	12.5 mm	12.5 mm	12.5 mm	12.5 mm	12.5 mm	12.5 mm	12.5 mm	12.5 mm	12.5 mm
Aggregate blend	42.2% #78 LS 14.3% #8 LS 36.7% #11 LS 6.8% Sand	44.3% #78 LS 44.5% #11 LS 11.2% Sand	41.0% #78 LS 23.6% #10 LS 20.2% #11 LS 15.2% Sand	59.4% #78 SST 21.4% #11 SST 19.2% #11 LS	49.8% #78 SST 43.6% #10 LS 6.6% Sand	41.3% #78 SST 48.4% #10 LS 10.3% Sand	57.1% #78 Granite 23.8% #11 Granite 14.1% #10 LS 5.0% Sand	48.3% #78 GR 29.7% #11 GR 15.4% #10 LS 6.6% Sand	36.5% #78 GR 30.2% #11 GR 22.4% #10 LS 10.9% Sand
Binder type	PG 76-22M	PG 76-22M	PG 76-22M	PG 76-22M	PG 76-22M	PG 76-22M	PG 76-22M	PG 76-22M	PG 76-22M
Design AC content, volumetric properties, and densification									
% G_{mm} at N_I	85.1	86.2	88.0	86.0	86.4	88.0	87.3	87.3	87.1
% G_{mm} at N_M	97.2	97.4	97.3	97.0	97.1	97.4	97.5	97.2	97.0
Design binder content, %	5.1	4.0	3.5	5.1	3.6	3.9	4.8	4.5	4.3
Design air void, %	4.0	4.0	4.0	4.0	4.0	4.0	4.0	4.0	4.0
VMA, %	13.5	11.3	9.4	13.1	8.4	8.5	12.7	11.3	10.9
VFA, %	71.0	62.7	58.5	69.0	50.0	54.0	66.2	62.4	60.6
Metric (U.S.) Sieve	Gradation, (% passing)								
19 mm (¾ in)	100	100	100	100	100	100	100	100.0	100.0
12.5 mm (½ in)	97.1	97.0	97.2	96.0	96.6	97.2	97.3	97.7	98.3
9.5 mm (⅜ in)	80.3	80.2	81.7	80.7	83.8	86.5	79.3	82.5	86.8
4.75 mm (No.4)	46.9	55.2	59.8	48.6	57.6	64.7	46.7	54.4	65.0
2.36 mm (No.8)	31.5	39.6	46.1	32.8	41.6	48.4	33.2	39.5	49.0
1.18 mm (No.16)	21.8	27.9	34.7	22.2	31.5	36.9	23.3	27.8	35.4
0.6 mm (No.30)	15.3	19.7	25.6	16.2	23.7	27.8	16.6	19.7	25.5
0.3 mm (No.50)	9.3	11.1	14.4	12.1	15.9	17.7	10.1	11.7	14.6
0.15 mm (No.100)	6.6	7.4	9.3	6.7	11.2	12.1	6.6	7.4	9.0
0.075 mm (No.200)	5.5	6.0	7.2	4.2	8.4	9.1	4.8	5.4	6.5

LS: Siliceous Limestone, SST: Sandstone, GR: Granite

Table 7
Job mix formula- 25.0-mm mixes- $N_{des} = 125$ gyrations

Mixture name	LS Coarse	LS Medium	LS Fine
Mix type	25.0	25.0 mm	25.0 mm
Aggregate blend	36.4 #57 LS	35.4 #57 LS	23.2% #57 LS
	26.7 #78 LS	20.9% #78 LS	25.7% #78 LS
	36.9 #11 LS	29.5% #11 LS	34.4% #11 LS
		14.2% Sand	16.7% Sand
Binder type	PG 76-22M	PG 76-22M	PG 76-22M
Design AC content, volumetric properties, and densification			
% G_{mm} at N_I	85.0	88.8	89.1
% G_{mm} at N_M	97.7	97.4	97.4
Design binder content, %	3.8	3.0	3.3
Design air void, %	4.0	4.0	4.0
VMA, %	11.1	9.6	10.0
VFA, %	63.5	58.2	60.5
Metric (U.S.) Sieve	Gradation, (% passing)		
37.5 mm (1½ in)	100	100	100
25 mm (1 in)	92.4	92.6	95.2
19 mm (¾ in)	78.8	79.3	86.5
12.5 mm (½ in)	64.7	66.0	76.9
9.5 mm (⅜ in)	52.5	56.1	65.8
4.75 mm (No.4)	36.4	43.2	50.3
2.36 mm (No.8)	24.5	32.7	38.1
1.18 mm (No.16)	15.8	24.3	28.2
0.6 mm (No.30)	10.6	17.6	20.4
0.3 mm (No.50)	7.7	8.7	10
0.15 mm (No.100)	6.1	5.2	5.9
0.075 mm (No.200)	5.1	4.2	4.8

Permeability Test

A SGC compacted specimen of 150 mm diameter and 63.5 mm height was soaked overnight to achieve full saturation. The specimen was then removed from the water bath and the side was treated with petroleum jelly in order to prevent any lateral flow of water. The specimen was then placed in the test apparatus and confined using a latex membrane. Air was evacuated from the membrane cavity. The membrane was inflated to 12.5 psi and this pressure was maintained throughout the test. Water was filled to a level above the graduated, upper timing mark. The timing device was started when the bottom of the meniscus of the water reached the upper timing mark. The test was run for 30 minutes and the final water level was recorded at the end of the test. The time was recorded to the nearest second. The coefficient of permeability is determined using the following equation:

$$K = \left(\frac{L}{T}\right) \times \left(\frac{d^2}{D^2}\right) \times \ln\left(\frac{H_1}{H_2}\right) \quad (8)$$

where,

K = Coefficient of Permeability (10^{-4} mm/s);

L = average specimen thickness (mm);

D = average specimen diameter (mm);

d = graduated cylinder diameter (mm);

T = total time of test, seconds (s);

H_1 = initial height of water (mm); and

H_2 = final height of water (mm).

Table 8 summarizes the permeability test results for all the mixtures. It is clearly shown that all the mixtures had very low permeability levels and that in many cases they were virtually impermeable. The extremely low permeability of the designed mixtures reflected the dense aggregate structures that resulted in minimal interconnectivity of air voids and hence prevented any water flow through the mixtures despite the fact that all the specimens were compacted to a 7.0% air void.

Table 8
Permeability data

Mixture	Gradation	Average Permeability (10^{-4} mm/sec)	Average Permeability (ft/day)
½" Limestone	Fine	0.82	0.02
	Medium	0.00	0.00
	Coarse	0.00	0.00
½" Sandstone	Fine	1.12	0.03
	Medium	3.12	0.09
	Coarse	0.00	0.00
½" Granite	Fine	1.91	0.05
	Medium	1.37	0.04
	Coarse	0.00	0.00
1" Limestone	Fine	0.21	0.01
	Medium	0.65	0.02
	Coarse	0.30	0.01

Asphalt Mixtures Compactability

The compactability of the designed asphalt mixtures was evaluated using results from the Superpave gyratory compactor (SGC) and the pressure distribution analyzer device (PDA). The densification curve obtained from the SGC was used to evaluate mixture

resistance to the compaction energy applied by the SGC. The behavior of the mixtures during compaction was also captured using the PDA. Two samples per mixture were tested for compactability evaluation. The following terms was used in the analysis of the results from the SGC and the PDA.

SGC Locking Point

The SGC locking point is the number of gyrations after which the rate of change in height is equal to or less than 0.05 mm/gyr for three consecutive gyrations (see Figure 15 and Table 9).

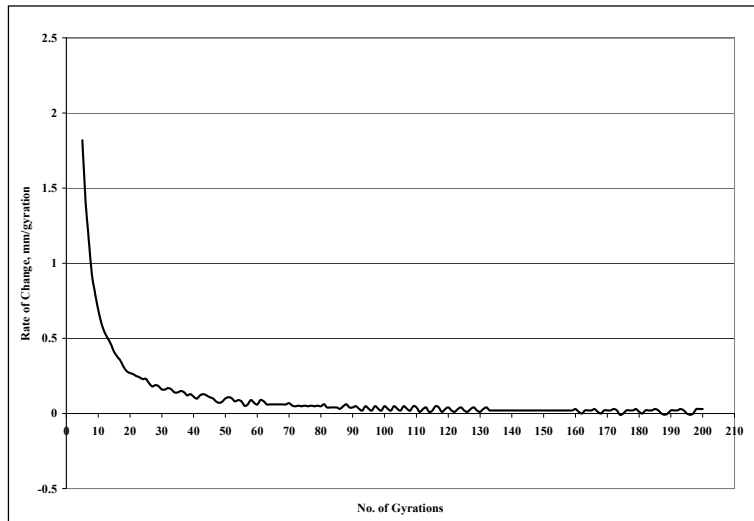


Figure 15
Rate of change of height during SGC compaction

Table 9
Example data set for SCG locking point determination

Number of Gyrations	Rate of Change
61	0.07
62	0.06
63	0.08
64	0.07
65	0.06
66	0.07
67	0.07
68	0.06
69	0.06
70	0.05
71	0.05
72	0.05
73	0.05
74	0.05

← **Locking Point**

PDA Locking Point

It is defined as the number of gyrations at which the rate of change of frictional resistance per gyration is equal or less than 0.01 psi/gyr (see Figure 16 and Table 10).

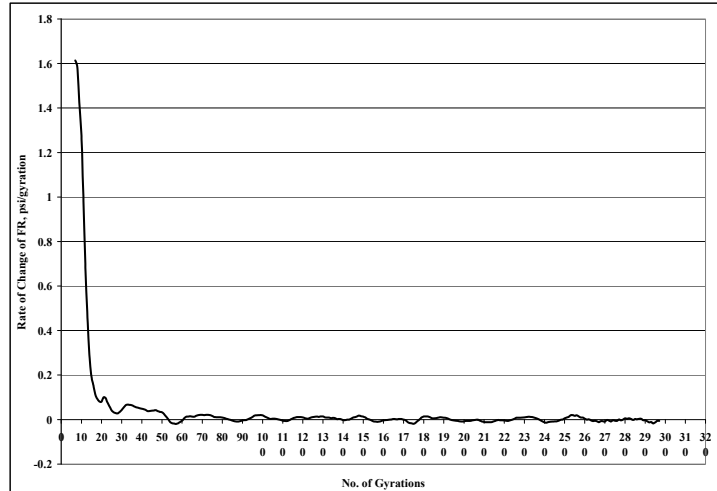


Figure 16
Rate of change of frictional resistance during SCG compaction

Table 10
Example data set for PDA locking point determination

No. of Gyrations	Rate of change of FR
36	0.05
37	0.05
38	0.05
39	0.05
40	0.05
41	0.04
42	0.03
43	0.05
44	0.05
45	0.05
46	0.04
47	0.04
48	0.03
49	0.03
50	0.03
51	0.01

← Locking Point

SGC Compaction Densification Index (CDI)

CDI is defined as the area under the SGC densification curve from the first gyration (i.e., $N = 1$) to the SGC locking point (see Figure 17). This index is hypothesized to be related to compactability of asphalt mixtures. Higher values of this index are associated with mixtures that are difficult to compact.

SGC Traffic Densification Index (TDI)

TDI is the area under the SGC densification curve from the SGC locking point to N at 98% G_{mm} or the end of compaction ($N = 205$ gyrations), whichever comes first (see Figure 17). This index is hypothesized to be related to the stability of mixtures under traffic loading. Theoretically, higher values are supposed to be indicative of better mixtures stability.

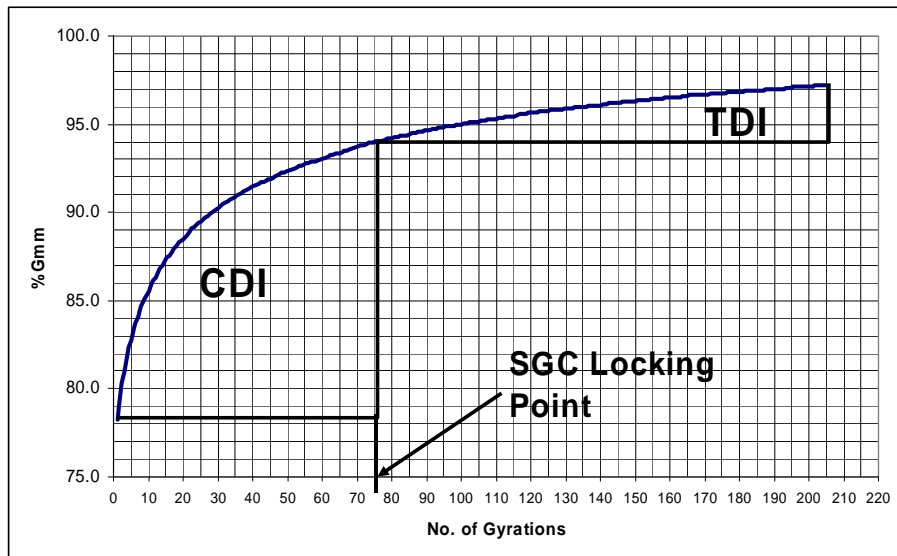


Figure 17
SGC compaction indices definition

PDA Compaction Force Index (CFI)

CFI is the area under frictional resistance vs. number of gyration curve from $N = 1$ to the SGC locking point. It is analogous to the CDI (see Figure 18). Higher values are associated with mixtures with poor compaction characteristics.

PDA Traffic Force Index (TFI)

TFI is the area under frictional resistance vs. number of gyration curve from the SGC locking point to $N = 205$ (see Figure 18). This index is analogous to TDI from the SGC. Higher values are supposed to be indicative of more stable mixtures.

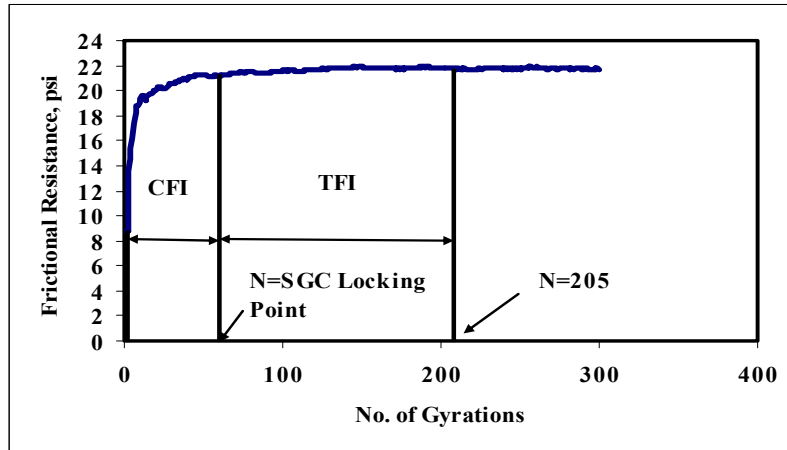


Figure 18
PDA compaction indices definition

The locking point data are presented in Figure 19 and Figure 20 for both the SGC and the PDA, respectively, suggesting that coarse mixtures take a higher number of gyrations to reach the locking point condition. This indicates that it takes more energy to densify coarse mixtures compared to the medium and fine mixtures. As the aggregate gradation becomes finer, the compactability of the mixtures was improved with the only exceptions of fine limestone mixture for SGC and fine granite mixture for PDA, in which locking points were slightly higher than that of the medium gradation mixtures. It was also found that the locking points for the mixture evaluated were much lower than the design number of gyrations recommended by the current Superpave design system. The highest locking point is less than 70% of the recommended design number of gyrations for the heavy-traffic category ($N_{des} = 125$). For 12.5-mm (1/2-in.) NMAS mixtures, the fine limestone mixture had the lowest locking points from both SGC and PDA (62 and 57, respectively). Both medium and fine limestone 25.0-mm (1-in.) NMAS mixtures showed similar response to the applied compaction energy in terms of locking point. Figure 21 shows a good correlation between the locking points determined from the SGC and those obtained from the PDA. On average, the PDA locking points were about four gyrations lower than those determined from the SGC data.

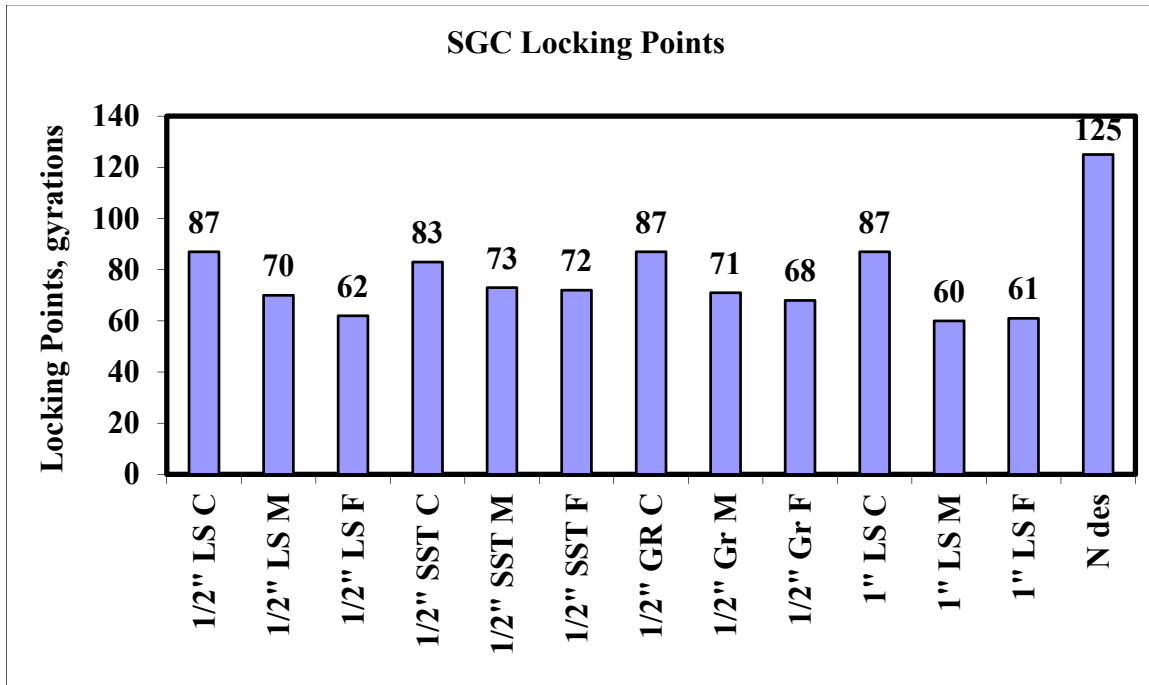


Figure 19
SCG locking point results

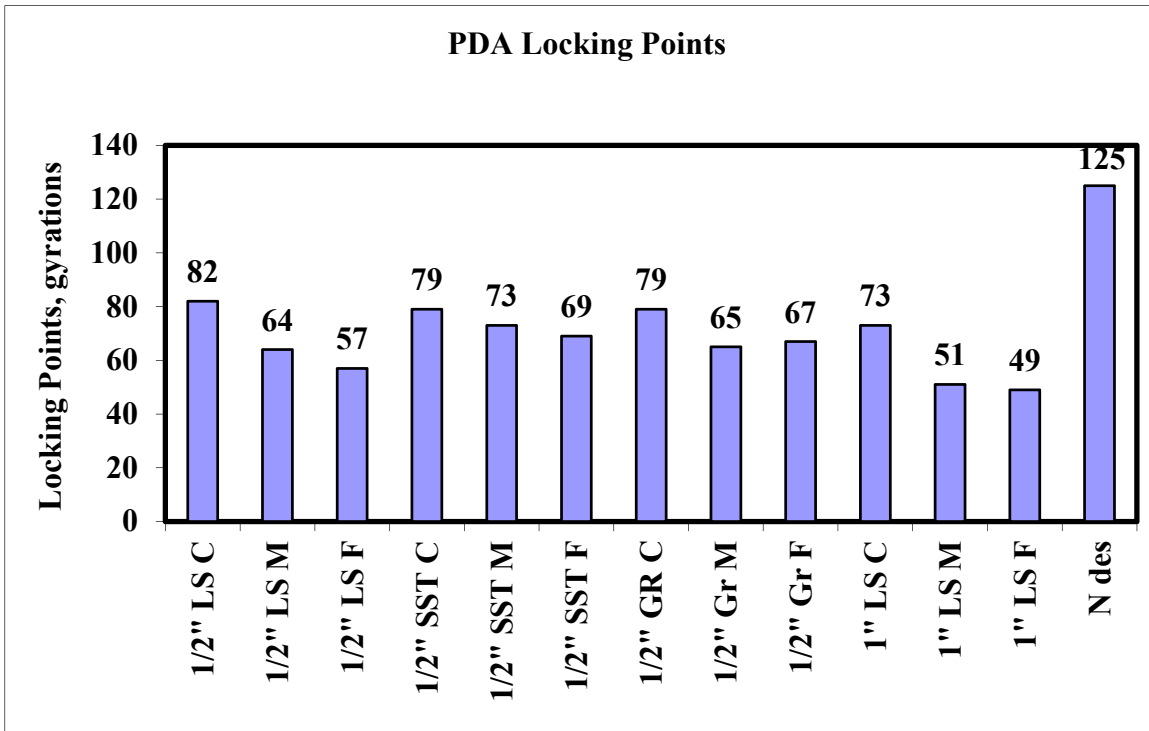


Figure 20
PDA locking point results

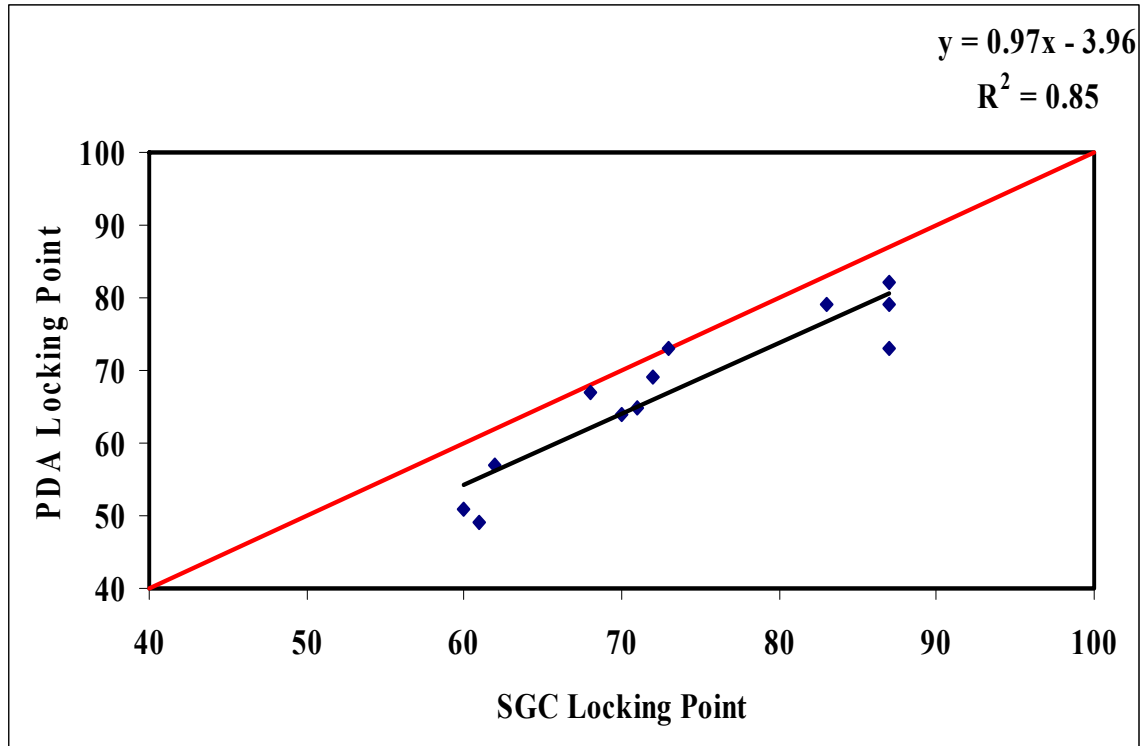


Figure 21
SCG and PDA locking points correlation

The concept of energy indices was first introduced by Bahia et al. [16]. In that study, the energy indices were calculated using the region from $N = 8$ to N at 92% G_{mm} for the CDI and from N at 96% G_{mm} to N at 98% G_{mm} for the TDI. It was assumed that the first eight gyrations represented the constant compaction energy applied by the paver screed. In the present study, however, that energy was considered as a part of the applied compaction effort and the densification curve was divided into two main regions: the densification region from $N = 1$ to the locking point, which was used to calculate the CDI and CFI from both the SGC and PDA. The post densification region from the locking point to $N = 205$ which represented the terminal densification of the mixture at the end of service life and was used to calculate the TDI and TFI. Figures 22 and 23 show the energy indices calculated for all the mixtures in Phase 1 of the study.

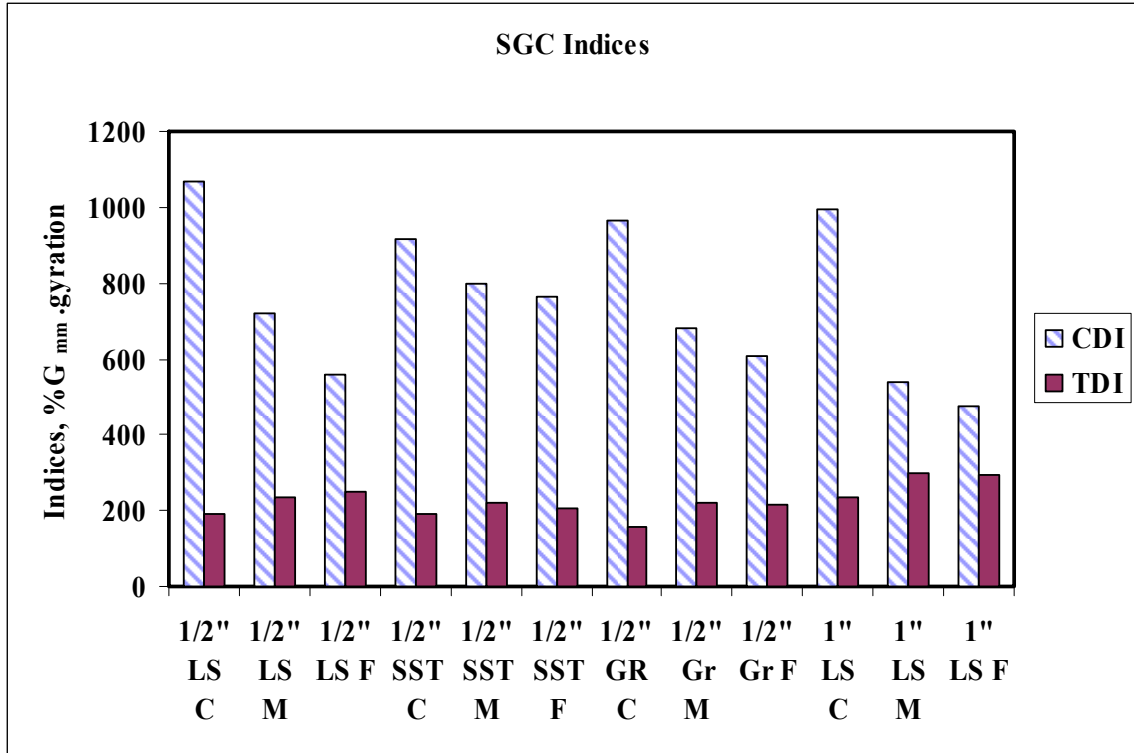


Figure 22
SCG densification indices

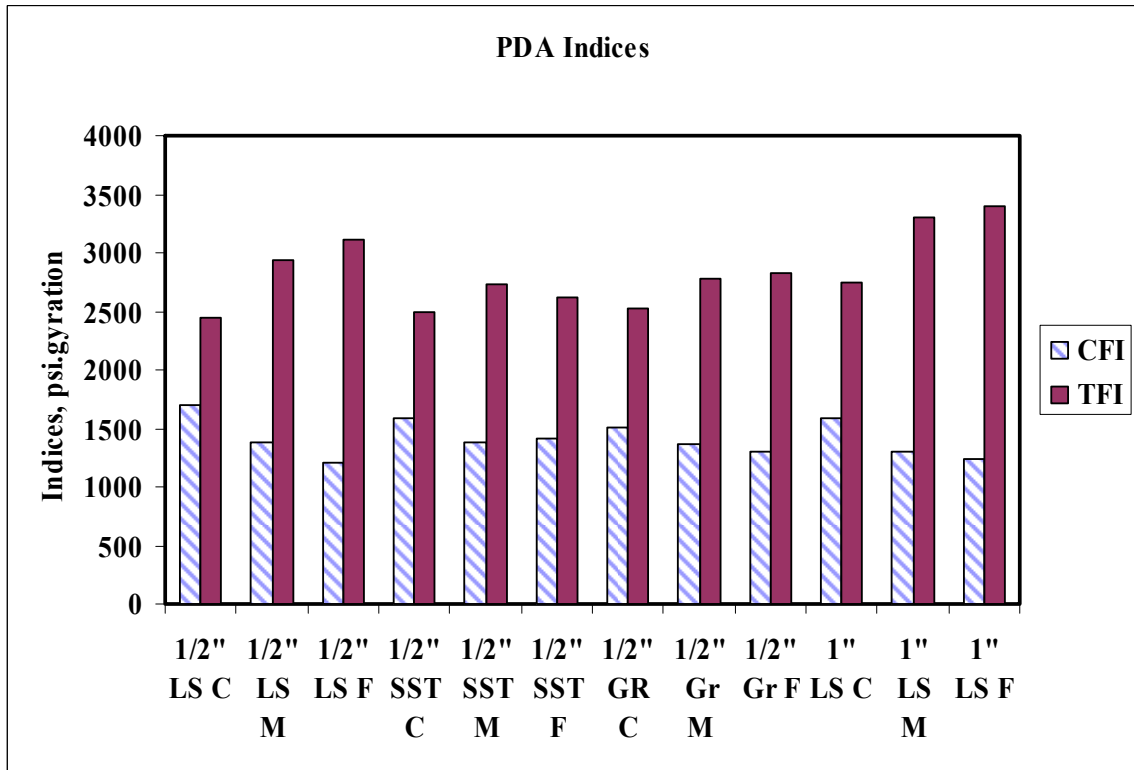


Figure 23
PDA densification indices

The compaction densification index CDI from the SGC had no considerable variations across the different gradations within the same NMA, indicating that it is sensitive to the size distribution of blends having the same NMA. For example, for 12.5-mm (1/2-in.) NMA limestone mixtures, the fine mixture required about 48% lower energy to reach the locking condition than the coarse mixture. The sandstone had lower variation in CDI across the different gradations. The fine sandstone mixtures took about 17% less compaction energy than the coarse one to reach to the locking condition. There was about an 11% difference in compaction energy between the medium and the fine granite gradations. Therefore, it is clear that it takes more energy to compact coarse mixtures in the first region of the densification curve, indicating that those mixtures might be less desirable for construction and more likely to have compactability problems. The same trend was observed with the compaction force index from the PDA. This is clearly shown in the strong correlation obtained between CDI and CFI ($R^2 = 0.92$), as shown in Figure 24.

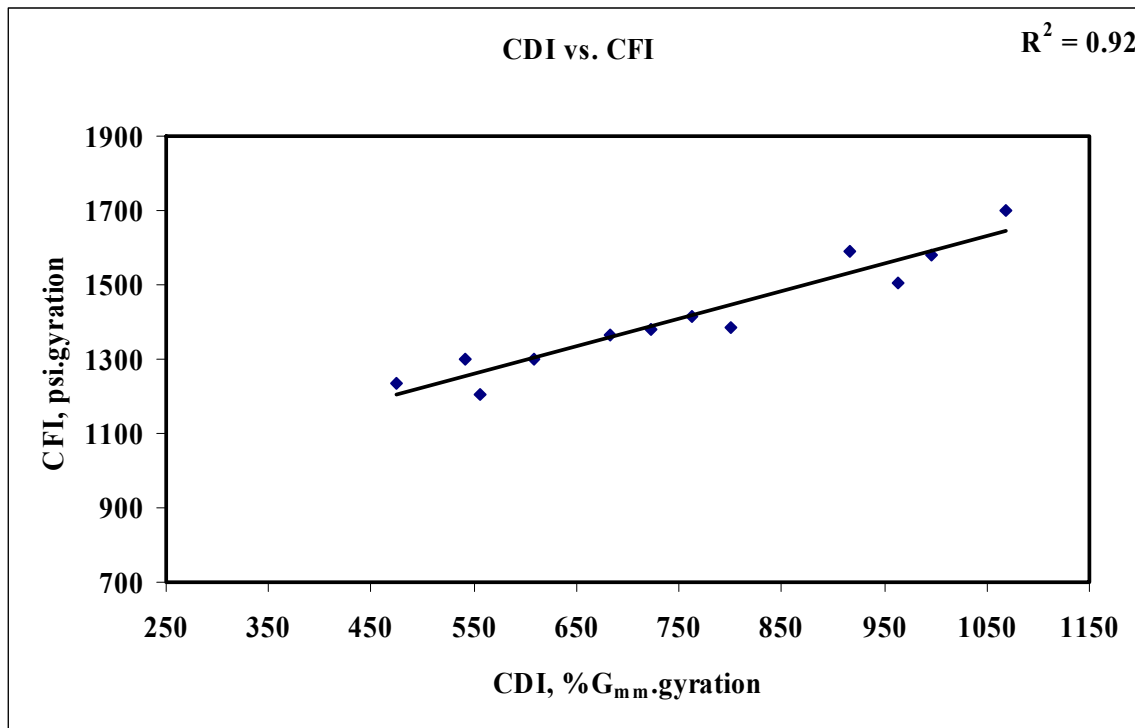


Figure 24
Correlation between PDA and SCG compaction indices

The aggregate resistance to further densification from traffic loading was explored using the TDI from the SGC and the TFI from the PDA. The variation of these two indices is less than that observed with the compaction indices. This was expected because the

behavior of the mixtures beyond their locking points was relatively similar, as shown in Figure 25. As shown in Figure 26, the mixtures maintained their frictional resistance until the end of compaction without showing noticeable loss in stability under the compaction load. The only mixture that showed some loss in stability was the fine sandstone mixture. This mixture had the highest amount of fine materials passing the No. 200 sieve (9.1%). In general, the magnitude of the frictional resistance varied in a narrow range between the mixtures at the locking point, suggesting that different aggregate structures can provide similar performances if they are properly designed with the aim of achieving mix stability.

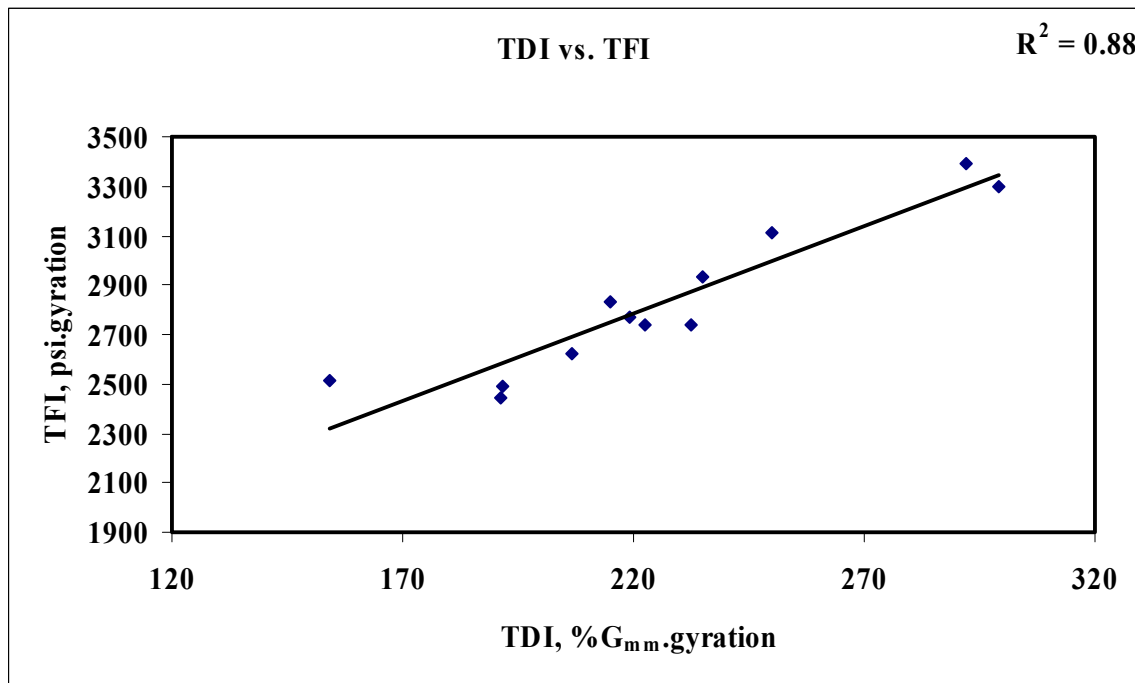


Figure 25
Comparison of traffic indices from SCG and PDA

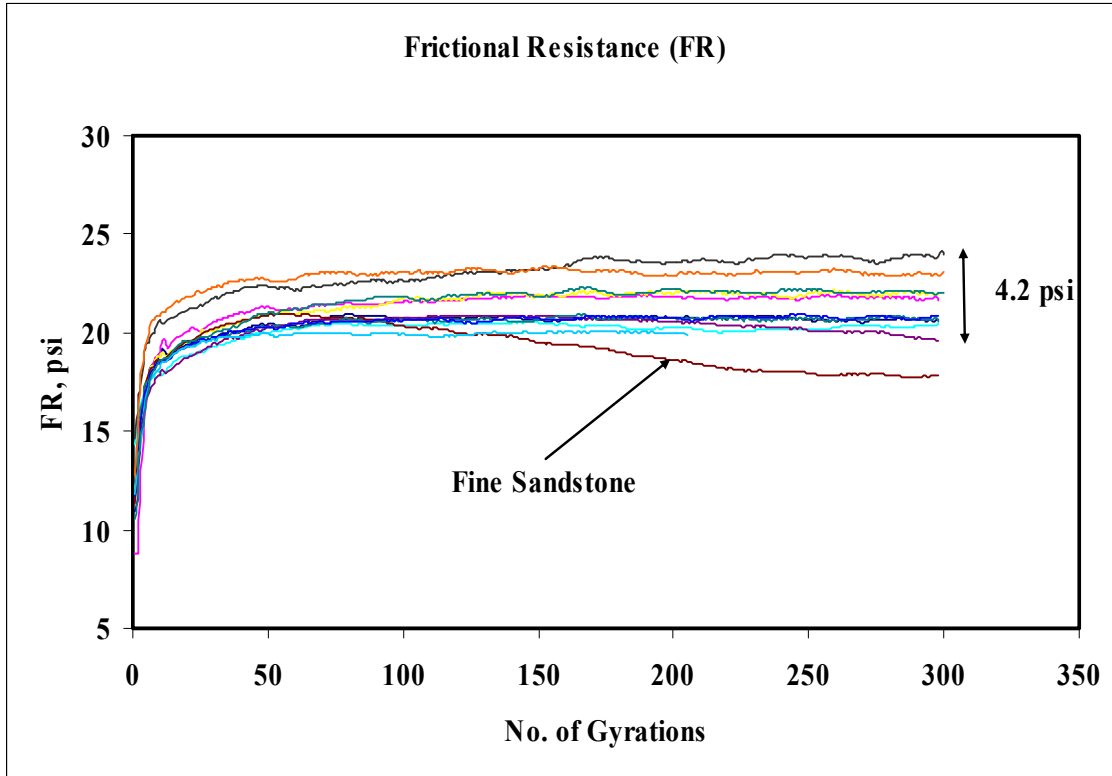


Figure 26
Frictional resistance of asphalt mixtures

Estimating Locking Point

A multiple linear regression model was developed using Statistical Analysis System (SAS) software to estimate the locking point of the mixture based on certain properties that is thought to influence the performance of the mixture during compaction. The response parameter used was the locking point (*LP*). Since the compaction process was always performed at elevated temperatures, the effect of aggregate structure on the mixture performance was thought to be more pronounced than that of the binder even if the binder still maintained some lubrication effect that could contribute to the mixture response to the applied compaction energy. Several parameters, including different characteristics of the gradation curves of the designed aggregate structure as well as binder content, were introduced in the model. A stepwise variable selection procedure was performed on a general model that contains those variables. The purpose of such a procedure was to remove insignificant variables from the general model. The regression analysis was then conducted on the reduced model determined using the stepwise variable selection procedure. Three parameters were selected for the regression analyses, which were found to be significant when included in the model as independent variables. These parameters are:

- Volume of coarse aggregate in the aggregate structure (VCA),
- Percent Passing #200 sieve for the aggregate structure in consideration (P_{200}),
and
- Estimated initial asphalt content (AC).

The predictive model used is:

$$LP = 1.38 \times VCA + 0.62 \times P_{200} \times AC - 6.86 \quad (9)$$

where,

LP = Locking Point to be estimated,

VCA = Volume of coarse aggregate in the aggregate structure, and

$DAC = P_{200} \times AC$ = Interaction between the effect of the amount of material passing #200 sieve (P_{200}) in the aggregate structure and the estimated asphalt content (AC).

The results of the regression procedure are summarized in Table 11. A f- value for the model was 45.44 with a p-value of 0.0001. This indicates that the model was significant in describing the relationship between the response variable (i.e., LP) and the independent variables. All the parameters estimated for the predictor variables in the model were found to be significant at the 95% significance level selected for the analysis.

The model was also checked for any collinearity between the predictor variables. When there is a perfect linear relationship among the predictors, the estimates for a regression model cannot be uniquely computed. The term collinearity describes two variables that are near perfect linear combinations of one another. When more than two variables are involved, it is often called multicollinearity, even if the two terms are often used interchangeably. The primary concern is that as the degree of multicollinearity increases, the regression model estimates of the coefficients become unstable and the standard errors for the coefficients can get wildly inflated. The “vif” option was used to check for multicollinearity, which stands for *variance inflation factor*. Generally, a variable with the “vif” value of greater than 10 may merit further investigation. A comparison between the measured locking point and predicted response variable by the model is presented in Figure 27.

Table 11
Linear regression analysis to estimate locking point

Analysis of Variance							
Source	DF	Sum of Squares	Mean Square	f-value	Pr > F		
Model	2	1413.28	706.64	45.44	<.0001		
Error	11	171.08	15.55				
Corrected Total	13	1584.36					
Root MSE	3.94	R-Square	0.89				
Dependent Mean	71.21	Adj R-Sq	0.87				
Coeff. Of Var.	5.54						
Parameter Estimates							
Variable	DF	Parameter Estimate	Standard Error	t Value	Pr > t	Tolerance	Variance Inflation
Intercept	1	-6.86	8.43	-0.81	0.4329		0
VCA	1	1.38	0.15	9.04	<.0001	0.99	1.00
DAC	1	0.62	0.18	3.45	0.0055	0.99	1.00

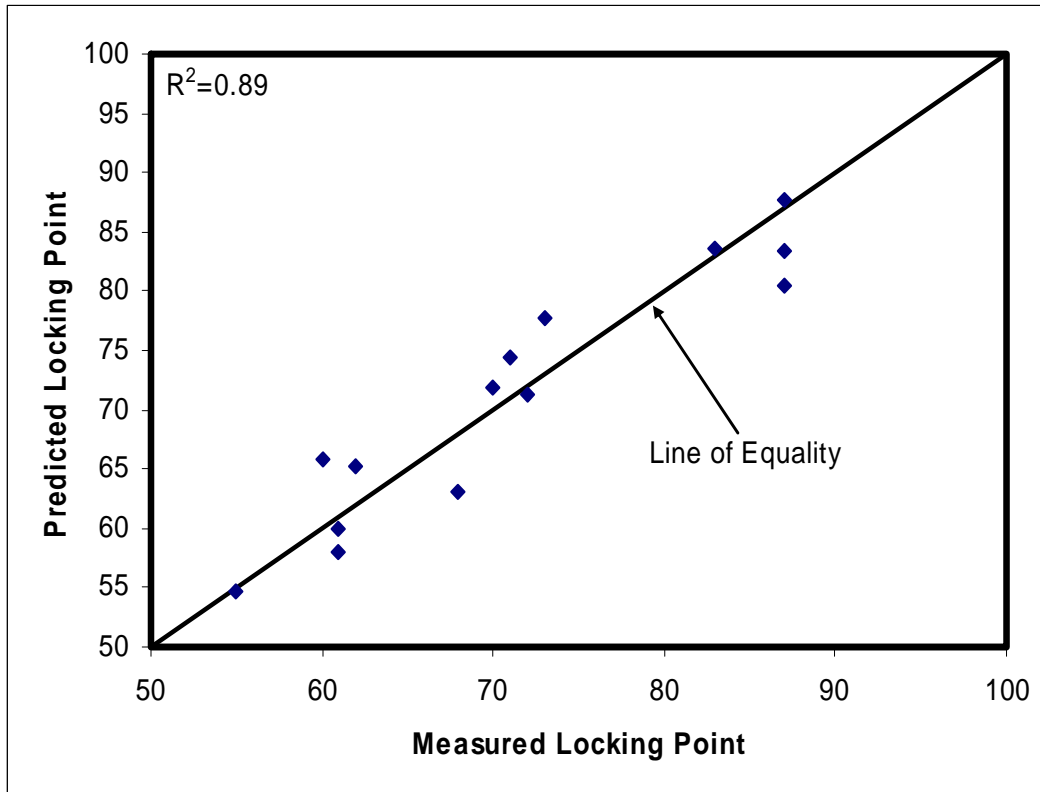


Figure 27

Accuracy of the locking point estimation model

Gradation Analysis

As mentioned earlier, the aggregate structures designed by the Bailey Method were further evaluated by the power law gradation evaluation method. Both methods looked at distinct regions in the gradation curve and described them using one or more indices that were related to the size distribution of the aggregates in those particular regions. An attempt was made to correlate the parameters from each method, as shown in Figures 28 and 29. The former figure shows that there is a good correlation between the parameters describing the coarse portion of the gradation curve from both methods (CA ratio, aCA, and nCA). From the same figure, it seems that the relationship between the intercept of aCA and CA ratio was dependent on NMAS. There was a clear distinction between the 25.0-mm (1-in.) NMAS mixtures and the 12.5-mm (½-in.) NMAS mixtures trend lines. The correlation between the parameters describing the fine portion of the aggregate gradation curve was, however, relatively weak, as seen in Figure 29. This is not unexpected because the F_{AC} from the Bailey Method described the middle portion of the curve only while the parameters from the power law method considered the whole portion of the gradation curve from the divider sieve to the No. 200 sieve. In other words, the parameters related to fine portion were described from different regions of the gradation curve in the two methods and, thus were not expected to be correlated well.

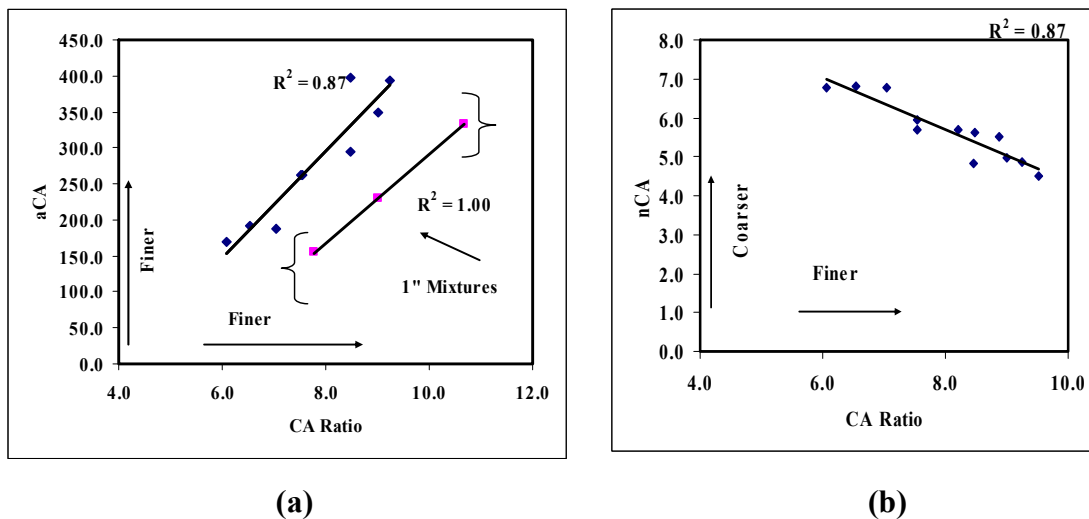


Figure 28
Relationship of the coarse gradation parameters from the Bailey and the power law methods (a) aCA vs. CA ration (b) nCA vs. CA ration

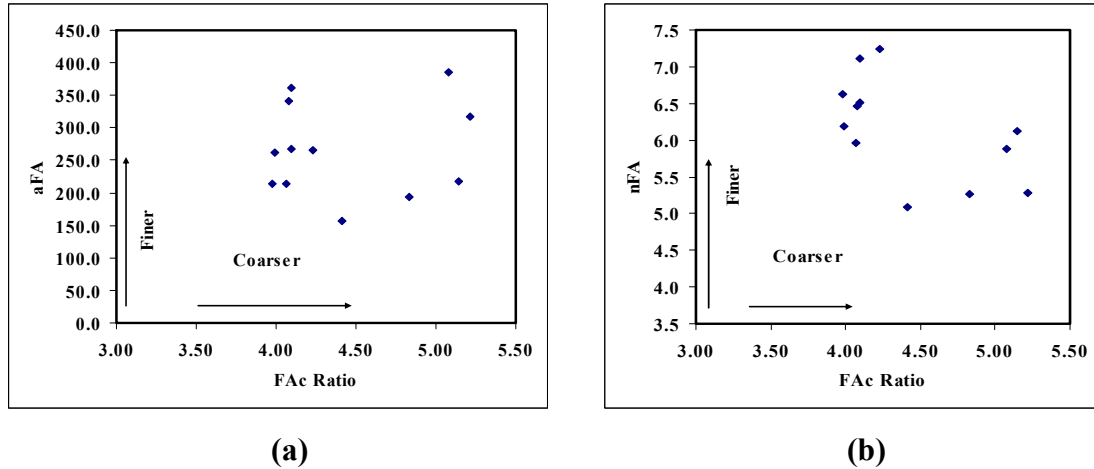


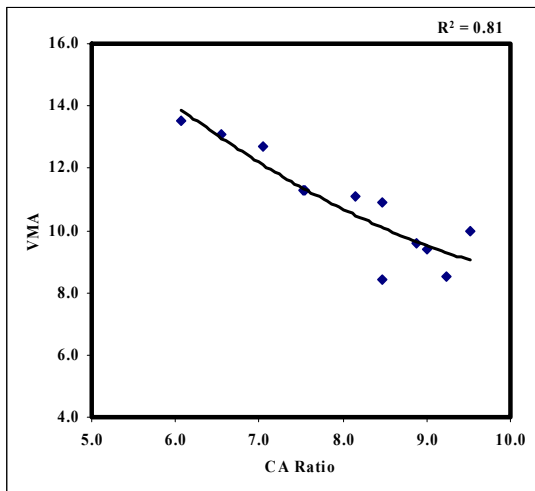
Figure 29
Fine gradation parameters from the Bailey Method and the power law method (a) aFA vs. F_{AC} ratio (b) nFA vs. F_{AC} ratio

Gradation Parameters and Mixture Design

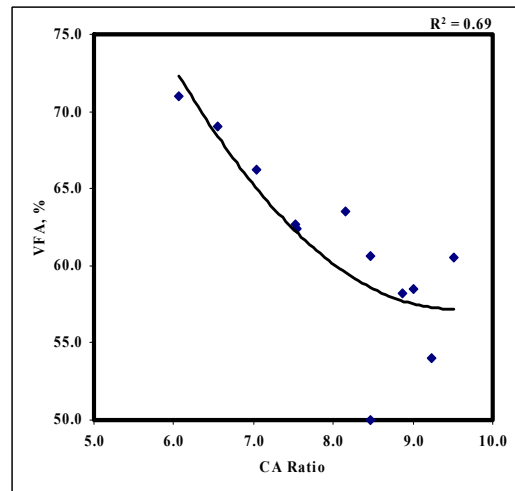
The effect of aggregate gradation on mixture volumetrics was investigated using the gradation parameters obtained from both the Bailey Method and the power law method. For this investigation, two parameters such as CA ratio and F_{AC} ratio from the Bailey were used while four parameters (i.e., aCA, nCA, aFA, and nFA) were selected from the power law method. Since different aggregate types were used, correlating the gradation parameters directly to mixture design might be misleading. Mixture design parameters were not only a function of the particle size distribution, but were also affected by the shape and surface texture characteristics of the aggregates used. Those characteristics were varied for different aggregate types.

The final blend was also affected by the amount and type of compaction applied to the mix. Therefore, those effects needed to be accounted for when such type of relationships between gradation and mixture design parameters were investigated. Regarding mixture compaction, all the mixtures were subjected to the same type and amount of compaction energy (SGC compaction, $N_{des} = 125$). In order to incorporate the variation of shape and surface texture of the different types of aggregates used, the gradation parameters from both the Bailey Method and the power law method were normalized by dividing them by the chosen unit weight of the blend for each mixture considered. The chosen unit weight was a percentage of the loose unit weight of the aggregates based on the degree of coarse aggregate interlock required. The loose unit weight was the minimum density (mass per volume) required to provide particle-to-particle contact of the coarse aggregates. Shape and surface texture play an important role in the packing of aggregate particles in a unit volume, and consequently have an influence on the measured unit weight. Therefore, by

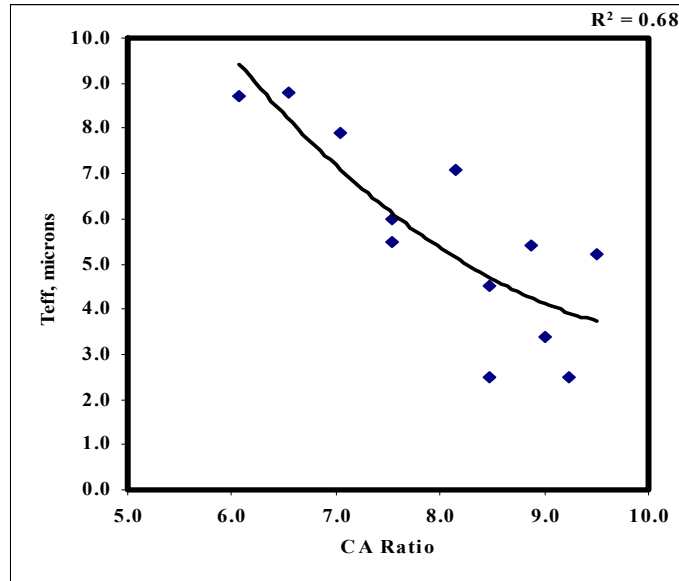
incorporating the unit weight in the relationship between the gradation parameters and mixture design properties, the shape and surface texture were indirectly accounted for. Figures 30 and 31 illustrate the relationship between the Bailey Method parameters and mixture physical properties. CA ratio, which is predominantly a function of the coarse aggregate blend by volume, seemed to have the strongest correlations with mixture physical properties. As the CA ratio increased, the smaller size particles in the coarse portion of the aggregate structure became more dominant, creating an inverse effect on the main volumetric parameters VMA and VFA. As shown in Figure 30(c), good correlation was also observed between CA ratio and the effective film thickness ($R^2 = 0.68$) in which film thickness was reduced by having high CA ratio. As indicated in Figure 31, mixture volumetrics seemed to be less sensitive to the change in the F_{AC} ratio. Clearly, no relationship could be established between the F_{AC} ratio and effective film thickness.



(a)



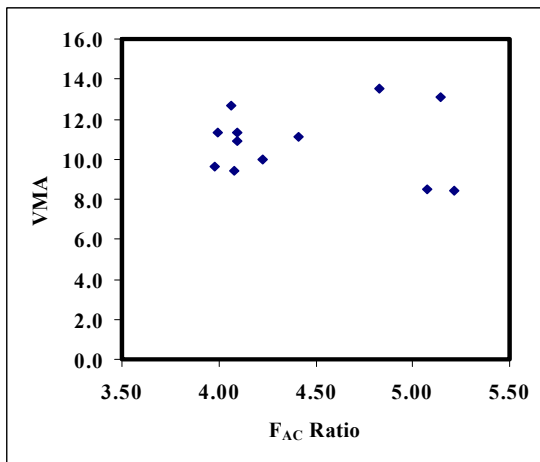
(b)



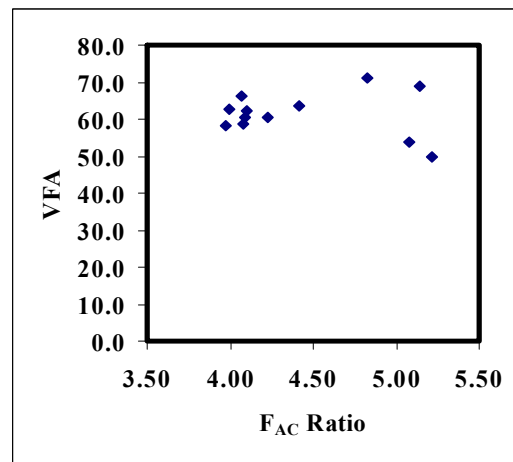
(c)

Figure 30

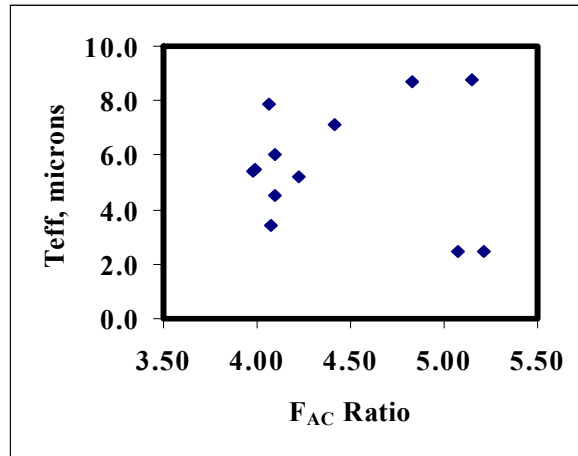
Bailey coarse gradation parameter; CA ratio and mixture physical properties: (a) CA ratio vs. VMA (b) CA ratio vs. VFA (c) CA ratio vs. effective film thickness



(a)



(b)



(c)

Figure 31

Bailey fine gradation parameter; F_{AC} ratio and mixture physical properties: (a) F_{AC} ratio vs. VMA; (b) F_{AC} ratio vs. VFA; (c) F_{AC} ratio vs. effective film thickness

The same analysis was conducted on the four parameters (i.e., aCA, nCA, aFA, and nFA) obtained from the power law method of aggregate evaluation, which is presented in Figures 32 through Figure 36. Among the mix properties considered, effective film thickness seems to be more sensitive to the gradation parameters from this method. Three of the four parameters (aCA, nCA, and aFA) had the strongest influence on effective film thickness with R² of 0.69, 0.63, and 0.70, respectively. The slope of the fine portion of the gradation curve nFA had the least influence on effective film thickness. In general, as the gradation became finer, effective film thickness tended to decrease. This is due to the fact that finer materials have higher surface area that allows them to absorb more asphalt and consequently reduce the amount of asphalt available to coat the aggregate particles. A trend was also observed in the relationship of the power-law gradation parameters with VMA and VFA. The slope of the coarse portion of the gradation curve nCA had a stronger relationship with both volumetric parameters VMA and VFA than the rest of the gradation parameters from this method. Again, the finer the gradation was, the lower the VMA and VFA became.

In summary, the analysis of the gradation parameters from both the Bailey Method and the power-law method clearly demonstrates the sensitivity of asphalt mixtures volumetrics to these parameters.

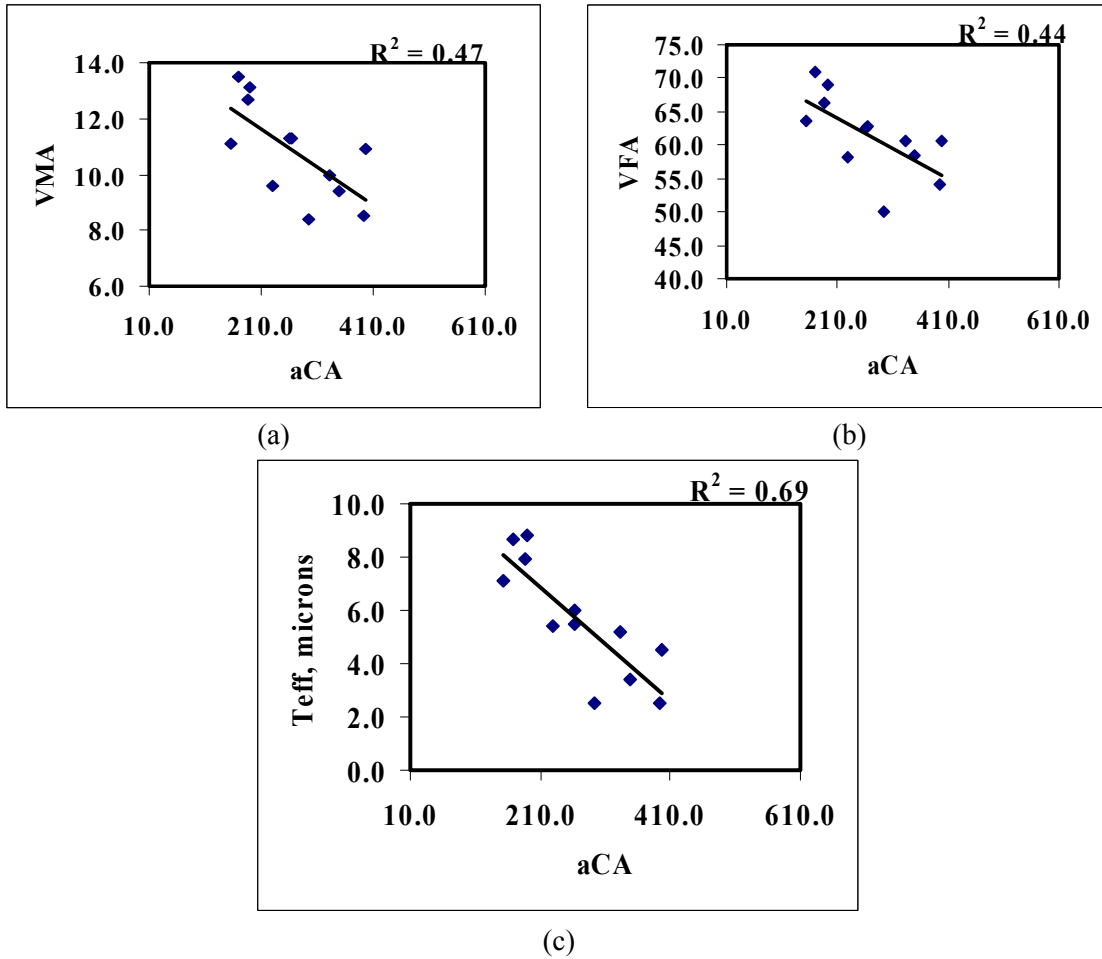
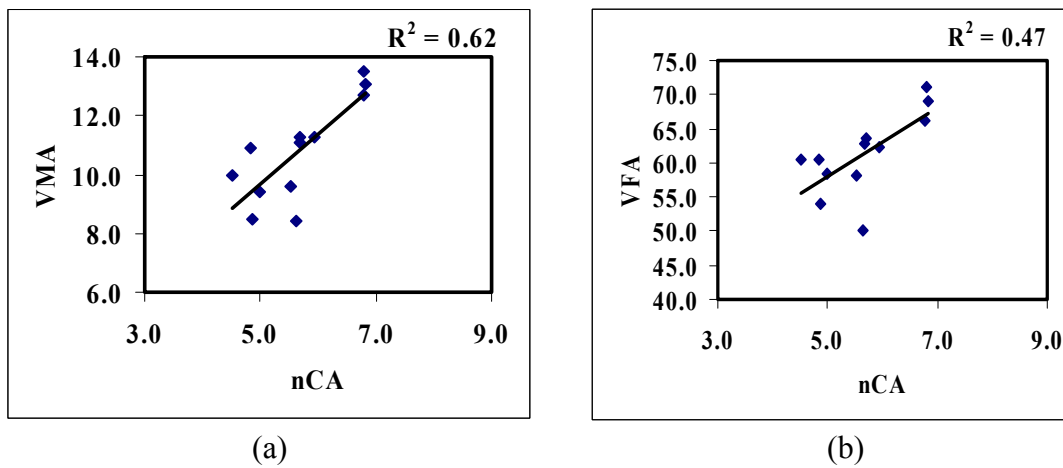
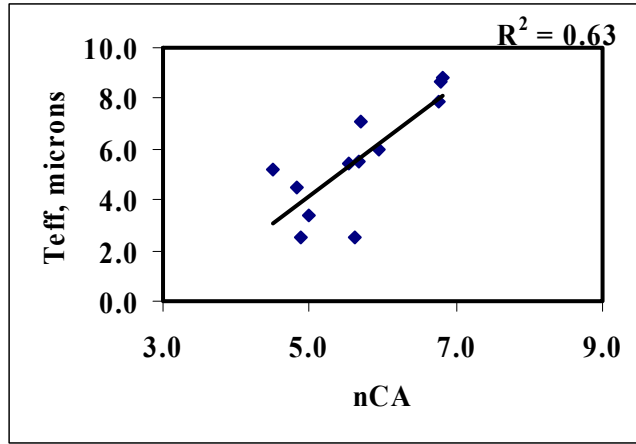


Figure 32
Power-law coarse gradation parameter aCA and mixture physical properties

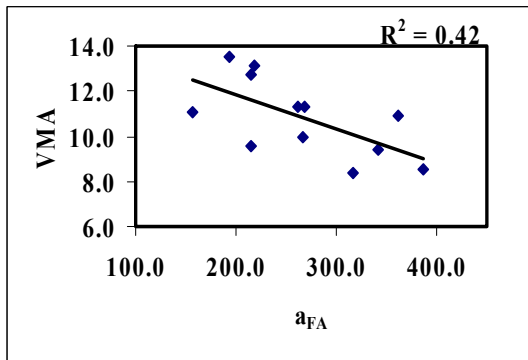




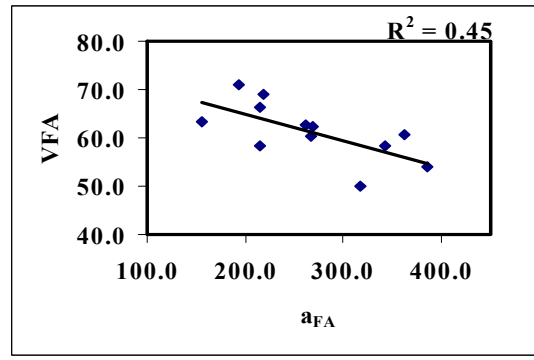
(c)

Figure 33

Power-law coarse gradation parameter nCA and mixture physical properties



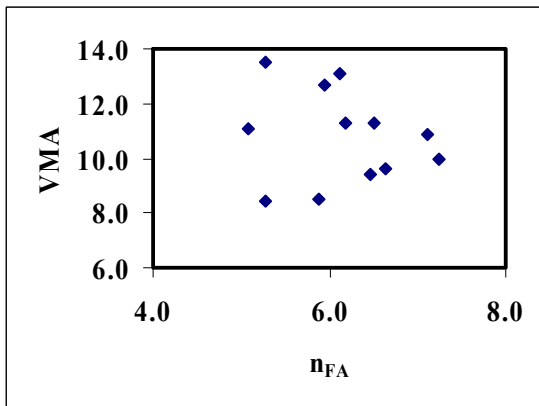
(a)



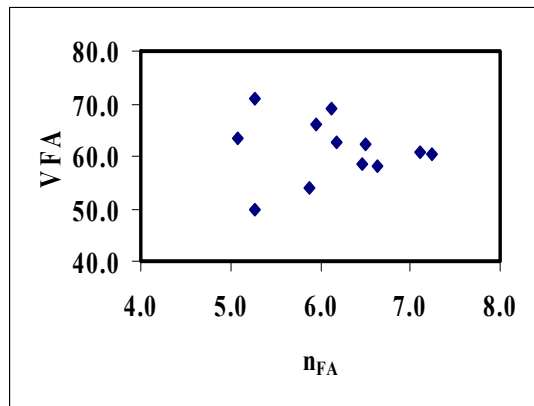
(b)

Figure 34

Power-law fine gradation parameter aFA and mixture volumetrics



(a)



(b)

Figure 35

Power-law fine gradation parameter nFA and mixture volumetrics

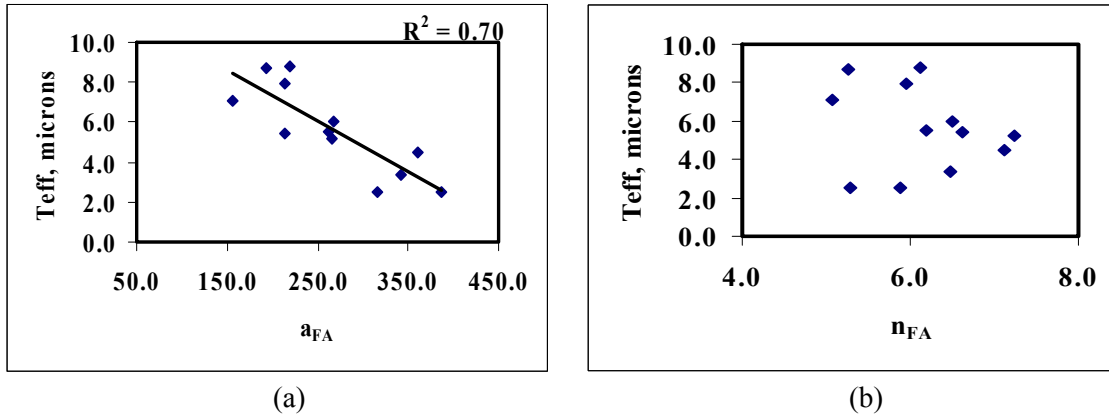


Figure 36
Power-law fine gradation parameters and effective film thickness

Gradation Parameters and Mixture Compactability

As was established earlier, compaction characteristics were varied for mixtures with different aggregate gradations. In order to quantify the effect of aggregate gradation on the compactability of the mixtures, the gradation parameters from the Bailey and the power law methods were utilized. Figures 37 to 39 present the relationship between mixture compactability, as represented by the SGC compaction densification index CDI, and those parameters from the gradation analysis. CDI did respond to change in the gradation parameters from the both methods, indicating that the compactability of the mixtures is a function (among other factors) of the particle size distribution as measured by those parameters. The CA ratio, n_{CA} , and n_{FA} had a better correlation with the CDI, when compared with other parameters.

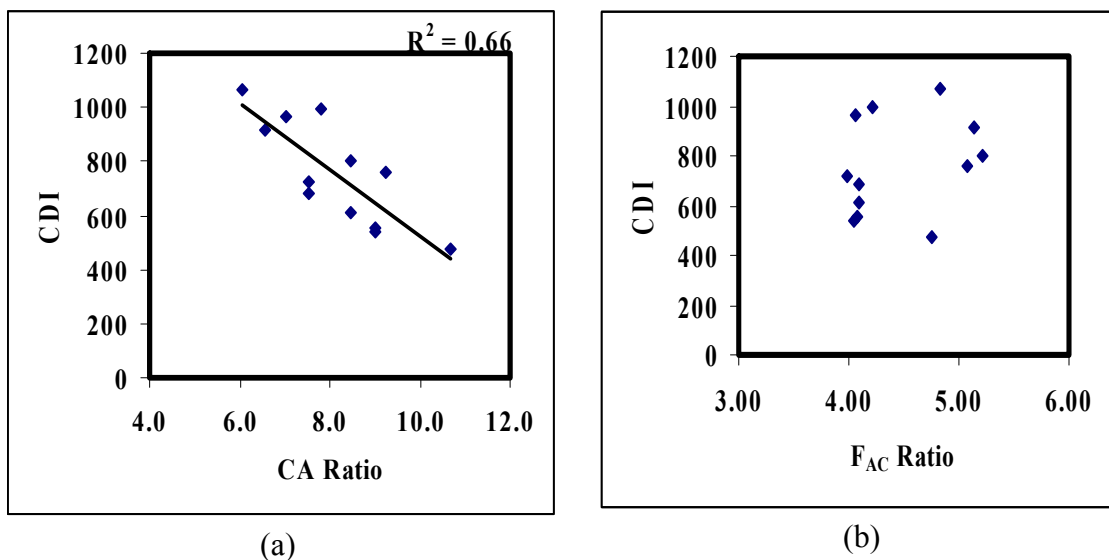


Figure 37
Relationship of the Bailey gradation parameters with mixture compactability

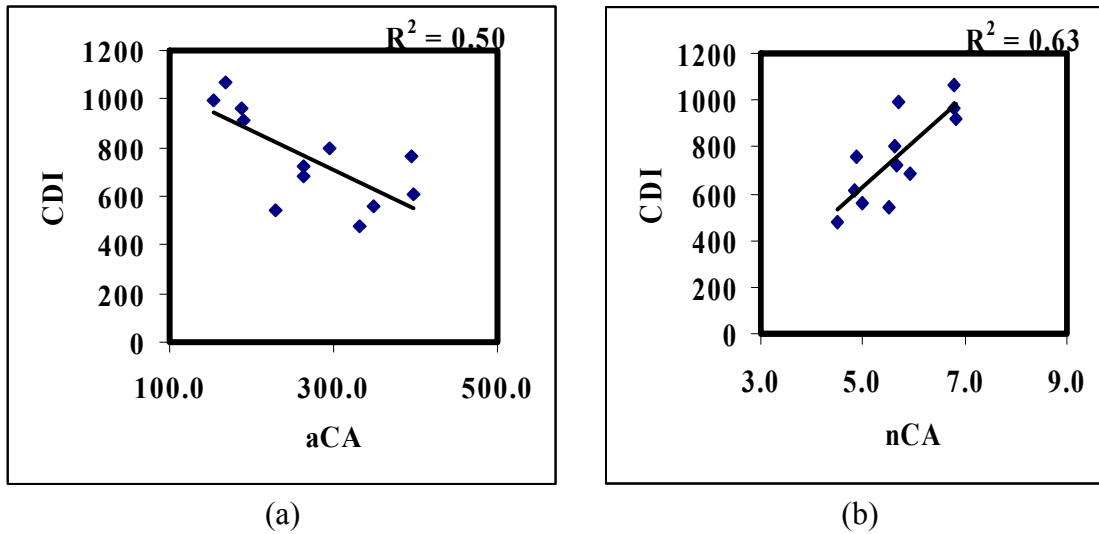


Figure 38
Relationship of power-law coarse gradation parameters and mixture compactability

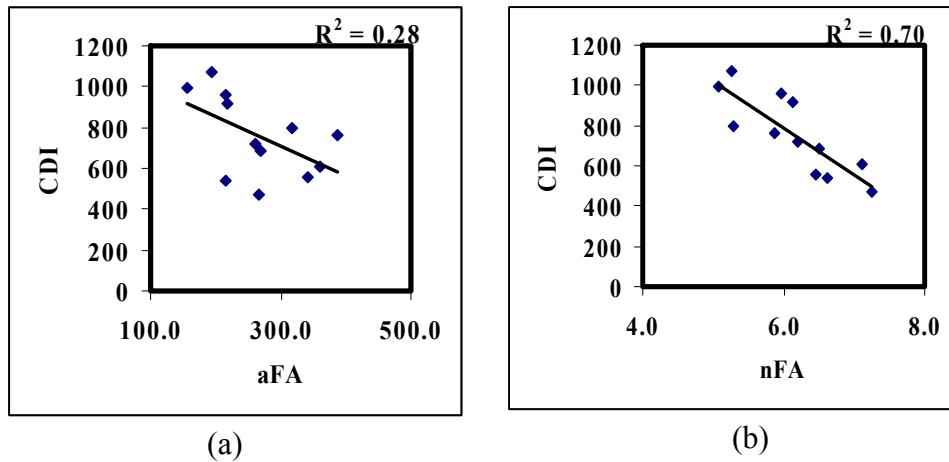


Figure 39
Relationship of power-law fine gradation parameters and mixture compactability

Mixture Performance

This section analyzes the performance of the asphalt mixtures as evaluated by the laboratory simulative and mechanistic tests.

Hamburg Loaded Wheel Tracking Test

The designed mixtures were evaluated for their performance under severe load and environmental conditions using the Hamburg Loaded Wheel Tracking test (LWT). This is a torture test to determine mixture resistance to rutting and moisture damage. The LWT

device measured the combined effects of rutting and moisture damage by rolling a steel wheel across the surface of an asphalt concrete slab, 260.8 mm wide by 320.3 mm long and 40.0 mm thick that was immersed in hot water at a temperature of 50°C. As shown in Figure 40, the examination of the rut profile from the LWT test indicated that rutting at the ends of the specimen should be taken with caution since the end effect of the rigid mold might prevent the lateral flow of the mix under loading. Therefore, it was decided to only use the middle portion of the profile in the determination of the rut depth. The average of the middle six point measurements was ultimately used. Figure 41 presents the mean rut depths for all the mixtures tested in Phase 1. All the mixtures had excellent performance with a maximum rut depth of 4.4 mm after 20,000 passes for the one in. limestone coarse mixture. No signs of stripping were found at the end of the test period for the mixtures evaluated. The lowest rut depth measured was the sandstone medium mixture with only 1.5 mm rut depth after 20,000 passes.

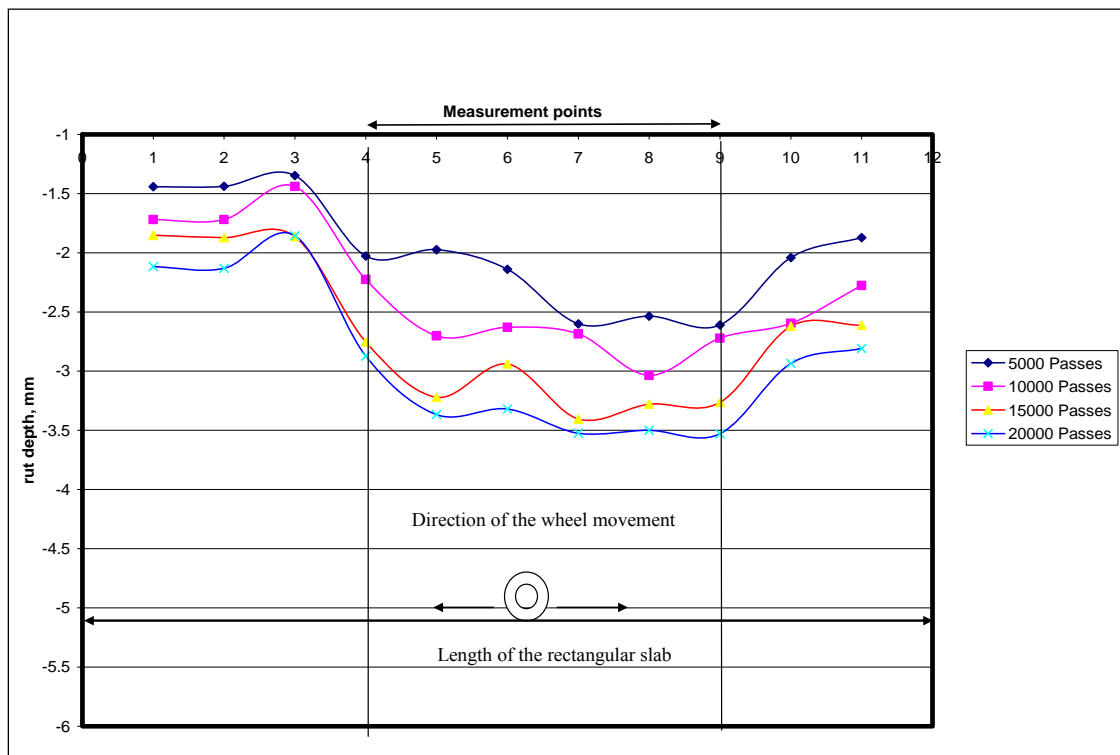


Figure 40
Rut profile from the LWT test

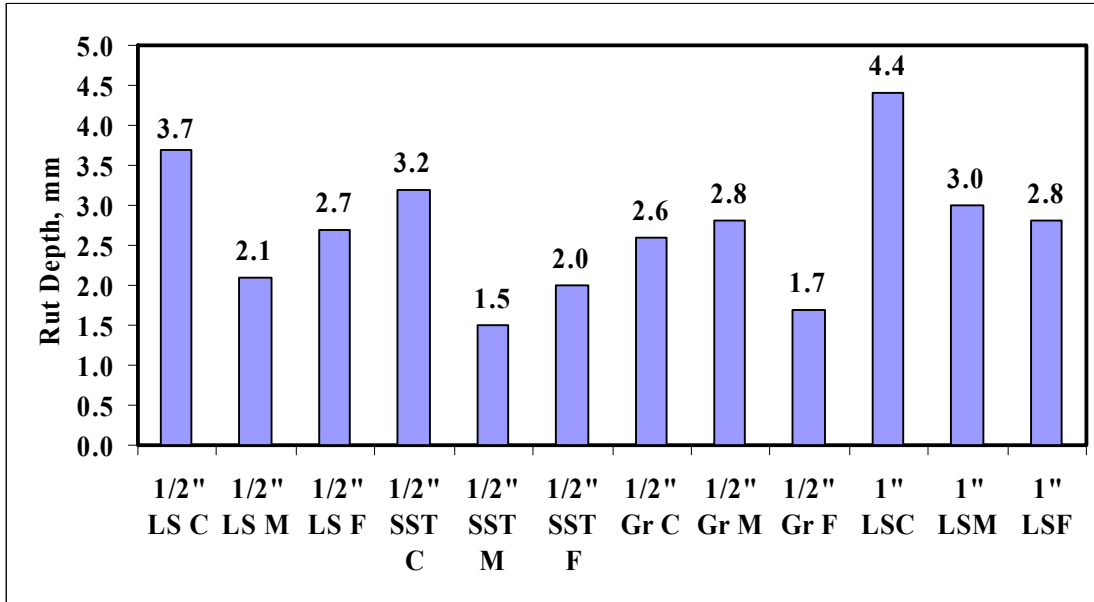


Figure 41
Rut depth at 20,000 passes of the LWT test

An analysis of variance (ANOVA) was conducted using Statistical Analysis Software (SAS) to detect the effects of gradation and type of aggregates on the Hamburg rut depths. The ANOVA analyses were performed using “MIXED” procedure available in SAS. The linear model used in these analyses was a completely randomized factorial design (Gradation × Type), as shown in equation (10). The dependent variable used in the analyses was the rut depth in mm.

$$Y_{ijk} = \mu + \tau_{i_i} + \tau_{2_j} + \tau_{1_1}\tau_{2_{ij}} + \epsilon_{ijk} \quad (10)$$

where,

μ = overall mean,

τ_{i_i} = effect of aggregate gradation,

τ_{2_j} = effect of aggregate type,

$\tau_{1_1}\tau_{2_{ij}}$ = effect of the interaction between the gradation and type,

ϵ_{ijk} = random sampling variation for observation k , at any level of gradation and type ij ,
and

Y_{ijk} = dependent variable (rut depth [mm] in this study).

Table 12 shows a summary of this analysis. The results of the ANOVA analyses showed that, at a 95% confidence level, the aggregate gradation and type had significant effect on the measured LWT rut depth. In addition, the results showed that aggregate gradation (τ_{i_i}

) had more significant effect on rut depth than aggregate type (τ_{2j}) did, as indicated by the higher F-value. The interaction effect of the aggregate gradation and type ($\tau_1\tau_{2ij}$) had no significant effect on the measured rut depth.

Table 12
Summary of the statistical analysis on LWT data

Type 3 Tests of Fixed Effects					
Effect	Num DF	Den DF	F Value	Pr > F	Significant?
GRADATION (τ_{ij})	2	15	8.89	0.0028	YES
TYPE (τ_{2j})	2	15	6.71	0.0083	YES
GRADATION*TYPE ($\tau_1\tau_{2ij}$)	4	15	2.61	0.0775	NO

Based on the result of the ANOVA analyses, post ANOVA Least Square Means (LSM) analyses were also conducted to compare the effect of all the different gradation and aggregate types used. Tukey adjustment was used in this analysis. Saxton’s macro was implemented to convert the results in the MIXED procedure to letter groupings [5]. The results of this grouping are presented in Tables 13 and 14. In these tables, the groups are listed in ascending order from the worst to the best. Groups with same letter are not significantly different. Medium and fine gradations showed similar performance (same letter group). Among the three aggregate types used, limestone showed the least rut resistance under the loading and environmental conditions of the LWT test, even if all the mixtures evaluated had acceptable LWT rut depth.

Table 13
Effect = GRA Method = Tukey-Kramer (P < .05)

Obs	GRADATION	Estimate	Standard Error	Letter Group
1	Coarse	3.27	0.20	A
2	Medium	2.25	0.20	B
3	Fine	2.19	0.20	B

Table 14
Effect = TYPE Method = Tukey-Kramer(P < .05)

Obs	TYPE	Estimate	Standard Error	Letter Group
4	Limestone	3.11	0.16	A
5	Granite	2.38	0.22	B
6	Sandstone	2.22	0.22	B

The effect of aggregate gradation on LWT results was further investigated using the parameters obtained from the Bailey and the power law methods. Linear multiple regression analysis using SAS software was performed on the data to determine what a gradation parameter was contributing to the significance effect of gradation. Table 15 summarizes the results of the regression analysis. Two parameters, which were aCA and aFA from the power law method of gradation analysis, showed significant correlation with LWT rut depth at 95% confidence level. As the mixes become finer, the resistance to permanent deformation improves (see Figure 42). In summary, the results show that the performance of the mixtures in the LWT test was sensitive to some of the gradation parameters used to analyze the aggregate gradation in this study.

Table 15
Statistical analysis of gradation parameters and LWT test data

Method		Pr>F	Correlation, $\alpha = 0.05$
Bailey Method	CA ratio	0.2699	Not significant
	F _{AC} ratio	0.7362	Not significant
Power-Law Method	aCA	0.0064	Significant
	nCA	0.1984	Not significant
	aFA	0.0014	Significant
	nFA	0.2824	Not significant

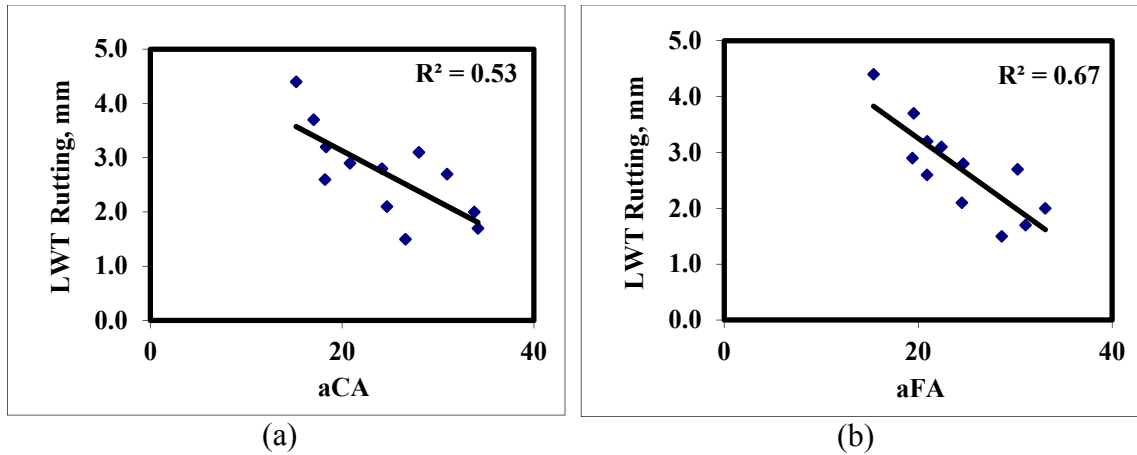


Figure 42
Gradation analysis on LWT test results (a) aCA vs. LWT (b) aFA vs. LWT

The results from the LWT test were also analyzed using the energy indices obtained from the SGC and the PDA. It was expected that the higher the TDI and TFI were, the lower rut depths obtained from the LWT test, if those indices truly provided indication of mixture stability. The data, however, showed no correlation between the two indices (i.e., TDI and TFI) and LWT rut depth, as shown in Figure 43. The inability of those indices for predicting the performance could be attributed to the fact that the mixture was contained within the rigid walls of the compaction mold, and consequently the equally rigid top and bottom platens prevented any type of lateral flow that constitutes the basic mechanism of permanent deformation in asphalt mixtures. Furthermore, mixtures evaluation for permanent deformation resistance was usually carried out at high pavement service temperature (54°C), which was much lower than the compaction temperature at which those indices were determined. This might have contributed to the absence of any relationship between the compaction indices and the LWT data. The effect of VMA, one of important HMA volumetric parameters on the rutting performance of asphalt mixtures measured by the LWT test was also investigated, as shown in Figure 44. A trend of increasing rut depth with higher VMA values was observed, while the correlation was not statistically considerable ($R^2 = 0.25$).

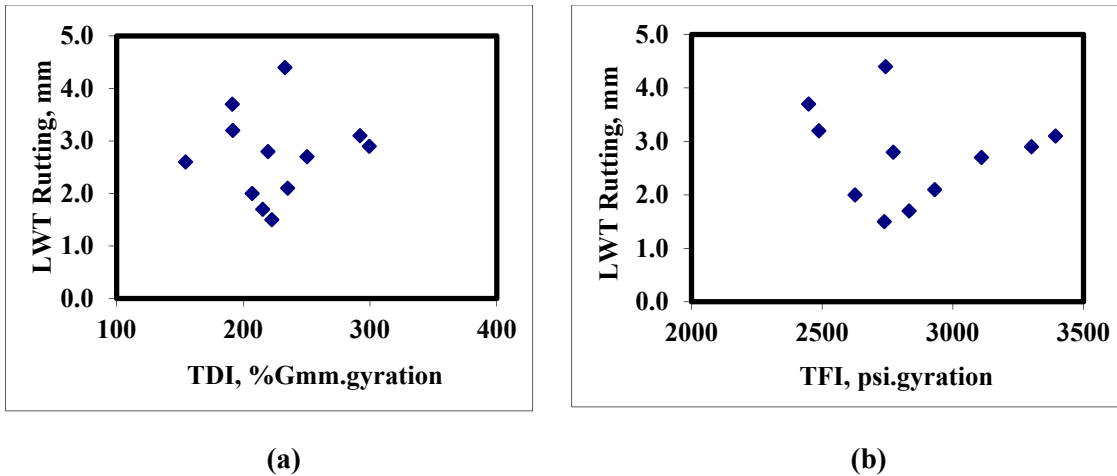


Figure 43
Relationship between the energy indices and LWT results (a) TDI vs. LWT rut depth. (b) TFI vs. LWT rut depth

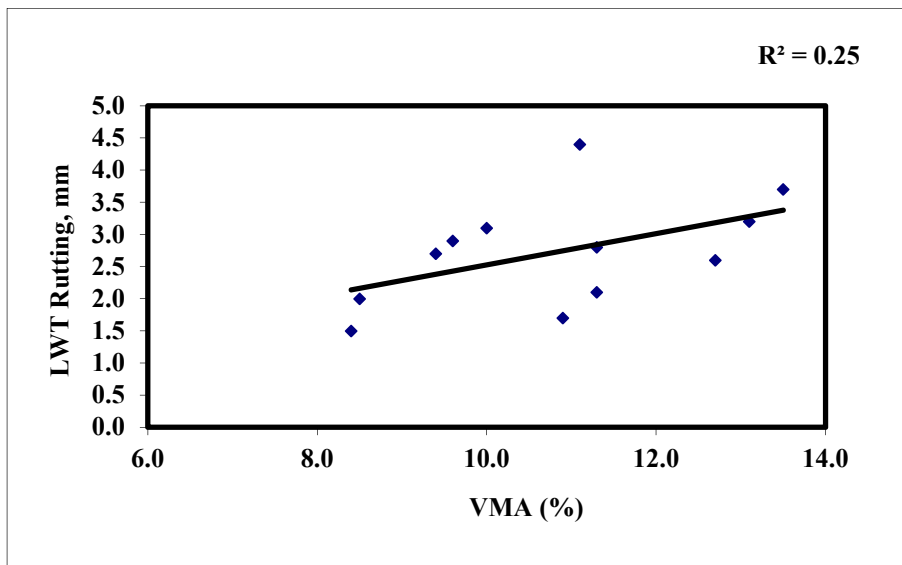


Figure 44
Effect of VMA on rutting from LWT test

Indirect Tensile Strength (ITS) Test

The Indirect Tensile Strength test is one of the most popular tests used for characterizing HMA mixtures and a fundamental test that describes mixture cohesion. The test was conducted at 25°C according to ASTM D6931. A cylindrical specimen was loaded to failure at deformation rate of 50 mm/min using a MTS machine. The indirect tensile strength and tensile strain at failure were used in the analysis. Three SGC specimens were tested for each mixture. The test was conducted on two sets of samples with two aging conditions: unaged and long-term oven aged. The long-term oven aging protocol

recommended by AASHTO PP2 was followed [17]. The specimens were placed in a force draft oven at 85°C for 5 days. Figure 45 presents the mean indirect tensile (IT) strength results of the unaged and aged mixtures. In this test, higher IT strength values at failure were desirable, indicating higher resistance to shear deformation. Figure 46 presents the corresponding strain values. The IT strength values ranged from 116.0 psi to 309.3 psi for the unaged mixes and from 146.4 psi to 357.1 psi for aged ones. The strain results ranged from 0.407% to 0.932% for the unaged mixes and from 0.293% to 0.770% for the aged ones. The IT strength and strain values obtained from this study were compared to typical values obtained for Louisiana Superpave mixtures that have shown good field performance [18]. For mixtures with PG76-22M, the reported IT strength values were in the range of 192.0 to 369.0 psi. The corresponding strain values ranged from 0.26 to 0.88%. The IT strain results from this study existed within that reported range, indicating that the designed mixtures in this study can offer good field performance despite the relatively lower mixture volumetrics than the recommended one. The medium sandstone mixture had the highest strength values of 309.3 and 357.1 psi for unaged and aged, respectively. The performance of limestone and sandstone fine mixtures was similar. The lowest strength values were obtained for coarse mixtures for all of the three types of aggregates. The values, however, were still high and fell within the established range for asphalt mixtures with good performance.

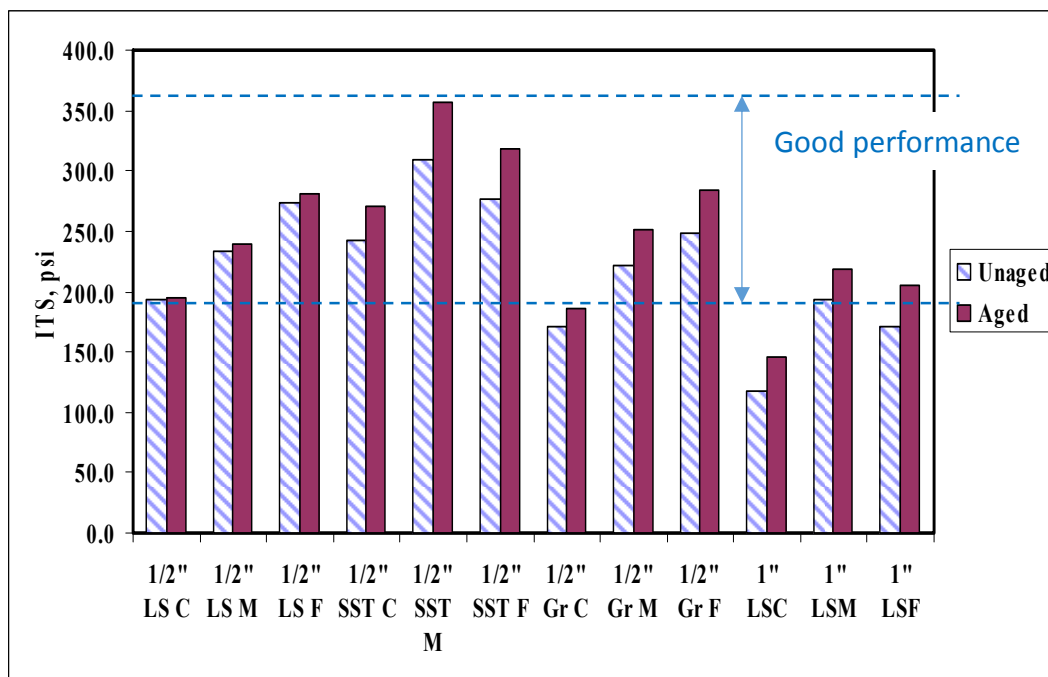


Figure 45
Indirect tensile strength results

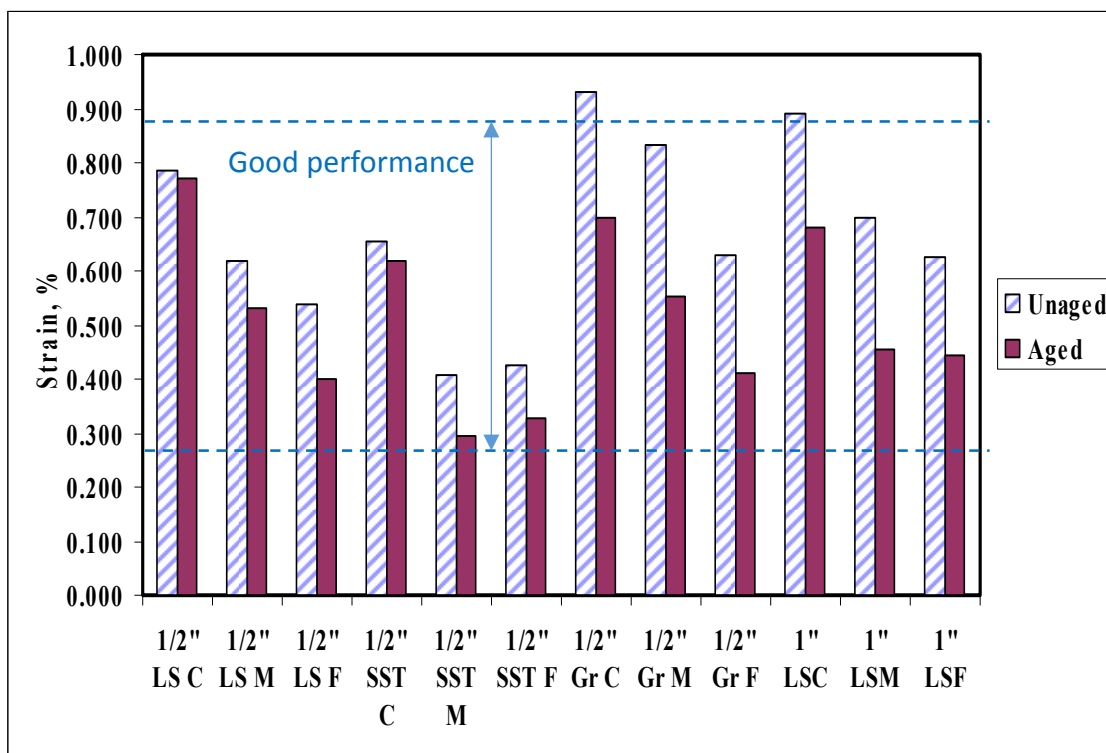


Figure 46
Indirect tensile strain results

Statistical analysis similar to that conducted on the LWT data was carried out on the IT strength and strain data, in order to determine if the test parameters used in the analysis are sensitive to gradation and type of aggregates, and the combination of these two factors. Table 16 summarizes the results of this analysis on the IT strength data. The fixed effect of gradation and type of aggregates was found to be significant at 95% confidence level. The interaction effect, however, did not seem to influence the results of the ITS test. The results of grouping the data based on gradation and type are presented in Tables 17 and 18, where the groups are listed in descending order from the best to the worst. Groups with same letter are not significantly different. Medium and fine gradations showed similar performance in terms of IT strength (i.e., same letter group). Although, among the three aggregate types, limestone had the lowest strength values, there was no significant difference between the limestone and granite aggregates, as shown in Table 18.

Table 16
Summary of the statistical analysis on IT strength data

Type 3 Tests of Fixed Effects				
Effect	Num DF	Den DF	F Value	Pr > F
Gradation	2	27	11.83	0.0002
Type	2	27	17.91	<.0001
Gradation*Type	4	27	0.82	0.5259

Table 17
Effect = GRADATION Method = Tukey-Kramer (P < .05)

Obs	Gradation	Estimate	Standard Error	Letter Group
1	Fine	249.80	9.9026	A
2	Medium	247.28	9.9026	A
3	Coarse	189.58	9.9026	B

Table 18
Effect = TYPE Method = Tukey-Kramer(P < .05)

Obs	Type	Estimate	Standard Error	Letter Group
4	SS	276.23	10.8477	A
5	GR	212.86	10.8477	B
6	LS	197.57	7.6705	B

SS: sandstone; GR: granite; LS: limestone

Similarly, the IT strain data showed that gradation and type had significant fixed effect on the strain values, but the interaction effect was not affecting the results significantly, as summarized in Tables 19 through 21. Coarse gradations had the highest strain values among the different gradations used. Sandstone mixtures were least favorable in terms of IT strain due to their lowest value among the three aggregate types. In the ITS test, high strength values are desired for better cohesion characteristics while high strain values are desirable for better cracking resistance.

Table 19
Summary of the statistical analysis on IT strain data

Type 3 Tests of Fixed Effects- Strain				
Effect	Num DF	Den DF	F Value	Pr > F
Gradation	2	27	29.05	<.0001
Type	2	27	19.29	<.0001
Gradation*Type	4	27	0.70	0.5968

Table 20
Effect = GRA Method = Tukey-Kramer (P < .05)

Obs	Gradation	Estimate	Standard Error	Letter Group
1	Coarse	0.8085	0.02715	A
2	Medium	0.5658	0.02715	B
3	Fine	0.5456	0.02715	B

Table 21
Effect = TYPE Method = Tukey-Kramer (P < .05)

Obs	Type	Estimate	Standard Error	Letter Group
4	GR	0.7311	0.02974	A
5	LS	0.6932	0.02103	A
6	SS	0.4956	0.02974	B

GR: granite; LS: limestone; SS: sandstone

Figure 47 presents the aging index calculated by dividing the aged IT strain by the unaged one. This index represents the amount of change in the IT strain values due to aging. Coarse mixtures of all the aggregate types were less affected by aging than the fine and medium gradations. Table 22 summarizes all the mixtures and their corresponding aging indices with the effect of aging as statistically described by the p-value from the t-test. The null hypothesis was that the unaged IT strain was the same as the aged one. The p-value was calculated and compared with the critical value of 0.05 to reject or accept the null hypothesis. The p-value indicated the extent to which a computed test statistic was unusual in comparison with what would be expected under the null hypothesis. A p-value greater than 0.05 indicated that the aged and unaged strains were statistically the same.

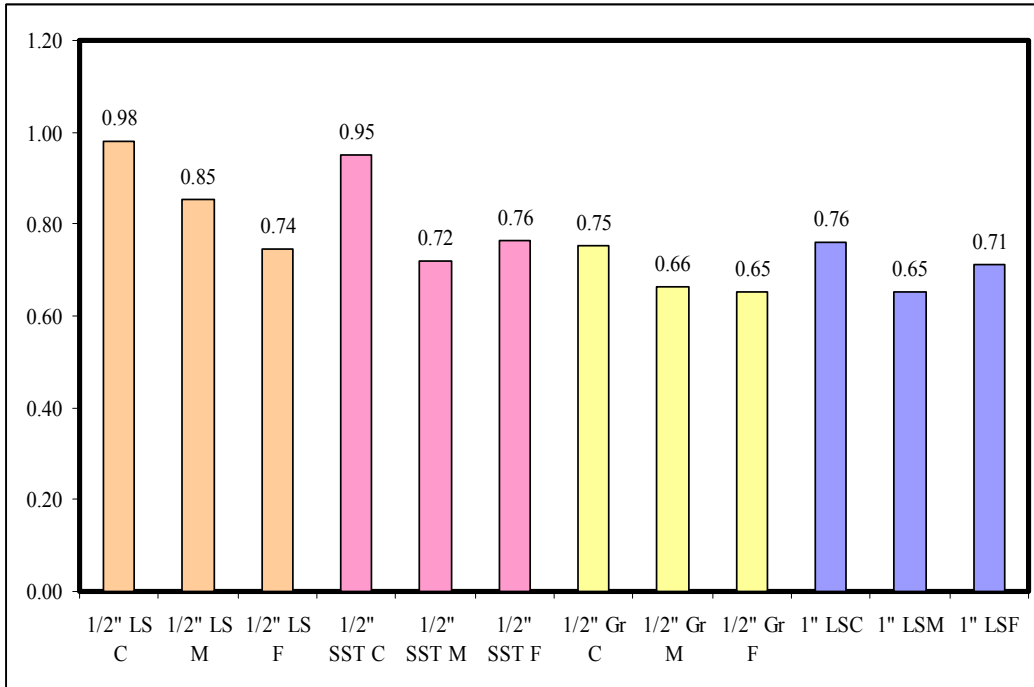


Figure 47
Aging index from the ITS test

Table 22
Statistical analyses on the effect of aging on IT strain

Mix Type	Mean Tensile Strain at Failure			p-value
	Unaged	Aged	Aging Index	
½ in. LSC	0.787	0.770	0.98	0.7582
½ in. LSM	0.620	0.530	0.85	0.0985
½ in. LSF	0.537	0.400	0.74	0.0765
½ in. SSC	0.653	0.620	0.95	0.6829
½ in. SSM	0.407	0.293	0.72	0.1695
½ in. SSF	0.427	0.326	0.76	0.0301
½ in. GRC	0.932	0.700	0.75	0.2747
½ in. GRM	0.843	0.553	0.66	0.0175
½ in. GRF	0.630	0.410	0.65	0.0057
1 in. LSC	0.891	0.679	0.76	0.0011
1 in. LSM	0.697	0.454	0.65	0.0065
1 in. LSF	0.625	0.445	0.71	0.0006

Among the mixture physical parameters considered, effective film thickness showed a strong correlation with the IT strain results for both aged and unaged mixtures (see Figure 48). A trend of increasing aging index with higher film thickness was observed in Figure 49, explaining why some mixtures were more affected by aging than others. Coarse

mixtures that were least affected by aging had the highest film thicknesses compared to the other mixtures did.

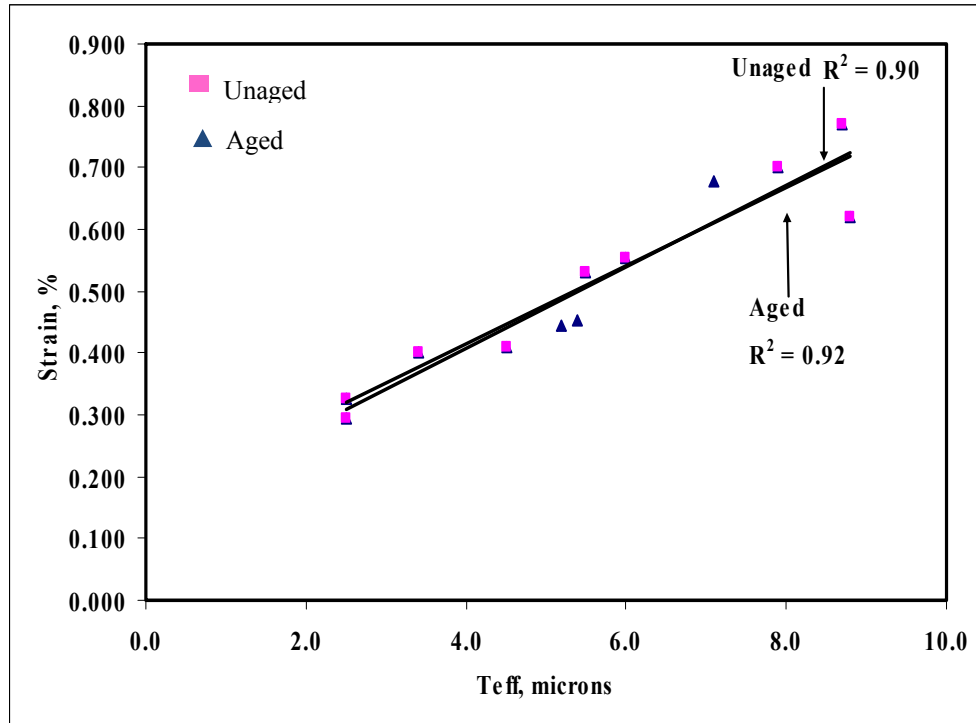


Figure 48
Relationship between effective film thickness and IT strain at failure

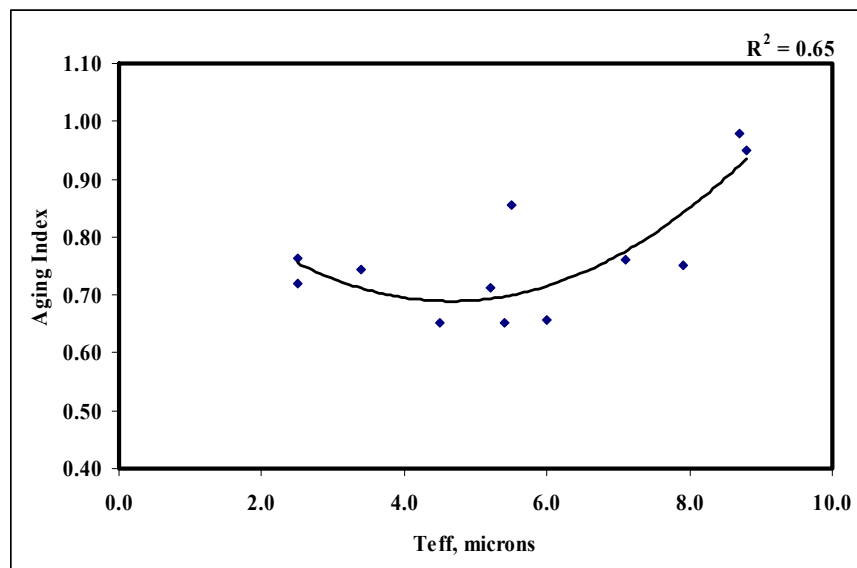


Figure 49
Film thickness and aging index using IT strain at failure

The influence of aggregate gradation on the tensile strength was explored using the different gradation parameters defined in this study. Only two gradation parameters such as aCA and aFA had significant correlation with the IT strength results, as shown in Table 23 and Figure 50. Similar to the trend observed with the LWT data, the finer the gradation was, the higher the IT strength of the mix was. The rest of the parameters did not show a significant correlation with the strength values.

Table 23
Statistical analysis of gradation parameters and IT strength

	Pr>F	Correlation, $\alpha = 0.05$
CA ratio	0.7955	Not significant
F _{AC} ratio	0.2130	Not significant
aCA	0.0270	Significant
nCA	0.4591	Not significant
aFA	0.0017	Significant
nFA	0.7955	Not significant

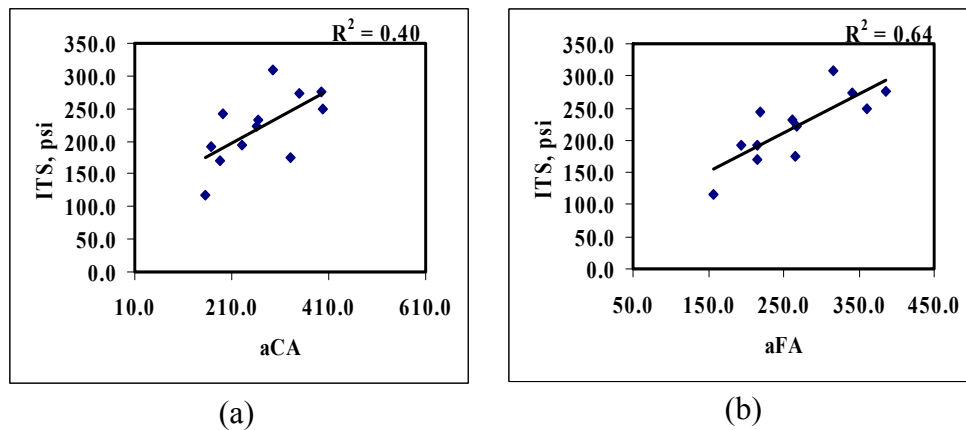


Figure 50
Gradation analysis on IT strength test results: (a) aCA vs. ITS (b) aFA vs. ITS

The IT strength results were also correlated with the compaction parameters obtained from the SGC and the PDA. As shown in Figures 51 and 52, there was no correlation between the compaction parameters and the IT strength values.

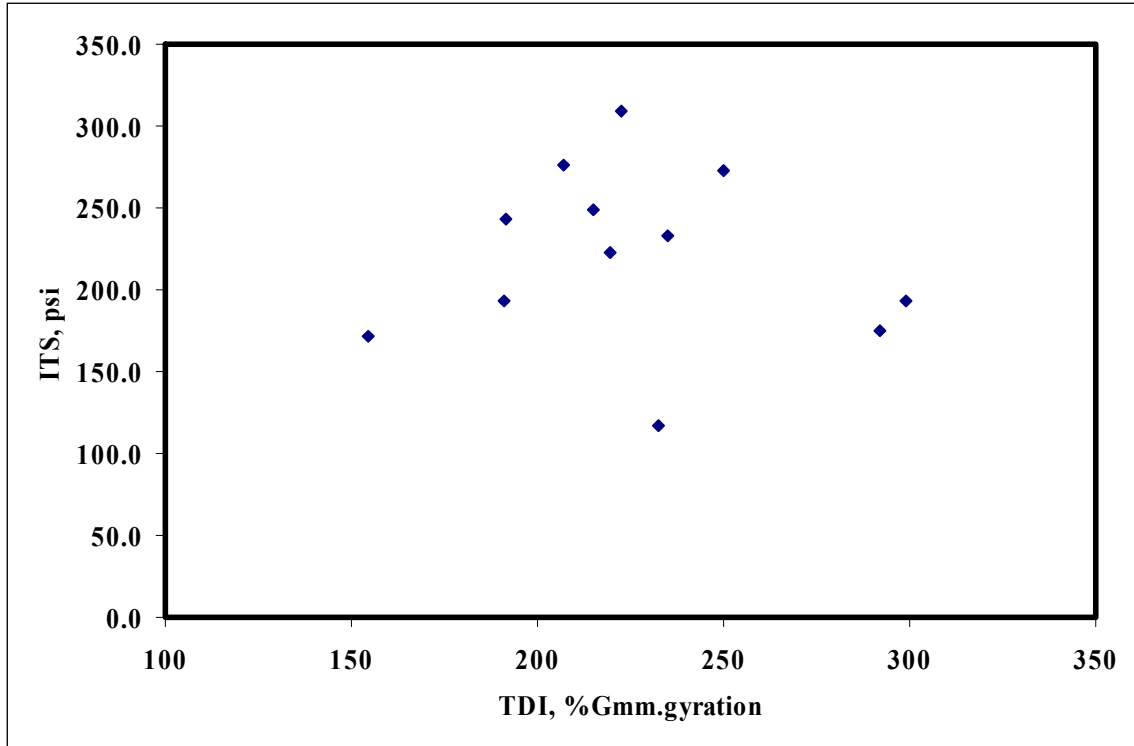


Figure 51
Traffic densification index (TDI) and IT strength

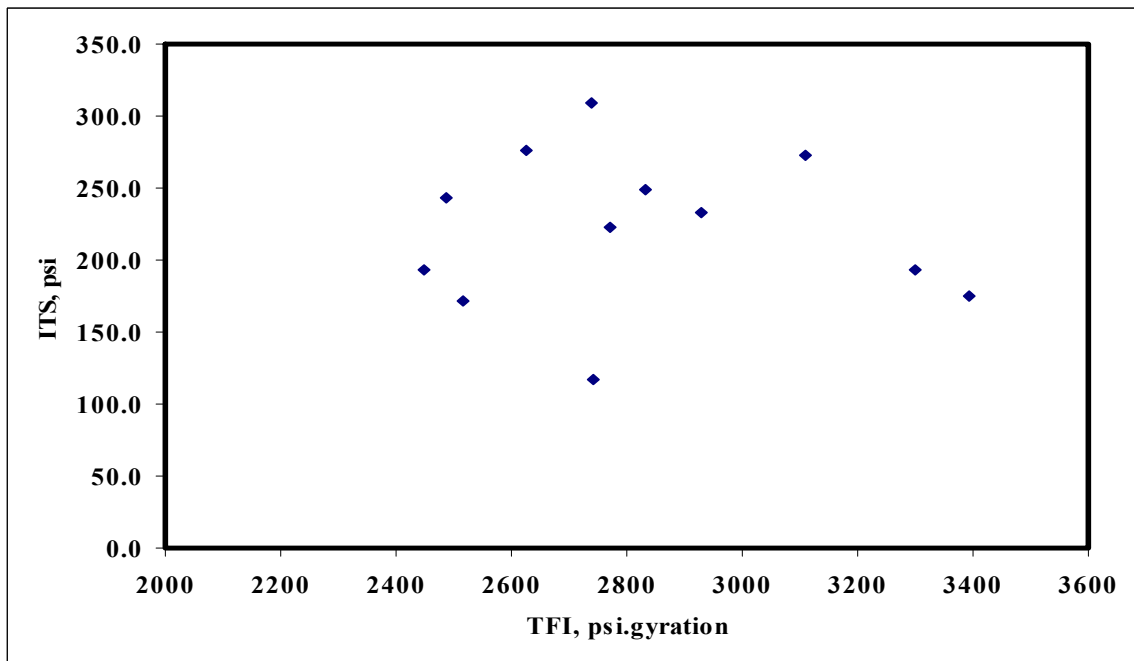


Figure 52
Traffic force index (TFI) and IT strength

Semi-Circular Bend Fracture Energy Test

The fracture resistance of the designed mixtures was investigated using the J-integral approach. The semi-circular bend (SCB) fracture test was conducted on two groups of specimens: unaged and oven aged. Figure 53 presents the calculated J_c from the semi-circular bend (SCB) fracture test for both groups. The J_c values ranged from 0.364 to 1.764 kJ/m² for the unaged mixes and from 0.599 to 1.761 kJ/m² for the aged ones. This J_c data range was on the same order of magnitude as those reported by Mohammad et al. for well-performing Superpave mixtures in Louisiana [18]. In that study, the field performance of 13 Superpave mixtures consisting of different gradations and binder types was investigated and found to be satisfactory. They reported a J_c range of 0.57 to 1.53 kJ/m². The three coarse mixtures with PG76-22M binder in that study had fracture resistance between 0.73 and 0.83 kJ/m² compared to 0.599 to 1.764 kJ/m² obtained for the coarse mixtures in this study with the same binder type. This clearly demonstrates that although those mixtures designed in this study did not meet the Superpave requirements in terms of volumetrics, they can still provide comparable cracking resistance to well-performing Superpave mixtures.

Data analysis showed that within each aggregate type, coarser mixtures had higher J_c compared to the medium and fine ones except for the 25.0-mm (1-in.) NMA limestone in which the coarse mix showed the lowest J_c value. The highest fracture resistance was obtained by the 12.5-mm (1/2-in.) NMA granite mixture.

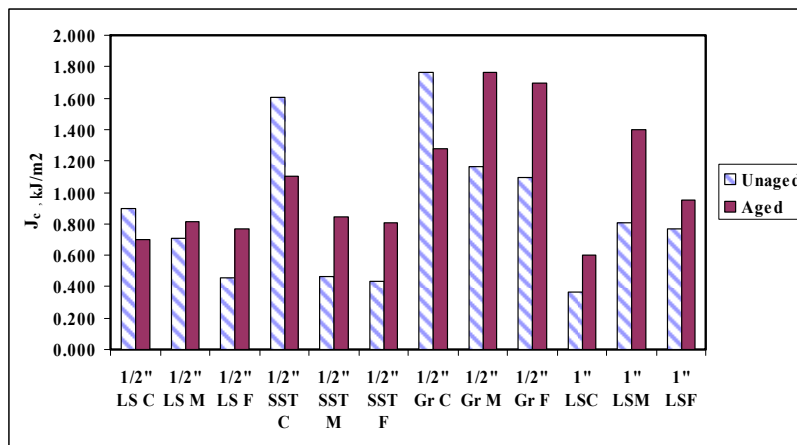


Figure 53
Fracture energy from the semi-circular fracture test

Figure 54 presents the effect of aging on the fracture resistance of the mixtures considered. It is seen that the aging of test specimens resulted in an increase in the fracture energy of the mixtures except for coarse mixtures. A good correlation was observed between the J_c aging index and the mixtures effective film thickness ($R^2 = 0.7$)

in which the effect of aging was reduced by having thicker binder film around the aggregates (see Figure 55).

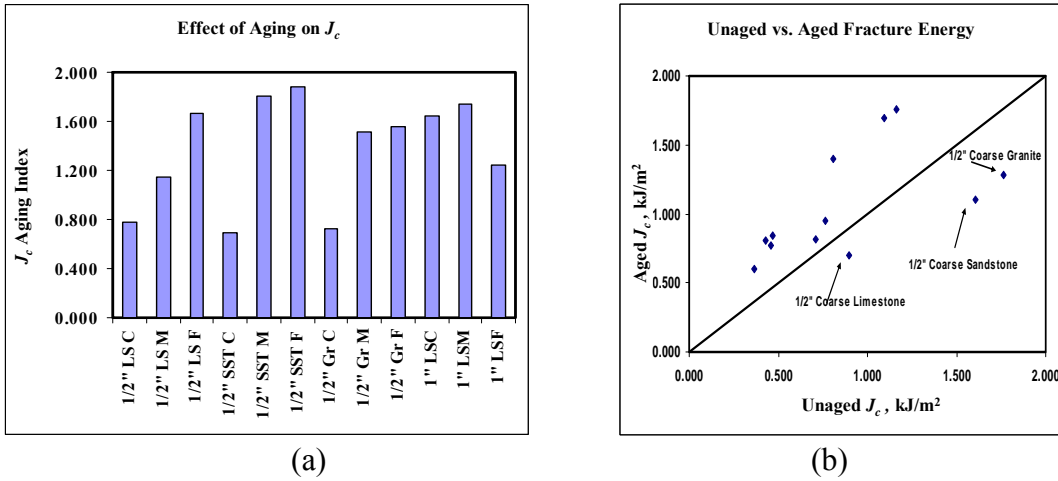
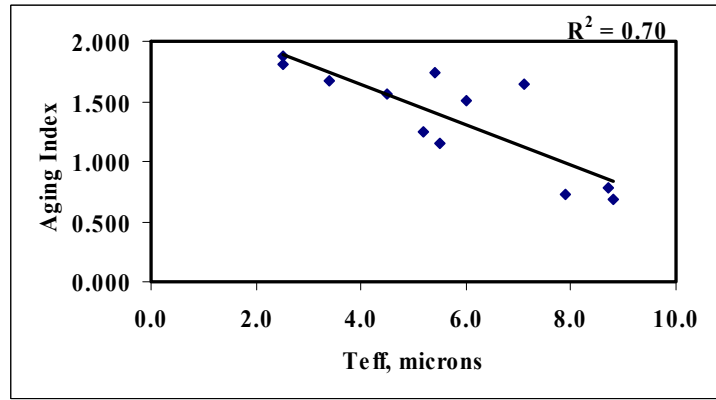


Figure 54
Effect of aging on J_c (a) aging index data and (b) Comparison of aged and unaged J_c



The relationship of the gradation parameters to fracture resistance is shown in Figures 56 and 57, presenting no significant correlation. However, the strength of this relationship was gained by statistical analysis. As shown in Table 24, two parameters showed a statistically significant correlation with J_c : the CA ratio from The Bailey Method and nCA from the power law method. It is noted that both describe the coarse portion of the gradation curve.

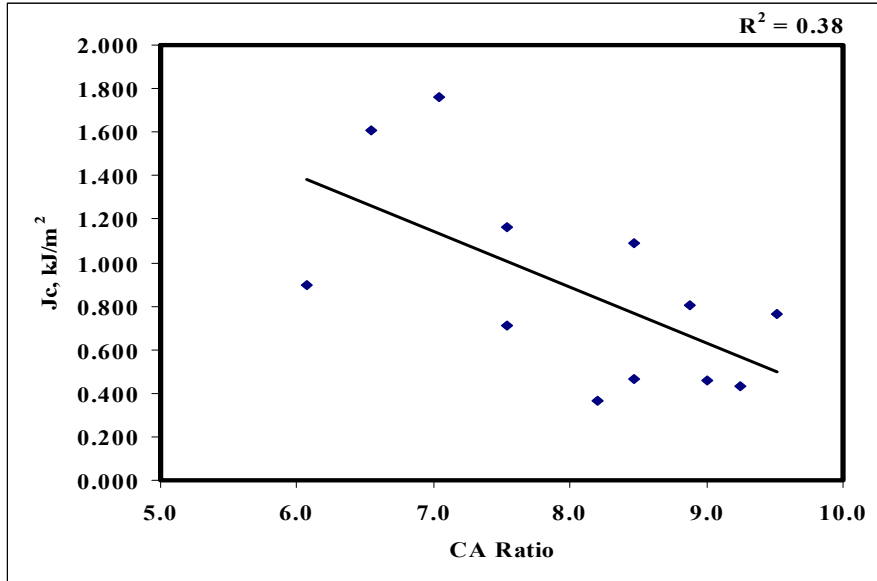


Figure 56
Effect of the gradation parameter CA ratio on J_c

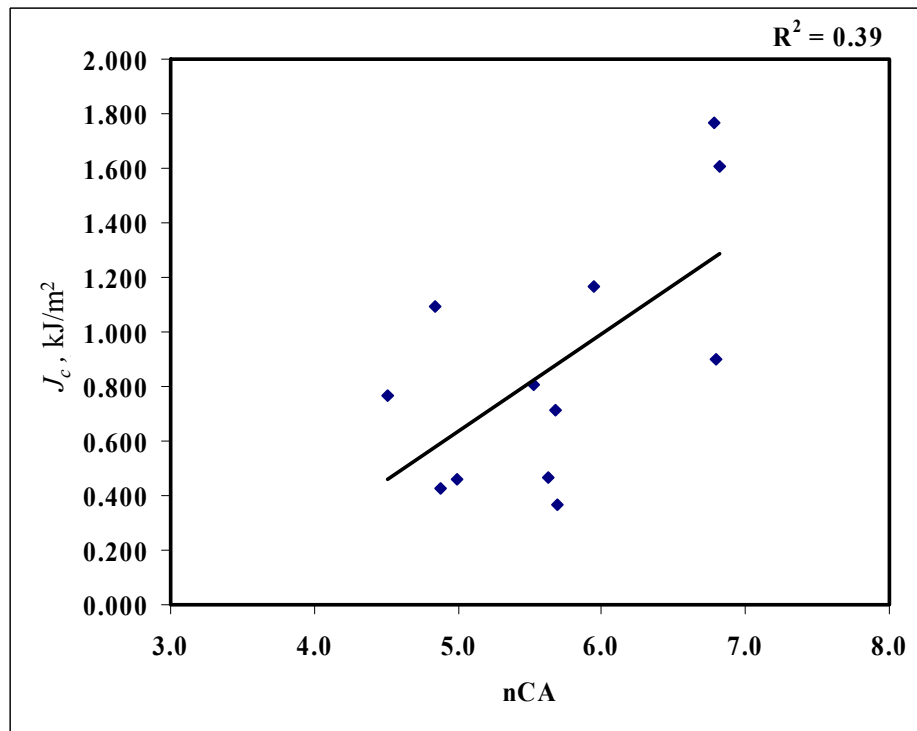


Figure 57
Effect of the gradation parameter nCA on J_c

Table 24
Statistical analysis of gradation parameters and J_c test data

	Pr>F	Correlation, $\alpha = 0.05$
CA ratio	0.0298	Significant
F _{AC} ratio	0.7546	Not significant
aCA	0.2657	Not significant
nCA	0.0286	Significant
aFA	0.3528	Not significant
nFA	0.4569	Not significant

PHASE 2: VERIFICATION OF PROPOSED MIXTURE DESIGN APPROACH

From the literature review presented in this document, it was evident that there were mainly two existing approaches for designing hot mix asphalt. The first approach was based on the concept of using adequate VMA, while the second one advocated the use of adequate asphalt film thickness. In both cases, the objective was to establish a systematic way of designing mixes through the specification of desirable levels of volumetric properties, and using specified compaction effort. It was also evident from the results in Phase 1 of this research that neither VMA nor the design number of gyrations was the same for various mixes with different aggregate types and structures. The response of different mixes to the applied compaction energy were different, which made the current approach of specifying the same design number of gyrations to all different mixes in the same traffic level questionable.

Based on the results obtained from Phase 1, a test plan was developed to determine if it is appropriate to improve mixtures durability by using a number of gyrations that was mix-specific and lower than that recommended by the current Superpave system. The premise was that using a lower number of gyrations would increase the design asphalt content and hence improve durability. The suggested approach was to utilize the concept of locking point in specifying the design number of gyrations. It was shown that the locking points of all the mixtures designed in this study were different and were lower than the currently specified single N_{des} for all the mixes in the traffic level considered. The devised plan involved the following tasks:

- Determine the design asphalt content for selected mixtures from Phase 1 using their locking points,
- Evaluate the rutting resistance of the mixtures designed in the previous step to ensure that stability is not compromised by using higher asphalt contents, and
- Run a suite of mechanistic tests on the mixtures with more emphasis on the durability aspect of mixture performance.

Mixture Selection for Phase 2

Phase 2 of this study required the selection of limited number of mixtures from Phase 1 for mixture design using the locking point concept as opposed to the traditional N_{des} in the Superpave approach. For the 25.0-mm (1-in.) NMA limestone mixture, three different aggregate structures were formulated. Because medium and fine mixtures

showed similar performance that was relatively better than the coarse mixture, the fine mixture was selected for Phase 2. For 12.5-mm (1/2-in.) NMAAS mixtures, a scoring system was developed to rationalize the selection process and assist in making an objective decision regarding what mixtures to be included in the second phase. The scoring system was based on some key mixtures properties that are related to mixture performance. The performance was quantified using the laboratory test parameters obtained from the first suite of testing on the mixtures in Phase 1. The mix attributes used in the scoring system are:

- Stability,
- Durability, and
- Compactability.

Table 25 lists the attributes used for this quantification process and their corresponding test parameters with their assigned numerical weights. A weighted score was calculated for each of the three mix attributes. The score was based on a seed value for each mix property considered. This seed value represents the maximum value obtained from that particular test parameter for the mixtures. For example, the maximum IT strength value obtained was 357.1 psi for the medium sandstone mixture. Therefore, the seed value for the IT strength parameter is 357.1 and therefore, IT strength score for the medium sandstone mixture is 1.0. On the other hand, the 12.5-mm (1/2-in.) NMAAS limestone mixture had a strength value of 195.1 psi which results in an IT score of 0.55 (195.1 divided by 357.1). The seed value for the LWT parameter, however, was taken as 6.0mm, which previous research showed that it was a critical value separating good performance mixtures from bad ones. The final rating assigned to the mix was based on the sum of the three individual scores as shown in Table 26 using the following equation:

$$\text{Total Score} = \text{ITS score} * w_1 + \text{Jc Score} * w_2 + (1 / \text{LWT score}) * w_3 + (1 / \text{CDI score}) * w_4$$

(11)

Table 25
Mixture attributes used in the selection procedure

Attribute	Laboratory Test Parameter	Weight
Stability	LWT Rutting	33.33
Durability	Aged Indirect Tensile Strength	16.67
	Aged Critical J-integral	16.67
Compactability	SGC Compaction Densification Index	33.33
Total		100.00

Table 26
Selection procedure for ½-in. mixtures

Mixture Type	Film Thickness	IT Strength	Score	J _c	Score	Durability Weighted Score	LWT	Score	Stability Weighted Score	CDI	Score	Compaction Weighted Score	Total Weighted Score
½" LS C	8.7	195.1	0.55	0.699	0.40	15.7	3.7	0.62	54.1	1067.8	1.00	33.33	103.1
½" LS M	5.5	238.7	0.67	0.817	0.46	18.9	2.1	0.35	95.2	721.9	0.68	49.30	163.4
½" LS F	3.4	281.7	0.79	0.768	0.44	20.4	2.7	0.45	74.1	556.6	0.52	63.95	158.4
½" SST C	8.8	270.3	0.76	1.106	0.63	23.1	3.2	0.53	62.5	916.1	0.86	38.85	124.4
½" SST M	2.5	357.1	1.00	0.842	0.48	24.6	1.5	0.25	133.3	800.2	0.75	44.48	202.4
½" SST F	2.5	317.7	0.89	0.807	0.46	22.5	2.0	0.33	100.0	762.0	0.71	46.71	169.2
½" GR C	7.9	185.3	0.52	1.279	0.73	20.8	2.6	0.43	76.9	963.3	0.90	36.95	134.6
½" Gr M	6.0	251.0	0.70	1.761	1.00	28.4	2.8	0.47	71.4	682.0	0.64	52.19	152.0
½" Gr F	4.5	284.7	0.80	1.699	0.96	29.4	1.7	0.28	117.6	609.3	0.57	58.42	205.4
Seed Value		357.1		1.761			6.0			1067.8			

The equation above was additive in nature and was formulated based on the desired mixture performance from each test. Higher ITS and J_c values were desired and therefore, those two parameters were multiplied directly by their weights. On the other hand, lower rutting from LWT was sought for adequate mixture stability and hence the inverse of rut depth from LWT was used to calculate the contribution of this parameter to the final score. Similarly, lower CDI indicated better compactability, which yielded the use of the inverse of this parameter in the calculation of the compactability contribution to the final score. Table 27 summarizes the ranking of the mixtures based on this scoring system. The three mixtures were selected as follows:

- Fine granite – The highest ranking mixture (ranked #1),
- Fine limestone – Medium ranking mixture (ranked #5), and
- Coarse limestone – The lowest ranking mixture (ranked # 9).

It was also decided to include a medium sandstone mixture that had a very high Dust/ P_{beff} ratio with the consideration of a durability problem.

Table 27
Overall ranking of the mixtures

Mixture	Total Score	Ranking
½" Gr F	205.4	1
½" SST M	202.4	2
½" SST F	169.2	3
½" LS M	163.4	4
½" LS F	158.4	5
½" Gr M	152.0	6
½" GR C	134.6	7
½" SST C	124.4	8
½" LS C	103.1	9
Maximum Possible Score*	226.7	

* This score can be obtained when the mixtures have the best score for all the attributes

Analysis of Results and Discussion

The physical properties and performance test results of the mixtures selected in Phase 2 and the ones designed using the Superpave recommended design number of gyrations in Phase 1 were compared.

Mixtures Physical Properties

Graphical comparisons of the mixtures physical properties of both sets of mixtures from Phases 1 and 2 are presented in Figures 58 to 62. As anticipated, compacting mixtures to their locking point yielded higher design asphalt contents than those obtained by Superpave design number of gyrations did. The design asphalt content for Phase 2 mixtures ranged from 3.9% to 5.4% compared to 3.3% to 5.1% for the same mixtures designed in Phase 1. It is worth noting that except for 12.5-mm (1/2-in.) NMA coarse limestone mixture, there was about 0.6% increase in asphalt content for all other mixtures when the mixtures were designed using their locking points at the same level of 4.0% air void.

The voids in mineral aggregates (VMA) values were about 0.2% to 1.2% higher for the mixtures designed in Phase 2. Again, this finding clearly indicates that VMA was compaction dependent and specifying it based on NMA only as currently adopted by the Superpave design system is questionable. Higher asphalt contents naturally resulted in higher VFA and lower D_{50}/P_{eff} ratio, and hence higher effective film thickness for the Phase 2 mixtures, as shown in Figures 60 to 62.

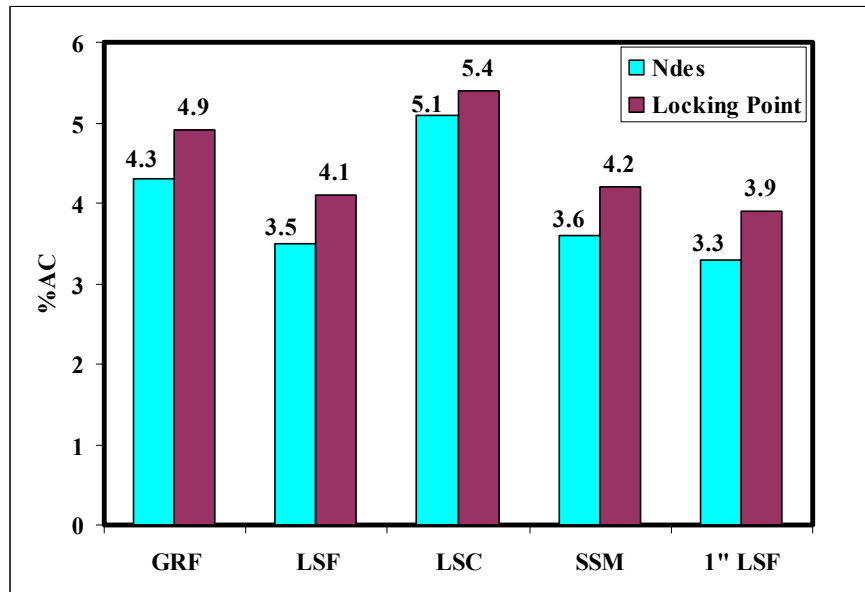


Figure 58
Design asphalt content

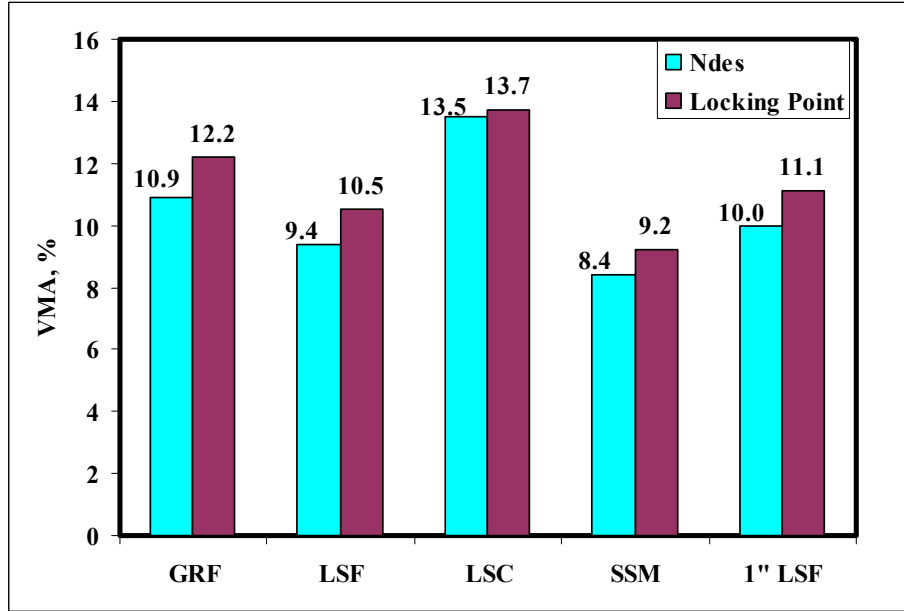


Figure 59
Voids in the mineral aggregate data

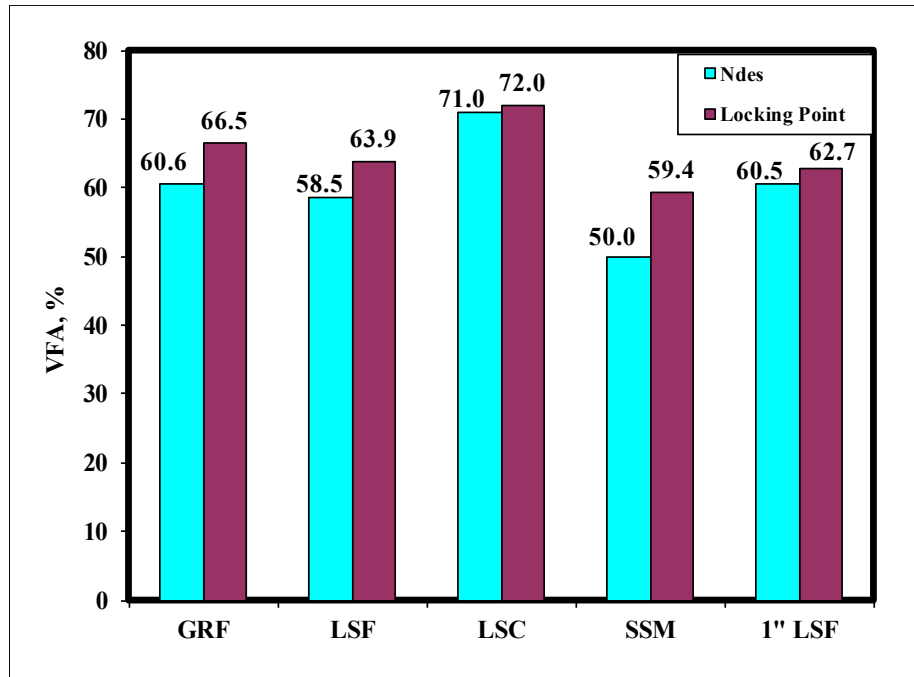


Figure 60
Voids filled with asphalt data

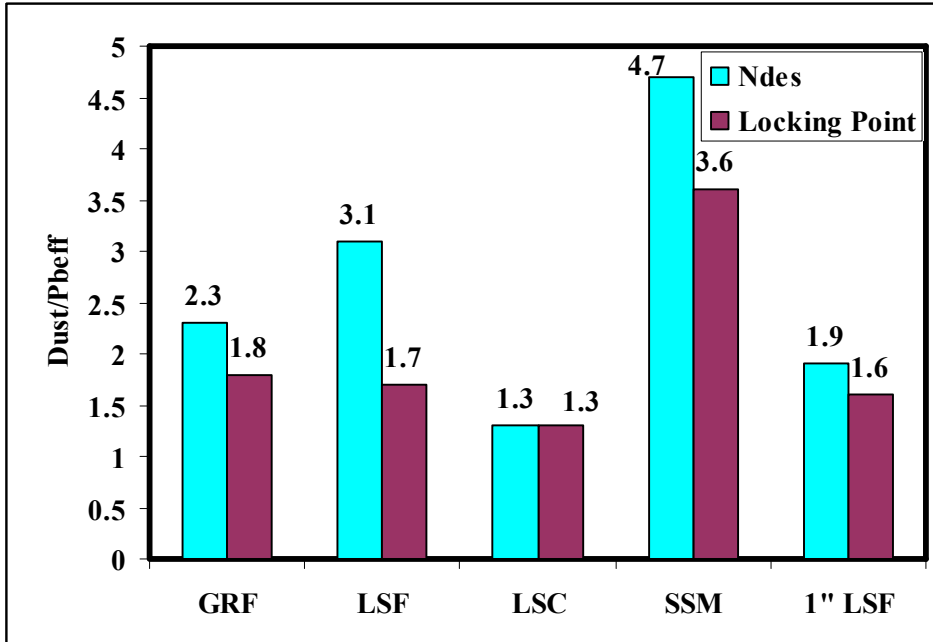


Figure 61
Dust/P_{beff} results

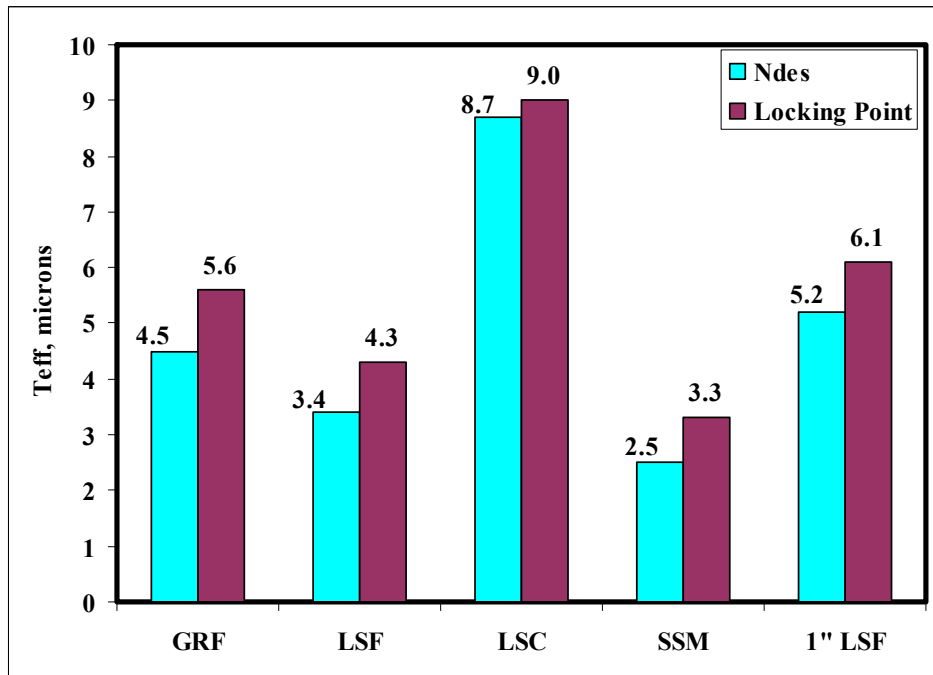


Figure 62
Effective film thickness

Performance Tests Results

For comparison and determination of relative performance, the Phase 2 mixtures were evaluated using similar suite of testing conducted in Phase 1, mainly Hamburg Loaded Wheel Tracking Test (LWT), IT strength test (ITS), and fracture resistance using the notched semi-circular fracture energy test (J_c). In addition, two more fundamental properties were determined for the Phase 2 mixtures: stiffness characteristics using the dynamic modulus test (E^*) and the cracking resistance using the concept of dissipated creep strain energy.

The performance of the Phase 2 mixtures in the LWT test is shown in Figure 63 with the corresponding data from Phase 1. There was a slight increase in the amount of rutting for the Phase 2 mixtures partly due to higher asphalt contents used. The highest rut depth was 4.0 mm for 12.5-mm (1/2-in.) NMAS coarse limestone. The results, however, were still within the range of good performing mixtures, indicating that stability was not compromised by designing the mixes using lower compaction levels.

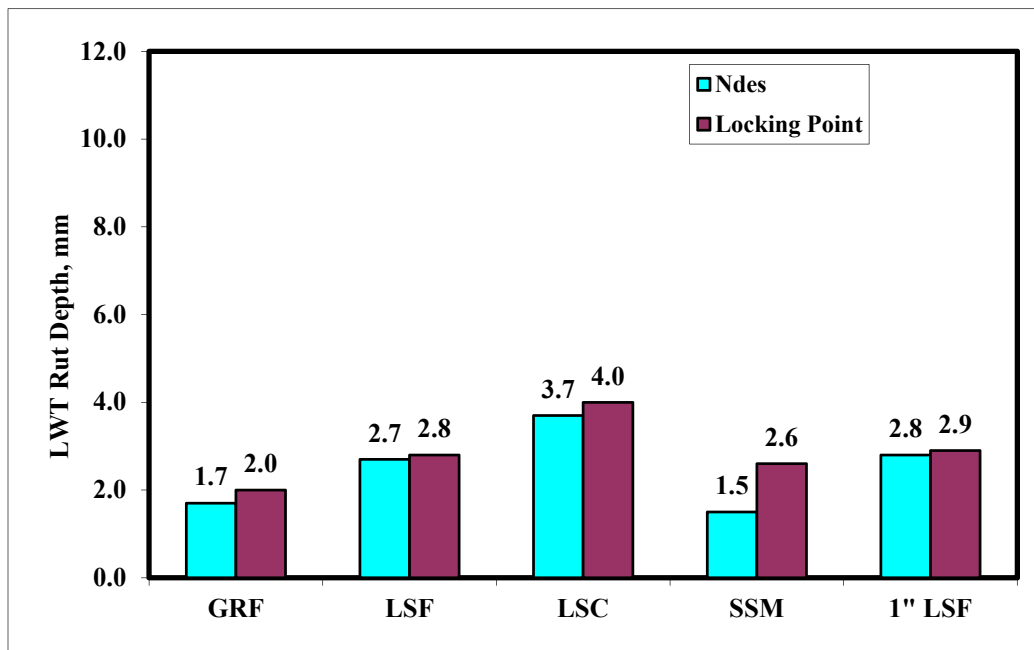


Figure 63
Loaded wheel tracking results

The cohesion characteristics of the mixtures were determined using the IT strength test. Three parameters from this test were used in the analysis: aged IT strength, aged IT strain, and toughness index (TI). Tensile strength values were slightly lower than those obtained for the mixtures compacted at N_{des} (i.e., for the Phase 1 mixtures). The strength values ranged from 168.3 for the 12.5-mm (1/2-in.) NMAS coarse limestone mixture to 325.0 psi for the 12.5-mm (1/2-in.) NMAS medium sandstone mixture, as shown in Figure 64. The highest

reduction in strength was observed for the 12.5-mm (1/2-in.) NMAS fine limestone mixture which had a strength value of 21.8% lower than that obtained for the same mix designed using the Superpave recommended N_{des} . The lowest change in strength was observed for the 25.0-mm (1-in.) NMAS fine limestone with only 4.1% reduction in strength. Moreover, analyzing the strain data in Figure 65 clearly presents that the Phase 2 mixtures exhibited higher IT strain values at failure. It implies that those mixtures can retain more flexibility over time compared to the Phase 1 mixtures and be relatively less prone to pre-mature failures due to aging.

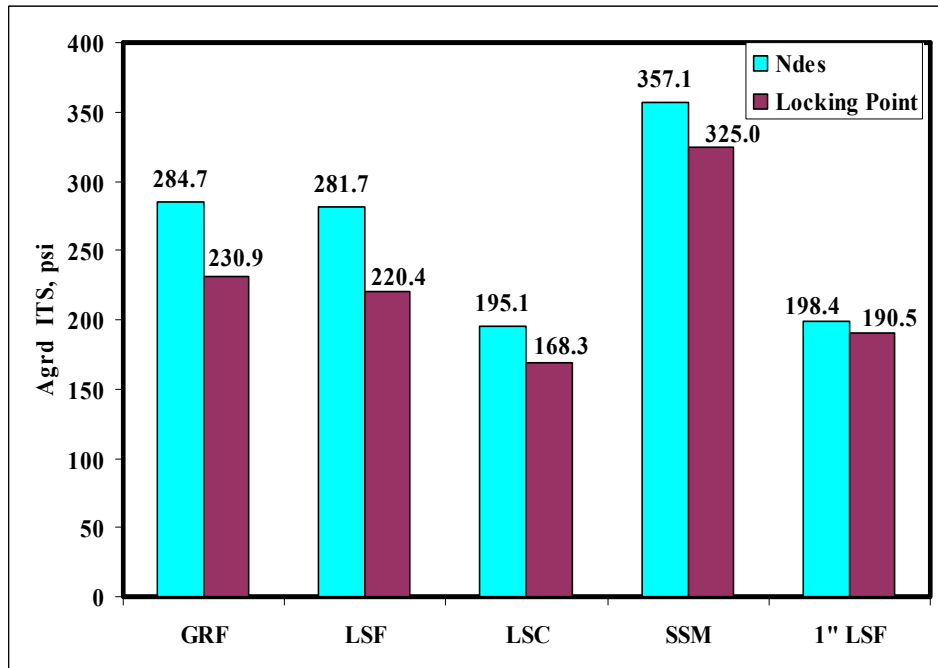


Figure 64
IT strength comparison

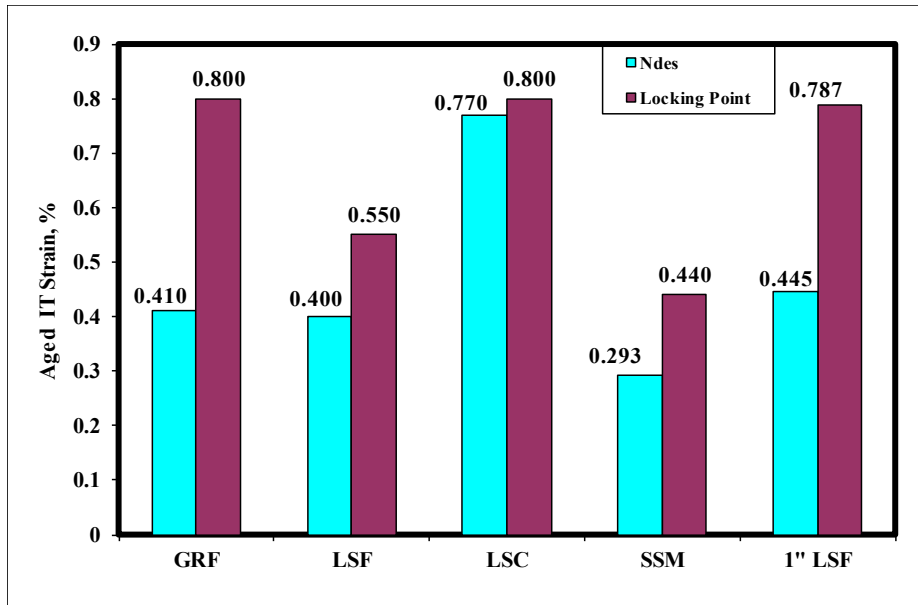


Figure 65
IT strain comparison

Both unaged and aged toughness index (TI) data are presented in Figures 66 and 67. The lowest toughness index was obtained for the medium sandstone mixture, followed by the 12.5-mm (1/2-in.) NMAS fine limestone. Those two mixtures had the lowest effective film thickness and the highest dust/ P_{beff} ratio. Although their TI values were still not considerably low (> 0.5), they were considered to be less favorable in terms of their ability to resist the aging effect over time. This was because the TI values of these mixtures (i.e., medium sandstone and fine limestone) were lower than the ones of other mixtures. It should be noted that all the mixtures showed better toughness properties at their locking points than at Superpave N_{des} , as shown in Figures 66 and 67.

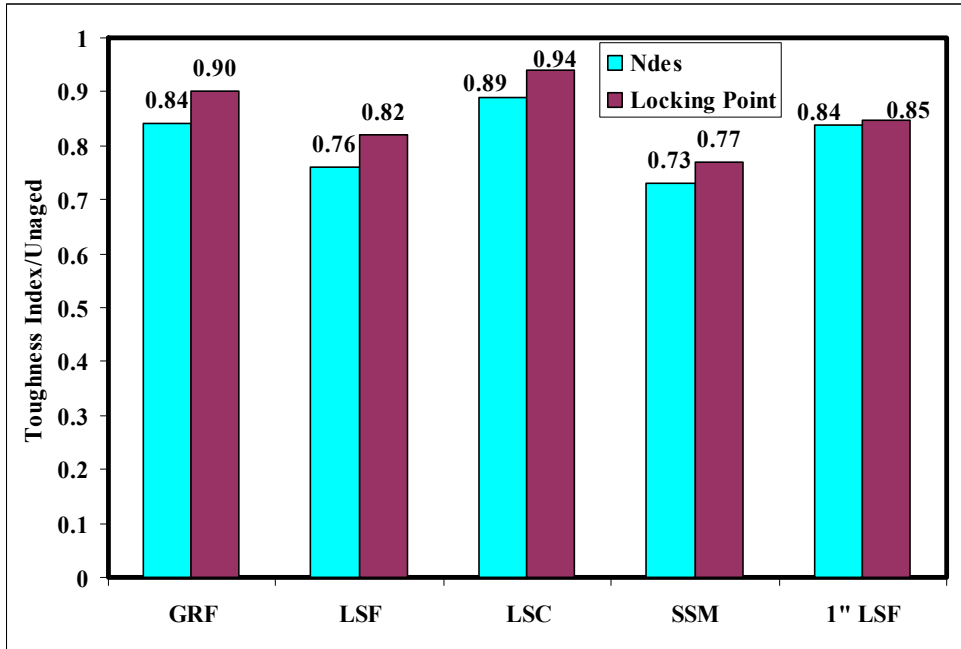


Figure 66
Unaged toughness index

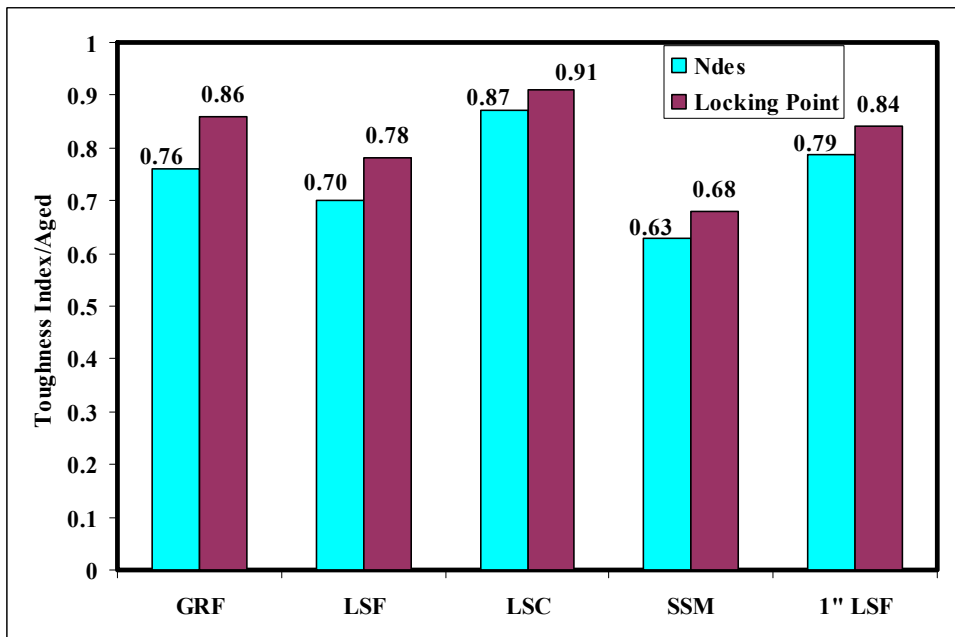


Figure 67
Aged toughness index

Figure 68 presents the calculated J-integral from the semi-circular bend notched fracture test. The test was conducted on mixtures that were aged for 5 days in a forced-draft oven at 85°C

(i.e., long-term aging condition). All the Phase 2 mixtures that were designed by the locking point exhibited an increase in their fracture resistance except for the 25.0-mm (1-in.) NMAS fine limestone mixture in which there was a drop of about 25.9% in J_c . The same fracture resistance under both N_{des} and locking point, which was the highest among the mixtures tested, was obtained from 12.5-mm (1/2-in.) NMAS granite fine mixture. The biggest improvement in the fracture resistance was observed for the 12.5-mm (1/2-in.) NMAS coarse limestone mixture for which there was about 49% increase in J_c when designed using the locking point followed by the 12.5-mm (1/2-in.) NMAS fine limestone mixture with about 35% increase in J_c . The 12.5-mm (1/2-in.) NMAS medium sandstone mixture gained about 20% increase in J_c .

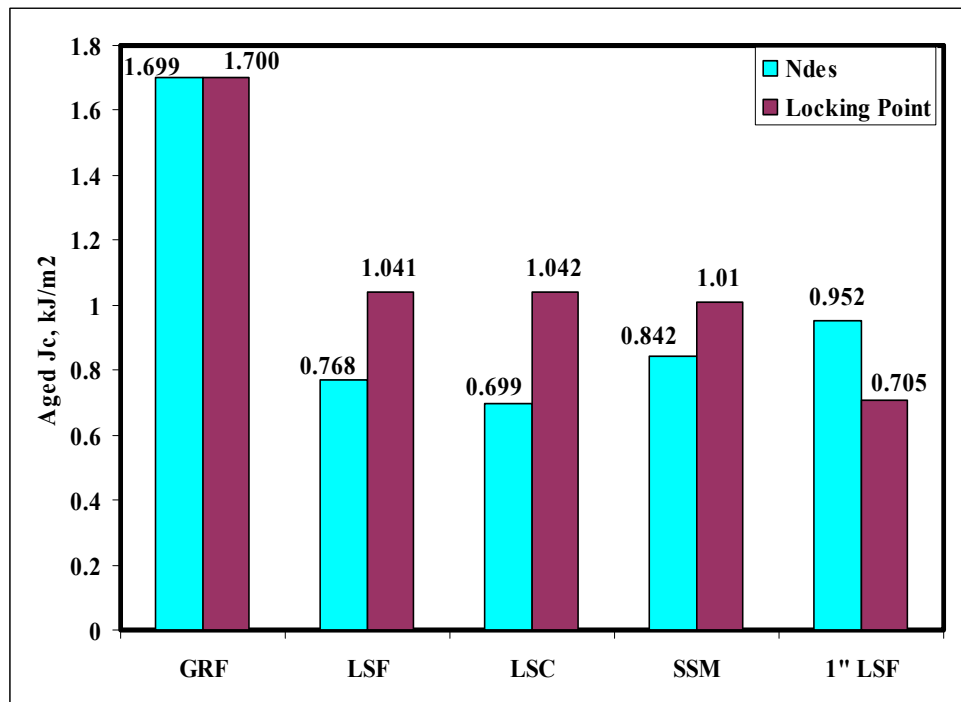


Figure 68
Fracture energy J_c results

Stiffness Characteristics

The stiffness of the mixtures designed in Phase 2 was evaluated using the dynamic modulus test, AASHTO TP 62-03 standard. Two parameters were obtained from this test: the dynamic modulus (E^*) and the phase angle (ϕ). Witczak et al. conducted a detailed study to evaluate candidate mechanistic parameters that correlates with mixtures performance [19]. The major finding of this study was the recommendation of a set of parameters for two distresses in asphalt layers of road pavement, including permanent deformation and load associated

cracking. One of the parameters recommended for the permanent deformation was the dynamic modulus term, $E^*/\sin\theta$ where θ is the phase angle. Higher values of this parameter indicate stiffer mixtures that have good permanent deformation resistance. For fatigue cracking, the recommended parameter was $E^*\sin\theta$.

Permanent deformation is a distress that is associated with excessive loading at relatively high pavement temperatures. The stiffness characteristics and ultimately the rutting resistance of the designed mixtures as defined by the parameter described above were evaluated under two loading conditions that were likely to cause the highest damage to the pavement. The first condition was a high temperature-high frequency of loading in which high traffic speed was simulated by a frequency of 10 Hz representing a speed of approximately 60 mph. The second was a high temperature-low frequency of loading in which slow moving traffic was simulated using a 0.5 Hz loading frequency approximating slow traffic at intersections. In both cases, the selected temperature was 54.4°C which was the highest testing temperature required by the dynamic modulus testing protocol (AASHTO TP 62-03 [20]).

Figures 69 and 70 presents the dynamic modulus and the rutting parameter (i.e., $E^*/\sin\theta$) for the mixtures considered. The sandstone mixture was clearly showing the highest rutting parameter among all the Phase 2 mixtures. The lowest rutting parameter was obtained for the coarse limestone mixture, which agreed with the LWT results showing that the coarse limestone mixture showed the highest rut depth. Both 25.0-mm (1-in.) and 12.5-mm (1/2-in.) NMAS limestone mixtures showed similar performance. It was also found that the relative performance of the mixtures under both loading conditions of fast and slow moving traffic was the same.

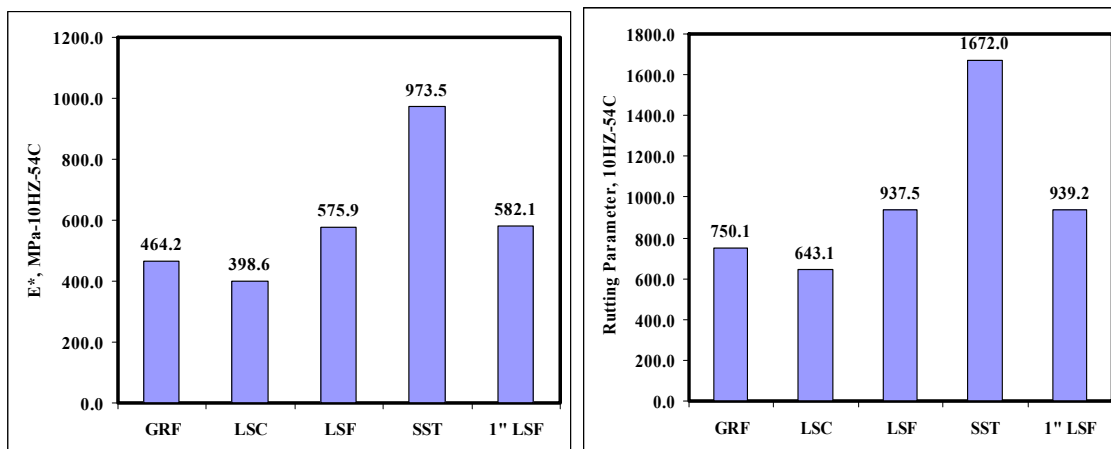


Figure 69
 E^* data at 10HZ, 54.4°C

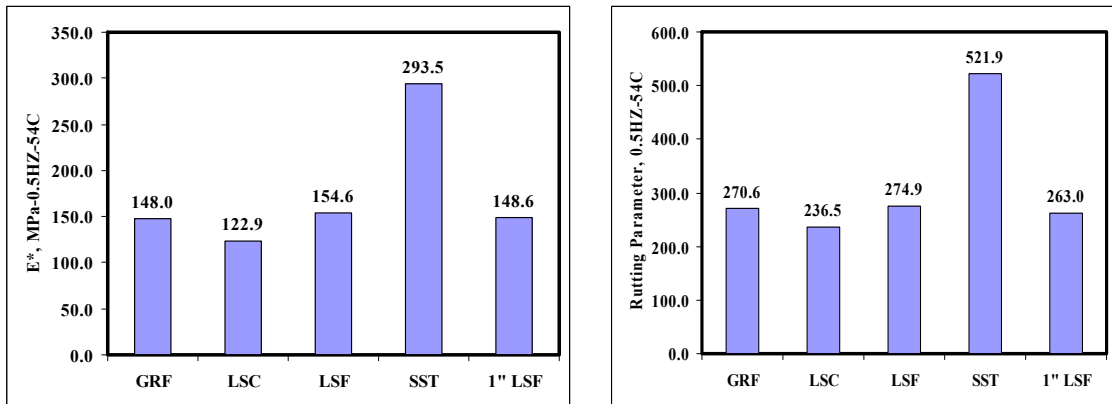


Figure 70
 E^* data at 0.5HZ, 54.4°C

Figure 71 presents the data for the fatigue parameter $E^* \sin \theta$. The mixtures were evaluated at a service temperature of 21.1°C and loading frequency of 10 Hz. The lower this parameter is, the better the fatigue resistance obtained is. It is evident from this figure that the coarse limestone mixture has the best fatigue performance as measured by the fatigue parameter described in here. That was expected since this mixture was relatively rich in asphalt content and had the lowest $Dust/P_{beff}$ ratio among all the mixtures considered. That resulted in a mixture with better flexibility characteristics that can tolerate relatively more repetitive loading without fracture. The granite mixture was ranked second in terms of fatigue resistance while the remaining three mixtures showed similar performance.

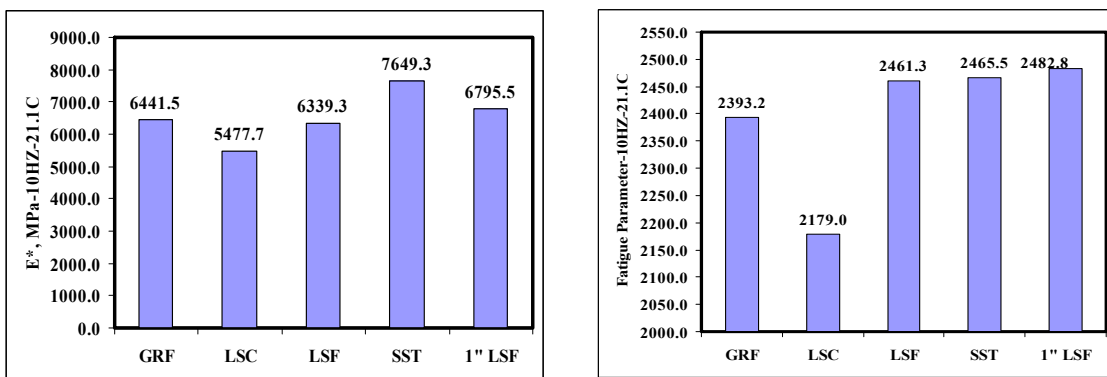


Figure 71
 E^* data at 10HZ, 21.1°C

Dissipated Creep Strain Energy

One of the main arguments presented in this project was that every HMA mixture is unique in its performance and, therefore, setting up general requirements (either volumetric or densification) that are empirical in nature and rely heavily on personal experiences with specific types of mixtures is very likely to limit the use of good performing mixtures, only on the basis of not meeting such empirical requirements. The mixtures designed in this study were likely to be rejected if they were to be judged using the traditional volumetric criteria adopted in the current Superpave design system. It was therefore imperative to validate the performance of these mixtures by comparing them to good performing field mixtures that were in place for a reasonable amount of time using a fundamental material property that described the behavior of the mixtures in consideration of durability in this case, specifically in terms of resistance to cracking.

It was mentioned earlier that there was a concern that the designed mixtures might have durability problems. To address that concern, the Dissipated Creep Strain Energy (DCSE) by Roque et al. was used [21]. In this study, the DCSE limit was proposed as one of the most important factors that control crack performance and hence durability of asphalt concrete mixtures. Roque et al. studied 22 field mixtures that had been in service for more than 10 years in Florida [21]. In order to determine this parameter, two laboratory tests such as indirect resilient modulus test (ITMr) and the indirect tensile strength (ITS) test were conducted at 10°C on 150-mm diameter and 50-mm thick specimens. From the strength test, failure strain (ϵ_f), tensile strength (S_t), and fracture energy (FE) were determined, while the resilient modulus (M_R) was obtained from the resilient modulus test (see Figure 72). The calculation of the DCSE was then determined as follows:

$$\epsilon_0 = (M_R \epsilon_f - S_t) / M_R \quad (11)$$

$$EE = \frac{1}{2} S_t (\epsilon_f - \epsilon_0) \quad (12)$$

$$DCSE = FE - EE \quad (13)$$

Table 28 summarizes the DCSE results obtained for all the mixtures in Phase 2. The results are also presented graphically in Figure 73. The dissipated creep strain energy (DCSE) threshold represents the energy that the mixture can tolerate before it fractures. Therefore, it is logical that mixtures with higher DCSE thresholds will exhibit better cracking performance than mixtures with lower DCSE thresholds when both are exposed to similar environmental and loading conditions. From the data presented, it is clear that the 12.5-mm (1/2-in.) NMAS limestone coarse mixture was favorable in terms of cracking resistance because it had the highest DCSE limit followed by the 12.5-mm (1/2-in.) NMAS fine granite mixture and then the 25.0-mm (1-in.) NMAS fine limestone mixture. The 12.5-mm (1/2-in.) NMAS fine

limestone and medium sandstone had the lowest DCSE. These two mixtures were relatively dry in asphalt and exhibited high stiffness characteristics in terms of E^* .

Based on the DCSE data obtained for Phase 2 mixtures, it is evident that the 12.5-mm (1/2-in.) NMAS fine limestone and medium sandstone mixtures were on the border line of the 0.75 kJ/m^3 DCSE limit below which cracking might be a problem [21]. The best performing mixtures was the 12.5-mm (1/2-in.) NMAS coarse limestone followed by fine granite and finally the 25.0-mm (1-in.) NMAS fine limestone. It should be noted that all four mixtures in Phase 2 had volumetric properties that were considered inferior using the current Superpave mix design criteria.

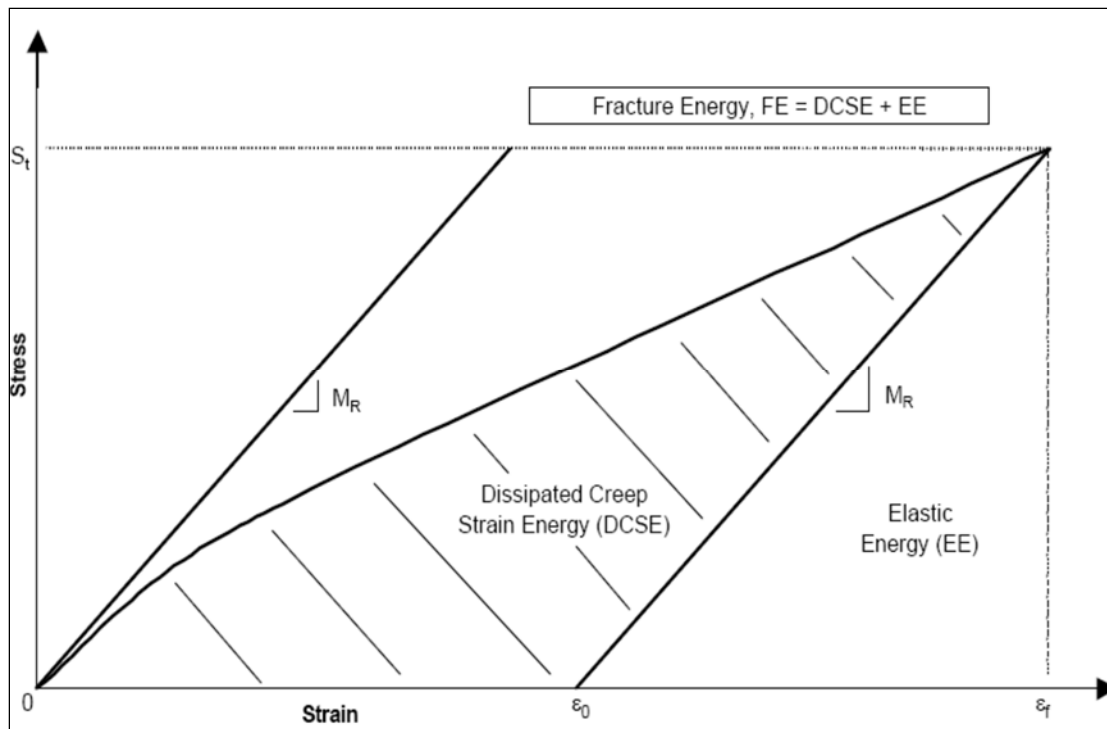


Figure 72
Calculations of the dissipated creep strain energy

Table 28
Calculations of the dissipated creep strain energy

Mixture	Mr, Gpa	Fracture Energy, kJ/m ³	ITS, MPa	Final Strain, microns	Initial Strain, microns	Elastic Energy, kJ/m ³	DCSE- kJ/m ³
GRF	19.4	1.5	2.8	570	569.86	0.20	1.30
LSC	18.1	1.62	2.3	713	712.87	0.15	1.47
LSF	23.2	0.95	3	370	369.87	0.19	0.76
SST	25.5	0.97	3.4	350	349.87	0.23	0.74
1"LSF	25.5	1	2.815	431.6	431.49	0.16	0.84

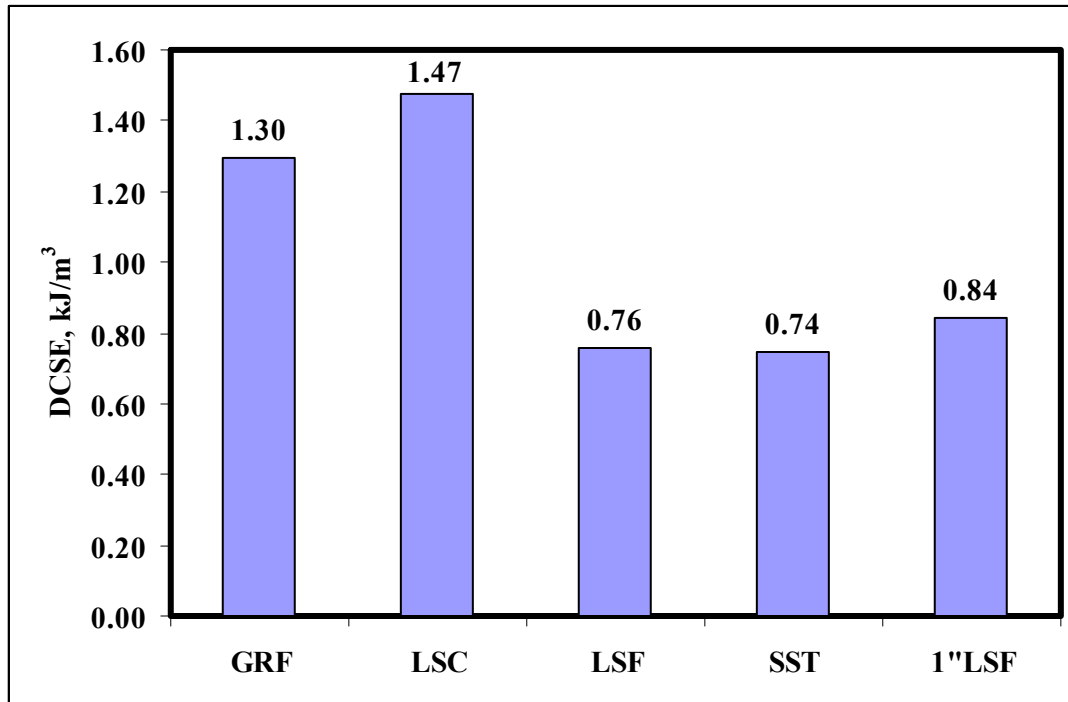


Figure 73
Dissipated creep strain energy of the designed mixtures

The performance of the mixtures as described by the DCSE concept was compared to their fatigue parameter, $E \cdot \sin \theta$ that was obtained from the dynamic modulus test. Both parameters (i.e., DCSE and $E \cdot \sin \theta$) gave similar ranking for coarse limestone and fine granite mixtures. The performance of the sandstone mixture and the two limestone mixtures was very similar when evaluated using both parameters, even if the ranking was different likely due to the small differences in magnitude of the parameter between the mixtures in both cases. Figure 74 shows that a reasonable correlation between the DCSE and the fatigue parameter (i.e., $E \cdot \sin \theta$) from the dynamic modulus test, indicating that both parameters follow the same trend in describing the cracking resistance of the mixtures.

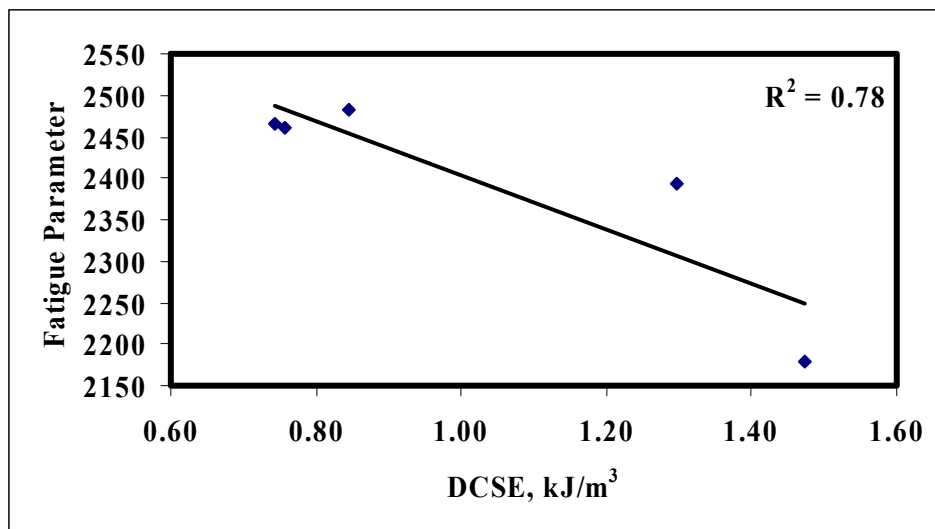


Figure 74
Relationship between DCSE and the fatigue parameter from the dynamic modulus test

Performance of Low Volume Mixtures

Low volume roads, which can be defined as roads with low number of vehicles per day and low cumulative equivalent single axle load (ESAL) in design period are generally built with lower quality materials compared to roads with higher traffic demands. Recipe type mix design is traditionally used for designing asphalt mixtures for this type of application. A small study was conducted as part of this research to evaluate the laboratory performance of asphalt mixtures which is intended for low volume application and contain high amount of natural sand. Natural sand is a fine material that is considered a cheap commodity and it is widely available across the country. The chosen aggregate for this research project was limestone, as it was one the most commonly used aggregate types in Louisiana. Two fine

limestone mixtures were designed for this study: 12.5-mm (½-in.) NMAS mixture and 25.0-mm (1-in.) NMAS mixture. The aggregate structures in those two mixtures were designed using the Bailey Method of aggregate gradation calculation procedure, where at least 25% natural sand should be included. The gradation characteristics of the low volume mixtures and the mixture design data for these two mixtures were summarized in Table 29 and Table 30, respectively.

Table 29
Bailey gradation properties for low volume mixtures

Mixture	CA Volume	FA Volume	CUW	%PCS	CA Ratio	F _{AC} Ratio	F _{AF} Ratio
LSF-1"	37.3	62.7	70	52.9	1.134	0.617	0.317
LSF-1/2"	37.1	62.9	68	49.2	0.842	0.246	N/A

Table 30
Mix design properties for low volume mixes

Mixture Type	1/2" Limestone- LV	1.0" Limestone- LV
OAC @ 4.0% AV (Ndes = 75)	4.9	4.3
Effective AC content @ 4.0% AV	0.0	0.0
VMA	13.1	12.2
VFA	69.0	67.2
Effective Film Thickness @ 4.0% AV and OAC	6.9	7.4
Dust/P _{beff}	1.4	1.2
Sand Content (%)	25.3	25.2

The low-volume mixtures were further evaluated using similar suite of laboratory tests, such as LWT, J_c , E^* , and DCSE. The results are presented in Figures 75 through 80. As expected, the high-volume mixture outperformed the low volume ones in all the tests conducted. The 25.0-mm (1-in.) NMAS low-volume mix showed a lower rutting performance as described by the rutting parameter ($E^*/\sin\theta$) from the dynamic modulus (E^*) test. The same mixture also was less fatigue resistant using the fatigue parameter (i.e., $E^*\sin\theta$). That observation, however, was contradicted by the results of the DCSE test in which the 25.0-mm (1-in.) NMAS low volume mixture had a higher DCSE than the 12.5-mm (1/2-in.) NMAS mixture. Mixture design properties, mainly effective film thickness and Dust/P_{beff} ratio were more in line with the DCSE results. The 25.0-mm (1-in.) NMAS limestone mixture had a higher

effective film thickness and lower dust/ P_{beff} ratio, indicating its better durability than the 12.5-mm (1/2-in.) NMAS mixture.

The resistance of low volume mixtures to permanent deformation was evaluated using the LWT test. The test was run for 20,000 passes or until specimen failed. Both mixtures did not meet the 6.0-mm rutting criterion generally specified. Figures 78 and 79 show the results of the LWT for these two mixtures. It should be noted that applying the same criterion (i.e., 6.0 mm at 20,000 passes) for both high-and low-volume mixtures was unjustifiable. Low-volume mixes are subjected to a significantly less amount of traffic than the high-volume ones are. Therefore, the low-volume mixtures might not experience the same level of loads that is equivalent to the 20,000 passes used in the LWT test. Figures 78 and 79 clearly present that the mixtures maintained reasonable rut resistance by about 10,000 passes indicating that those mixtures might still provide adequate performance for the purpose they were intended for. Figure 80 shows the number of passes required to cause 6.0-mm rutting for both mixtures. It took about 11,226 passes for the 25.0-mm (1-in.) NMAS mixture compared to 7426 passes for the 12.5-mm (1/2-in.) NMAS mixture, indicating that higher rut resistance was offered by the mixture with greater NMAS for the low volume mixtures.

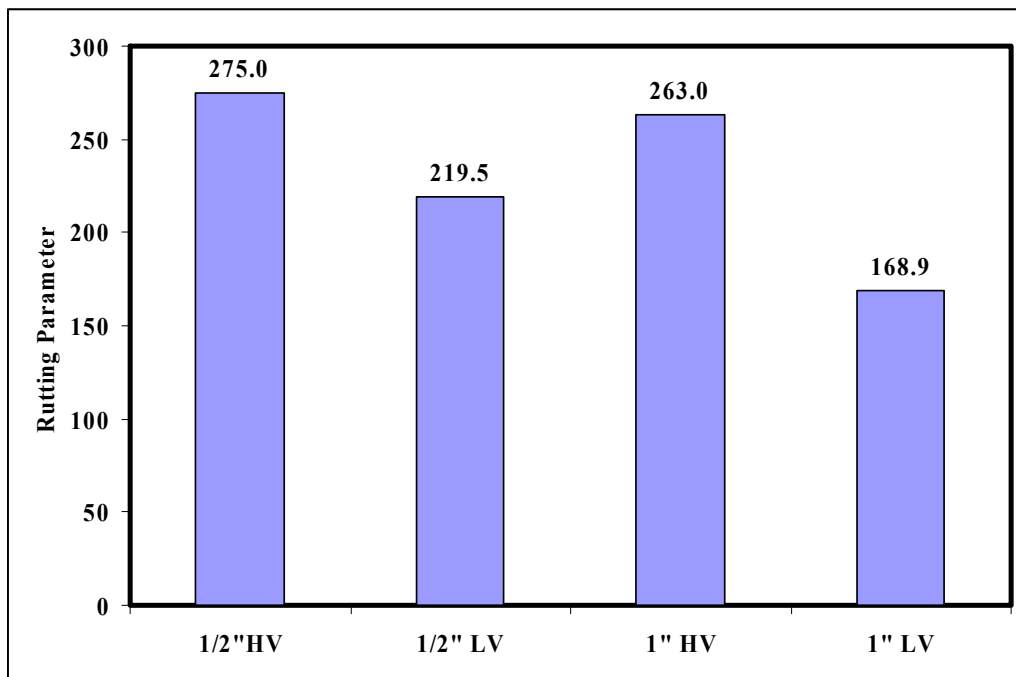


Figure 75
Comparison of rutting parameter of both high and low volume limestone mixtures

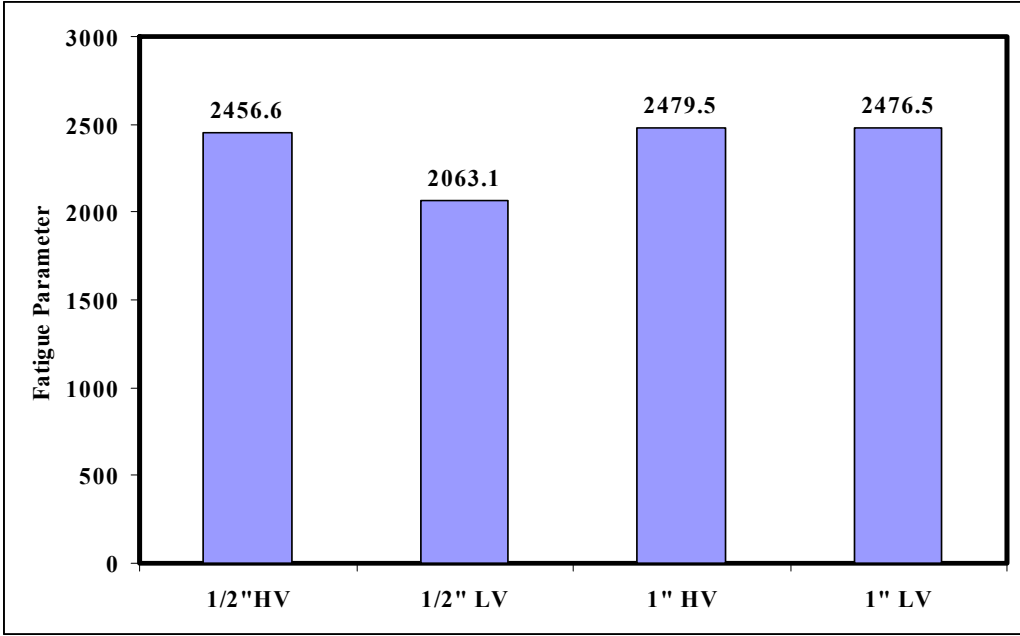


Figure 76
Comparison of fatigue parameter of both high and low volume limestone mixtures

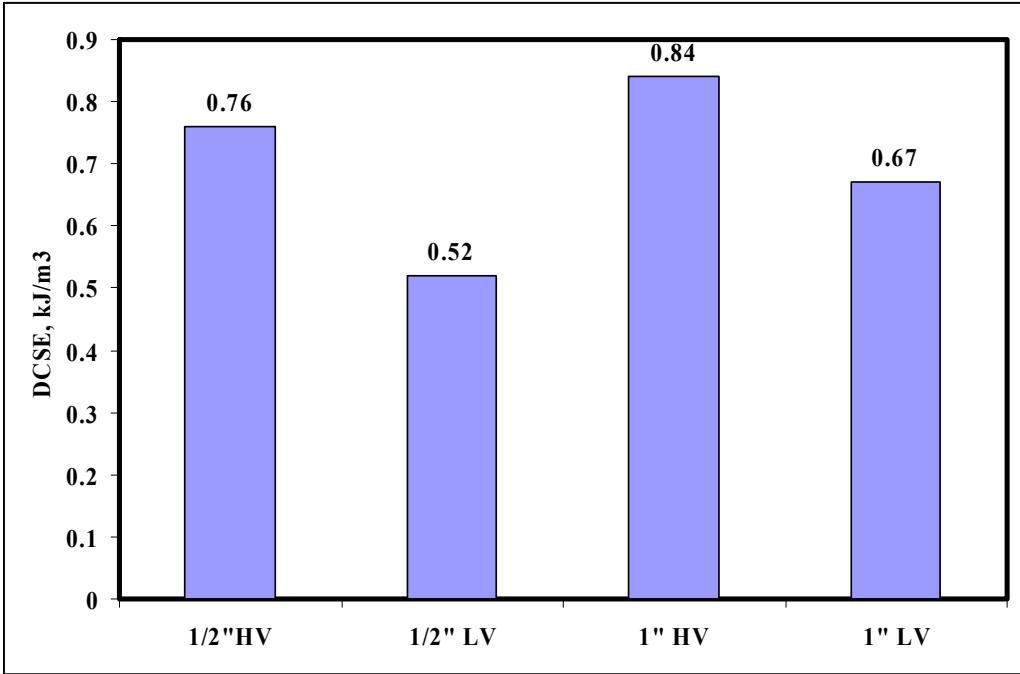


Figure 77
DCSE results for low volume mixtures

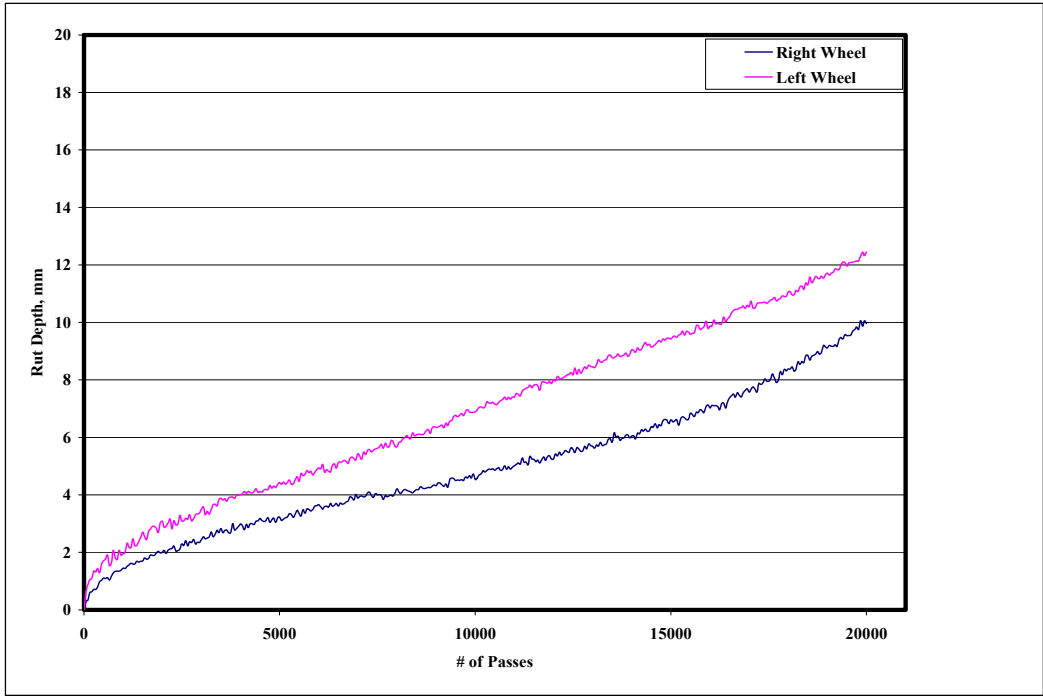


Figure 78
Performance of 1 in. limestone low volume mixtures in LWT test

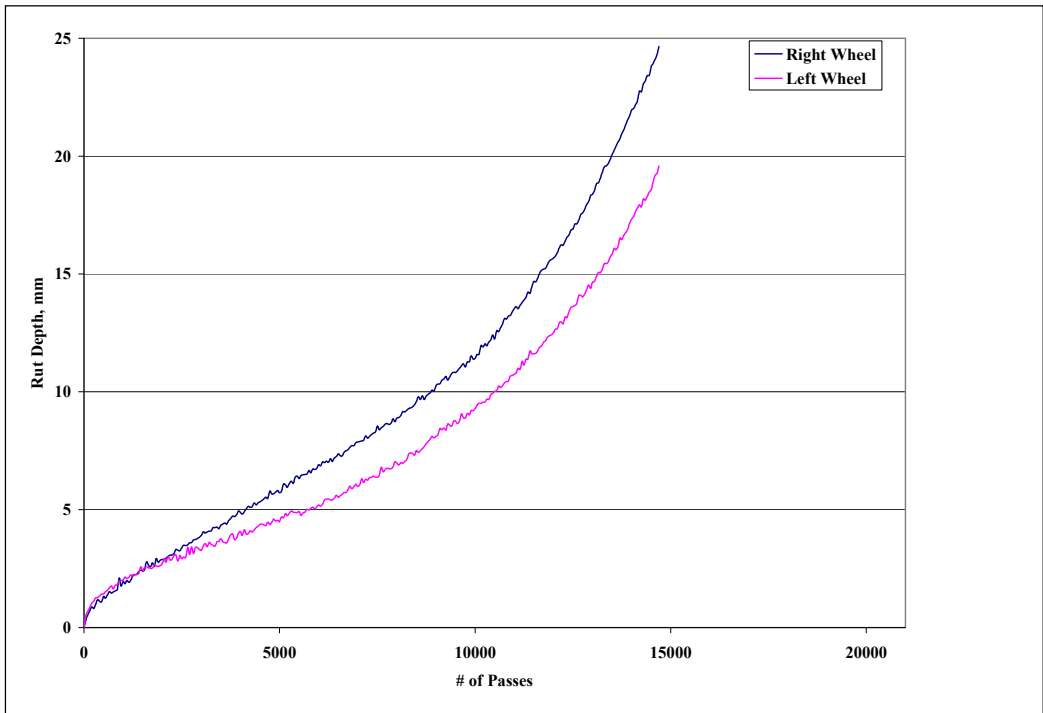


Figure 79
Performance of 1/2 in. limestone low volume mixture in LWT test

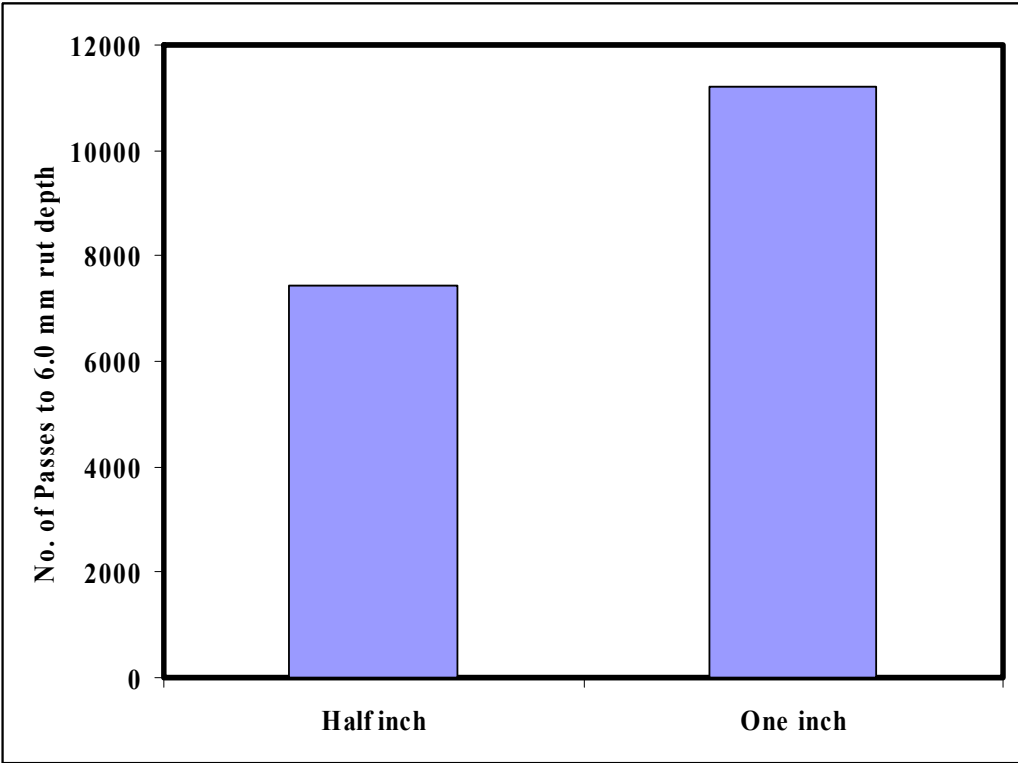


Figure 80
Performance comparison of low volume mixes in LWT test

CONCLUSIONS

This report documented the findings of an extensive research study on design and characterization of asphalt mixtures used as road pavement materials. The mixture design method using the concept of locking point was developed and a suite of tests were performed to evaluate the proposed mixture design method. The test results were compared to the corresponding results on the mixtures by the current Superpave design approach. The following is a summary of some of the major findings from this research:

- The Bailey Method provided a rational approach of aggregate blending and evaluation.
- Adhering to the currently recommended Bailey ratios produced results in terms of volumetrics that are more in line with the generally accepted levels for coarse graded mixtures. Fine and medium mixtures, however, had lower voids in mineral aggregates (VMA) than the current Superpave recommendations.
- Both SGC and PDA results showed that coarse mixtures were more difficult to compact compared to the medium and fine ones.
- The compaction data indicated that the current recommended Superpave design number of gyrations was too high and subject the mixtures to unnecessary high compaction loads for extended period of time, which might have an adverse effect on the final mixture volumetrics.
- There was a strong correlation between the data from the SGC and PDA, implying that the data from the SGC provides good indication of mixture compatibility.
- The CA ratio, a gradation parameter from the Bailey Method, which is predominantly a function of the coarse aggregate blend by volume, seemed to have the strongest correlations with mixtures volumetrics (e.g., $R^2 = 0.81$ for VMA). On the other hand, mixture volumetrics was less sensitive to the change in the other gradation parameter, F_{AC} ratio.
- Three parameters, such as CA ratio from the Bailey Method and nCA and nFA from the power law gradation analysis method, had the best correlation with the Compaction Densification Index (CDI), indicating that those parameters described the actual gradation characteristics of the mixtures and that the compactability of the mixtures is a function (among other factors) of the particle size distribution as measured by those parameters.
- Traffic Indices from Superpave Gyrotory Compactor (SGC) and the Pressure Distribution Analyzer (PDA) failed to capture plastic instability of asphalt mixtures as measured by the Hamburg Loaded Wheel Tracking Test (LWT).

- All the mixtures designed using the Bailey Method had highly dense aggregate structures that exhibited superior performance in the LWT test with a maximum rut depth of 4.0 mm after 20,000 passes. No signs of stripping were found at the end of the test period for all the mixtures.
- Designing mixtures to their locking points resulted in improved durability without compromising stability.
- The use of strict volumetric requirements was cautioned. Such requirements are likely to eliminate potential well-performing mixtures.

RECOMMENDATIONS

The area of asphalt mixture design is a versatile research platform that evolves as traffic levels and vehicle design constantly changes. This research provided a foundation for more elaborate work on developing mixture design methodologies that can reliably produce asphalt mixtures with performance characteristics that matches the demand of the transportation industry. A recommended design approach is documented in Appendix D. It is strongly recommended that the findings of this research should be evaluated using large scale testing facilities such as the Louisiana Accelerated Loading Facility (ALF). This will provide the opportunity to monitor the performance of the designed asphalt mixtures over time as a part of a full pavement structure with different structural properties and thickness design. It is also recommended that wider range of mixture types and gradations be designed and evaluated using the recommended design approach in order to develop well established ranges of performance criteria adopted for this design methodology.

ACRONYMS, ABBREVIATIONS, AND SYMBOLS

$ E^* $	dynamic modulus
ϵ_f	failure strain
ϵ_0	peak recoverable axial strain
σ_0	dynamic stress
AASHTO	American Association of State Highway and Transportation Officials
AC	asphalt content
ALF	accelerated loading facility
ANCOVA	analysis of covariance
ANOVA	analysis of variance
AV	air voids
CA	coarse aggregate volume
CDI	compaction densification index
CFI	compaction Force Index
cm	centimeter(s)
CUW	chosen unit weight
DCSE	dynamic creep strain energy
DOT	Department of Transportation
DOTD	Department of Transportation and Development
EE	elastic energy
ESAL	equivalent single axle load
ETG	expert task group
FA	fine aggregate volume
FE	fracture energy
FR	frictional resistance
GR	granite
HMA	hot mix asphalt
in.	inch(es)
ITMr	indirect tensile resilient modulus test
ITS	indirect tensile strength
Jc	critical strain energy release rate
kJ	kilojoules
km	kilometer(s)
lb.	pound(s)
LP	locking point
LS	siliceous limestone

LSM	least square means
LTRC	Louisiana Transportation Research Center
LWT	loaded wheel tracking
MF	mineral filler
m	meter(s)
mm	millimeter(s)
MR	resilient modulus
NMAS	nominal maximum aggregate size
NMPS	nominal maximum particle size
P_{beff}	effective asphalt content
PCS	primary control sieve
PDA	pressure distribution analyzer
RAP	recycled asphalt pavement
S_t	tensile strength
SAS	statistical analysis system
SCB	semi-circular bending
SGC	superpave gyratory compactor
SHRP	strategic highway research program
SST	sandstone
TCS	tertiary control sieve
TDI	traffic densification index
TFI	traffic force index
TI	toughness index
VCA	volume of coarse aggregate
VMA	voids in mineral aggregates
VFA	voids filled with asphalt

REFERENCES

1. Roberts, F.L., P.S. Kandhal, E.R. Brown, D.-Y. Lee, and T.W. Kennedy, *Hot mix asphalt materials, mixture design and construction*. 1991, NAPA Research and Education Foundation: Lanham, Maryland.
2. National Asphalt Pavement Association, *A Guide for Hot Mix Asphalt Pavement*. Information Series 131. 2002.
3. Hveem, F.N., *The Centrifuge Kerosene Equivalent as Used in Establishing the Oil Content for Dense Graded Bituminous Mixtures*. 1946.
4. Asphalt Institute, *Construction of Hot Mix Asphalt Pavements*, in *Manual Series No. 22*,. Lexington, KY.
5. Asphalt Institute, *Mix Design Methods for Asphalt Concrete and Other Hot-Mix Types*, in *Manual Series*. 1993: Lexington, KY.
6. Asphalt Institute, *SP-2 Superpave Mix Design*. 2001: Lexington, KY.
7. Anderson, R.M. and R.A. Bentsen, *INFLUENCE OF VOIDS IN THE MINERAL AGGREGATE (VMA) ON THE MECHANICAL PROPERTIES OF COARSE AND FINE ASPHALT MIXTURES (WITH DISCUSSION)*. Journal of the Association of Asphalt paving Technologists, 2001. 70: p. 1-37.
8. Coree, B. and W. Hislop. *The difficult nature of minimum VMA: A historical perspective, Presented to the Annual meeting*. in *Transportation Research Board 78th Annual Meeting*. 1999. Washington, DC: Transportation Research Board.
9. Coree, B.J. and W.P. Hislop, *A LABORATORY INVESTIGATION INTO THE EFFECTS OF AGGREGATE-RELATED FACTORS ON CRITICAL VMA IN ASPHALT PAVING MIXTURES (WITH DISCUSSION)*. Journal of the Association of Asphalt Paving Technologists, 2001. 70.
10. Haddock, J., C. Pan, A. Feng, and T. White, *Effect of gradation on asphalt mixture performance*. Transportation Research Record: Journal of the Transportation Research Board, 1999(1681): p. 59-68.
11. Kandhal, P., K. Foo, and R. Mallick, *Critical review of voids in mineral aggregate requirements in Superpave*. Transportation Research Record: Journal of the Transportation Research Board, 1998(1609): p. 21-27.
12. Mallick, R., *Use of Superpave gyratory compactor to characterize hot-mix asphalt*. Transportation Research Record: Journal of the Transportation Research Board, 1999(1681): p. 86-96.
13. Mohammad, L., I. Negulescu, Z. Wu, C. Daranga, W. Daly, and C. Abadie, *Investigation of the use of recycled polymer modified asphalt binder in asphalt concrete pavements (with discussion and closure)*. Journal of the Association of

- Asphalt Paving Technologists, 2003. 72: p. 551-594.
14. Mohammad, L., Z. Wu, and M. Aglan. *Characterization of fracture and fatigue resistance on recycled polymer-modified asphalt pavements*. in *Proceedings, 5th International Conference*. 2004.
 15. Ruth, B.E., R. Roque, and B. Nukunya, *Aggregate gradation characterization factors and their relationship to fracture energy and failure strain on asphalt mixtures (with discussion)*. Journal of the Association of Asphalt Paving Technologists, 2002. 71.
 16. Bahia, H.U., T.P. Friemel, P.A. Peterson, J.S. Russell, and B. Poehnelt, *Optimization of constructibility and resistance to traffic: a new design approach for HMA using the superpave compactor*. Journal of the Association of Asphalt Paving Technologists, 1998. 67: p. 189-232.
 17. American Association of State Highways and Transportation Officials, *Practice for Short and long Term Aging of HOT Mix Asphalt*, in *AASHTO Designation PP2*,. 1994: Washington, D.C.
 18. Mohammad, L.N., Z. Wu, and A. Raghavendra, *Performance Evaluation of Louisiana Superpave Mixtures*, in *Final Report No. FHWA/LA*. 2005, Louisiana Transportation Research Center: Baton Rouge, LA.
 19. Witczack, M.W., K. Kaloush, T. Pellinen, M. El-Basyouny, and H.V. Quintus, *Simple Performance Test for SUPERPAVE*, in *NCHRP Report 465*. 2002, Transportation Research Board, National Cooperative Highway Research Council: Washington, D. C.
 20. American Association of State Highways and Transportation Officials, *Determining the Dynamic Modulus of Hot-Mix Asphalt Concrete Mixtures*, in *AASHTO Designation TP-62-03*. 2003: Washington, DC.
 21. Roque, R., B. Birgisson, C. Drakos, and B. Dietrich, *Development and field evaluation of energy-based criteria for top-down cracking performance of hot mix asphalt (with discussion)*. Journal of the Association of Asphalt Paving Technologists, 2004. 73.
 22. ASTM, *Standard Test Method for Specific Gravity and Absorption of Coarse Aggregate*, in *ASTM C127*.
 23. ASTM, *Standard Test Method for Specific Gravity and Absorption of Fine Aggregate*, in *ASTM C128*.
 24. American Association of State Highways and Transportation Officials, *Bulk Density (Unit Weight) and Voids in Aggregate*, in *AASHTO Designation T 19*. 2004.
 25. American Association of State Highways and Transportation Officials, *Standard Test Method for Uncompacted Void Content of Fine Aggregate*, in *AASHTO*

- Designation T 304-96*. 2000: Washington, D.C.
26. Transportation Research Circular, *Bailey Method for Gradation Selection in Hot-Mix Asphalt Mixture Design*. 2002, Washington, DC: Transportation Research Board.
 27. Vavrik, W.R., W.J. Pine, G. Huber, S.H. Carpenter, and R. Bailey, *The bailey method of gradation evaluation: the influence of aggregate gradation and packing characteristics on voids in the mineral aggregate (with discussion)*. Journal of the Association of Asphalt Paving Technologists, 2001. 70.

APPENDIX A

List of Laboratory Tests for Aggregate Stockpiles

- Materials finer than no. 200 (75- μm) sieve in mineral aggregates by washing (AASHTO T 11),
- Specific Gravity and Absorption of Coarse Aggregate (AASHTO T 85 & ASTM C127 [22]),
- Specific gravity and absorption of fine aggregates (AASHTO T 84 & ASTM C128 [23]),
- Bulk density (“unit weight”) & voids in aggregate (AASHTO T19 [24]),
- Standard Test Method for Determining the Percentage of Fractured Particles in Coarse Aggregate (ASTM D 5821),
- Uncompacted void content of fine aggregate (AASHTO T 304 [25]),
- Standard Test Method for Flat Particles, Elongated Particles or Flat and Elongated Particles in Coarse Aggregate (ASTM D 4791), and
- Plastic fines in graded aggregates and soils by use of the sand equivalent test (AASHTO T176).

Individual Aggregate Stockpiles Properties

Table A.1
Limestone stockpile gradations and physical properties

Stockpile No.	#57 LS	#67 LS	#78 LS	#8 LS	#11 LS	#10 LS
Metric (U.S.) Sieve						
37.5 mm (1.5 in)	100.0	100.0	100.0	100.0	100.0	100.0
25 mm (1 in)	79.1	100.0	100.0	100.0	100.0	100.0
19 mm (¾ in)	41.6	91.3	100.0	100.0	100.0	100.0
12.5 mm (½ in)	8.0	44.3	93.2	100.0	100.0	100.0
9.5 mm (⅜ in)	2.3	23.1	55.3	94.6	100.0	100.0
4.75 mm (No. 4)	1.4	4.6	7.0	24.3	92.1	98.8
2.36 mm (No. 8)	1.3	2.5	3.1	6.0	62.8	77.2
1.18 mm (No. 16)	1.3	2.1	2.5	4.1	39.7	56.1
0.6 mm (No. 30)	1.2	1.9	2.3	3.5	25.9	41.3
0.3 mm (No. 50)	1.1	1.8	2.1	3.2	18.3	30.4
0.15 mm (No. 100)	1.0	1.6	2.0	3.0	14.1	22.6
0.075 mm (No. 200)	0.9	1.5	1.8	2.8	11.6	17.0
Bulk specific gravity	2.673	2.674	2.658	2.654	2.567	2.496
Apparent specific gravity	2.701	2.703	2.697	2.688	2.706	2.716
Absorption, %	0.381	0.401	0.538	0.469	2.007	3.329
CAA	100	100	100	100	N/A	N/A
FAA	N/A	N/A	N/A	N/A	46.1	45.1
Flat & Elongated	0.0	0.0	0.0	0.0	N/A	N/A
SE value	N/A	N/A	N/A	N/A	58.1	51.6
Loose Unit Weight	86.8	88.4	90.6	88.5	N/A	N/A
Rodded Unit Weight	98.5	98.8	100.0	99.4	114.4	111.8

Table A.2
Sandstone stockpiles gradations and physical properties

Stockpile No.	#57 SST	#67 SST	#78 SST	#8 SST	#11 SST	#1/4 by 0 SST	Coarse Sand
Metric (U.S.) Sieve							
37.5 mm (1.5 in)	100.0	100.0	100.0	100.0	100.0	100.0	100.0
25 mm (1 in)	98.6	100.0	100.0	100.0	100.0	100.0	100.0
19 mm (¾ in)	68.5	95.9	100.0	100.0	100.0	100.0	100.0
12.5 mm (½ in)	29.0	50.3	93.2	100.0	100.0	100.0	100.0
9.5 mm (⅜ in)	14.0	27.2	67.4	96.3	100.0	100.0	100.0
4.75 mm (No. 4)	2.0	5.2	16.1	39.0	99.7	87.4	99.0
2.36 mm (No. 8)	1.6	3.0	3.8	7.4	86.6	69.3	92.0
1.18 mm (No. 16)	1.6	2.8	3.2	4.7	59.5	57.7	81.7
0.6 mm (No. 30)	1.6	2.8	3.0	4.2	44.0	50.0	63.8
0.3 mm (No. 50)	1.6	2.7	2.9	4.0	32.2	42.0	17.6
0.15 mm (No. 100)	1.4	2.1	2.4	3.1	11.8	23.6	1.6
0.075 mm (No. 200)	1.0	1.5	1.9	2.4	4.2	14.1	0.6
Bulk specific gravity	2.555	2.513	2.539	2.520	2.551	2.514	2.595
Apparent specific gravity	2.655	2.644	2.655	2.656	2.678	2.682	2.647
Absorption, %	1.466	1.966	1.721	2.027	1.874	2.501	0.700
CAA	100%	100%	100%	100%	N/A	N/A	N/A
FAA	N/A	N/A	N/A	N/A	47.8	-	38.0
Flat & Elongated	0	0	0	0	N/A	N/A	N/A
SE value	N/A	N/A	N/A	N/A	38.8	-	100
Loose Unit Weight	82.9	87.6	86.1	83.8	N/A	N/A	N/A
Rodded Unit Weight	93.9	97.5	95.9	95.5	103.6	110.6	109.6

**Table A.3
Granite stockpiles gradations and physical properties**

Stockpile No.	#5 Granite	#78 Granite	#11 Granite
Metric (U.S.) Sieve			
37.5 mm (1.5 in)	100.0	100.0	100.0
25 mm (1 in)	92.2	100.0	100.0
19 mm (¾ in)	63.3	100.0	100.0
12.5 mm (½ in)	22.1	95.2	100.0
9.5 mm (⅜ in)	10.8	63.8	100.0
4.75 mm (No. 4)	2.3	9.1	95.4
2.36 mm (No. 8)	1.2	2.3	68.9
1.18 mm (No. 16)	1.1	1.6	43.4
0.6 mm (No. 30)	1.1	1.5	27.5
0.3 mm (No. 50)	1.1	1.4	17.3
0.15 mm (No. 100)	1.0	1.2	11.0
0.075 mm (No. 200)	0.8	1.1	7.5
Bulk specific gravity	2.620	2.601	2.548
Apparent specific gravity	2.660	2.660	2.682
Absorption, %	0.580	0.851	1.957
CAA	100%	100%	N/A
FAA	N/A	N/A	46.2
Flat & Elongated	0	0	N/A
SE value	N/A	N/A	64.2
Loose Unit Weight (lb/ft³)	96.3	91.8	N/A
Rodded Unit Weight (lb/ft³)	106.8	101.4	109.6

Binder Laboratory Test Results

Table A.4
DOTD performance graded asphalt cement specification & test results

Property	AASHTO Test Method	PG 76-22M		PG 70-22M	
		Spec.	Results	Spec.	Results
Rotational Viscosity @ 135°C, Pa.s	TP 48	3.0-	1.7	3.0-	0.9
Dynamic Shear, 10 rad/s, G*/Sin Delta, kpa @ Spec. Temp.	TP 5	1.00+	1.82	1.00+	1.64
Flash Point, °C	T 48	232+	305	232+	295
Solubility, %	T 44	99.0+	99.5	99.0+	99.6
Force Ductility Ratio (F2/F1, 4°C, 5 cm/min, F2 @ 30 cm elongation)	T 300	0.30+	0.49	0.30+	0.31
Mass loss, %	T 240	1.00-	0.08	1.00-	0.03
Dynamic Shear, 10 rad/s, G*/Sin Delta, kpa @ Spec. Temp.	TP 5	2.20+	2.84	2.20+	3.14
Elastic Recovery, 25°C, 10 cm, % elongation, %	T 301	60+	70	40+	45
Dynamic Shear, @ 25°C, 10 rad/s, G* Sin Delta, kpa	TP 5	5000-	2297	5000-	4615
Bending Beam Creep Stiffness, S, Mpa @ -12°C.	T 313	300-	162	300-	193
Bending Beam Creep Slope, m value, @ -12°C	T 313	0.300+	0.327	0.3+	0.315

APPENDIX B

The Bailey Method

The Bailey Method is a systematic approach to blending aggregates that provides aggregate interlock as the backbone of the structure and a balanced continuous gradation to complete the mixture [26, 27]. The method provides a set of tools that allows the evaluation of aggregate blends. These tools provide a better understanding in the relationship between aggregate gradation and mixture voids. The Bailey Method gives the practitioner tools to develop and adjust aggregate blends. The new procedures help to ensure aggregate interlock (if desired) and good aggregate packing, giving resistance to permanent deformation, while maintaining volumetric properties that provide resistance to environmental distress. In the Bailey Method, aggregate interlock is selected as a design input. Aggregate interlock provides a rut-resistant mixture. To ensure that the mixture contains adequate asphalt binder, VMA is changed by changing the packing of the coarse and fine aggregates. In this way asphalt mixtures developed with the Bailey Method can have a strong skeleton for high stability and adequate VMA for good durability.

Basic Principles

To develop a method for combining aggregates to optimize aggregate interlock and provide the proper volumetric properties, it is necessary to understand some of the controlling factors that affect the design and performance of these mixtures. The explanation of coarse and fine aggregates given in the following section provide a background for understanding the combination of aggregates. The Bailey Method builds on that understanding and provides more insight into the combination of aggregates for use in an asphalt mixture.

The Bailey Method uses two principles that are the basis of the relationship between aggregate gradation and mixture volumetrics: Aggregate packing, and Definition of coarse and fine aggregate. With these principles, the primary steps in the Bailey Method are to combine aggregates by volume and to analyze the combined blend.

Aggregate Packing

Aggregate particles cannot be packed together to fill a volume completely. There will always be space between the aggregate particles. The degree of packing depends on:

- Type and amount of compactive energy. Several types of compactive force can be used, including static pressure, impact (e.g., Marshall hammer), or shearing (e.g., gyratory shear compactor or California kneading compactor). Higher density can

be achieved by increasing the compactive effort (i.e., higher static pressure, more blows of the hammer, or more tamps or gyrations).

- Shape of the particles. Flat and elongated particles tend to resist packing in a dense configuration. Cubical particles tend to arrange in dense configurations.
- Surface texture of the particles. Particles with smooth textures will re-orient more easily into denser configurations. Particles with rough surfaces will resist sliding against one another.
- Size distribution (gradation) of the particles. Single-sized particles will not pack as densely as a mixture of particle sizes.
- Strength of the particles. Strength of the aggregate particles directly affects the amount of degradation that occurs in a compactor or under rollers. Softer aggregates typically degrade more than strong aggregates and allow denser aggregate packing to be achieved.

The properties listed above can be used to characterize both coarse and fine aggregates. The individual characteristics of a given aggregate, along with the amount used in the blend, have a direct impact on the resulting mix properties. When comparing different sources of comparably sized aggregates, the designer should consider these individual characteristics in addition to the Bailey Method principles presented. Even though an aggregate may have acceptable characteristics, it may not combine well with the other proposed aggregates for use in the design. The final combination of coarse and fine aggregates, and their corresponding individual properties, determines the packing characteristics of the overall blend for a given type and amount of compaction. Therefore, aggregate source selection is an important part of the asphalt mix design process.

Coarse and Fine Aggregate

The traditional definition of coarse aggregate is any particle that is retained by the 4.75-mm sieve. Fine aggregate is defined as any aggregate that passes the 4.75-mm sieve (sand, silt, and clay size material). The same sieve is used for 9.5-mm mixtures as 25.0-mm mixtures. In the Bailey Method, the definition of coarse and fine is more specific in order to determine the packing and aggregate interlock provided by the combination of aggregates in various sized mixtures. The Bailey Method definitions are:

- Coarse Aggregate: large aggregate particles that when placed in a unit volume create voids.
- Fine Aggregate: aggregate particles that can fill the voids created by the coarse aggregate in the mixture.

From these definitions, more than a single aggregate size is needed to define coarse or fine. The definition of coarse and fine depends on the nominal maximum particle size (NMPS) of the mixture. In a dense-graded blend of aggregate with a NMPS of 37.5 mm, the 37.5-mm particles come together to make voids. Those voids are large enough to be filled with 9.5-mm aggregate particles, making the 9.5-mm particles fine aggregate. Now consider a typical surface mix with a NMPS of 9.5 mm. In this blend of aggregates, the 9.5-mm particles are considered coarse aggregate. In the Bailey Method, the sieve which defines coarse and fine aggregate is known as the primary control sieve (PCS), and the PCS is based on the NMPS of the aggregate blend. The break between coarse and fine aggregate is shown in Figure B1. The PCS is defined as the closest sized sieve to the result of the PCS formula in equation (B.1).

$$PCS = NMPS \times 0.22 \tag{B.1}$$

where,

PCS = Primary Control Sieve for the overall blend,

NMPS = Nominal Maximum Particle Size for the overall blend, which is one sieve larger than the first sieve that retains more than 10% (as defined by Superpave terminology).

The value of 0.22 used in the control sieve equation was determined from a two- (2D) and three-dimensional (3-D) analysis of the packing of different shaped particles. The 2-D analysis of the combination of particles shows that the particle diameter ratio ranges from 0.155 (all round) to 0.289 (all flat) with an average value of 0.22. The 3-D analysis of the combination of particles gives a similar result with the particle diameter ratio ranging from 0.15 (hexagonal close-packed spheres) to 0.42 (cubical packing of spheres). In addition, research on particle packing distinctly shows that the packing of particles follows different models when the characteristic diameter is above or below 0.22 ratio.

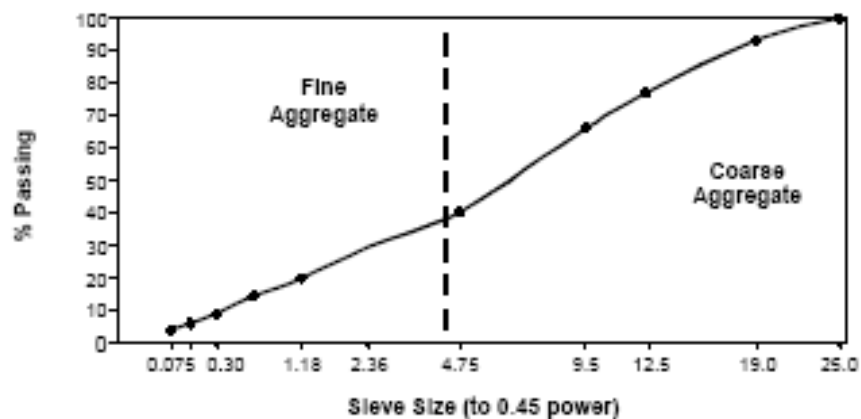


Figure B.1

The break between coarse and fine aggregate for 19.0-mm mixtures

While 0.22 may not be exactly correct for every asphalt mixture, the analysis of gradation is not affected if the value ranges from 0.18 to 0.28. The 0.22 factor is the average condition of many different packing configurations.

Combining Aggregates by Volume

All aggregate blends contain an amount and size of voids, which are a function of the packing characteristics of the blend. In combining aggregates we must first determine the amount and size of the voids created by the coarse aggregates and fill those voids with the appropriate amount of fine aggregate. Mix design methods generally are based on volumetric analysis, but for simplicity, aggregates are combined on a weight basis. Most mix design methods correct the percent passing by weight to percent passing by volume when significant differences exist among the aggregate stockpiles. To evaluate the degree of aggregate interlock in a mixture the designer needs to evaluate a mixture based on volume. To evaluate the volumetric combination of aggregates, additional information must be gathered. For each of the coarse aggregate stockpiles, the loose and rodded unit weights must be determined, and for each fine aggregate stockpile, the rodded unit weight must be determined. These measurements provide the volumetric data at the specific void structure required to evaluate interlock properties.

Loose Unit Weight of Coarse Aggregate

The loose unit weight of an aggregate is the amount of aggregate that fills a unit volume without any compactive effort applied. This condition represents the beginning of coarse aggregate interlock (i.e., particle-to-particle contact) without any compactive effort applied. The loose unit weight is depicted in Figure B.2. The loose unit weight is determined on each coarse aggregate using the shoveling procedure outlined in AASHTO T-19: "Unit Weight and Voids in Aggregate", which leaves the aggregate in a loose condition in the metal unit weight bucket [24]. The loose unit weight (density in kg/m^3) is calculated by dividing the weight of aggregate by the volume of the metal bucket. Using the aggregate bulk specific gravity and the loose unit weight, the volume of voids for this condition is also determined. This condition represents the volume of voids present when the particles are just into contact without any outside compactive effort being applied.

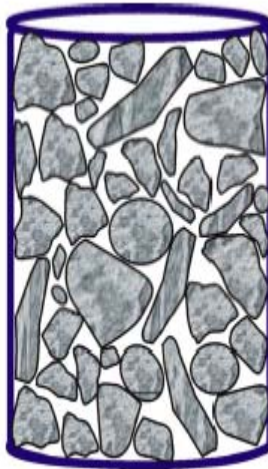


Figure B.2
Loose unit weight condition

Rodded Unit Weight of Coarse Aggregate

The rodded unit weight of aggregate is the amount of aggregate that fills a unit volume with compactive effort applied. The compactive effort increases the particle to particle contact and decreases the volume of voids in the aggregate. Rodded unit weight is depicted in Figure B.3. The rodded unit weight is determined on each coarse aggregate using the rodding procedure outlined in AASHTO T-19: “Unit Weight and Voids in Aggregate,” which leaves the aggregate in a compacted condition in the metal unit weight bucket [24]. The rodded unit weight (density in kg/m^3) is calculated by dividing the weight of aggregate by the volume of the metal bucket. Using the aggregate bulk specific gravity and the rodded unit weight, the volume of voids for this condition is also determined. This condition represents the volume of voids present when the particles are further into contact due to the compactive effort applied.



Figure B.3
Rodded unit weight condition

Chosen Unit Weight of Coarse Aggregate

The designer needs to select the interlock of coarse aggregate desired in their mix design. Therefore, they choose a unit weight of coarse aggregate, which establishes the volume of coarse aggregate in the aggregate blend and the degree of aggregate interlock.

In the Bailey Method, coarse-graded is defined as mixtures which have a coarse aggregate skeleton. Fine-graded mixtures do not have enough coarse aggregate particles (larger than the PCS) to form a skeleton, and therefore the load is carried predominantly by the fine aggregate. To select a chosen unit weight the designer needs to decide if the mixture is to be coarse-graded or fine-graded. Considerations for selecting a chosen unit weight are shown in Figure B.4.

The loose unit weight is the lower limit of coarse aggregate interlock. Theoretically, it is the dividing line between fine-graded and coarse-graded mixtures. If the mix designer chooses a unit weight of coarse aggregate less than the loose unit weight, the coarse aggregate particles are spread apart and are not in a uniform particle-to-particle contact condition. Therefore, a fine aggregate skeleton is developed and properties for these blends are primarily related to the fine aggregate characteristics.

The rodded unit weight is generally considered to be the upper limit of coarse aggregate interlock for dense-graded mixtures. This value is typically near 110% of the loose unit weight. As the chosen unit weight approaches the rodded unit weight, the amount of compactive effort required for densification increases significantly, which can make a mixture difficult to construct in the field.

For dense-graded mixtures, the chosen unit weight is selected as a percentage of the loose unit weight of coarse aggregate. If it is required to obtain some degree of coarse aggregate interlock (as with coarse-graded mixtures), the percentage used should range from 95% to 105% of the loose unit weight. For soft aggregates prone to degradation the chosen unit weight should be nearer to 105% of the loose unit weight. Values exceeding 105% of the loose unit weight should be avoided due to the increased probability of aggregate degradation and increased difficulty with field compaction.

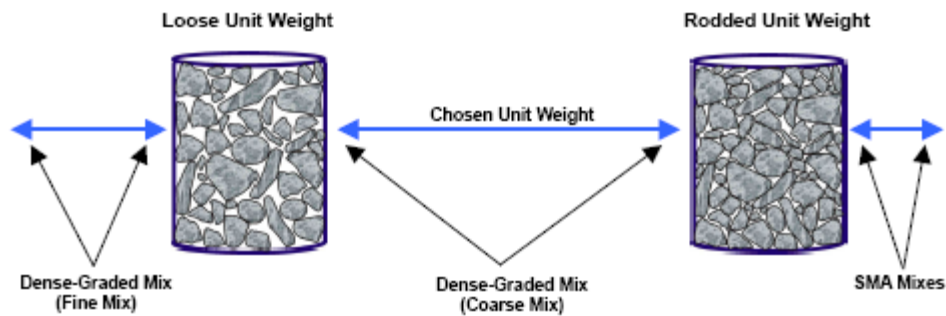


Figure B.4
Selection of chosen unit weight of coarse aggregate

With fine-graded mixtures, the chosen unit weight should be less than 90% of the loose unit weight, to ensure the predominant skeleton is controlled by the fine aggregate structure. For all dense-graded mixtures, it is recommended the designer should not use a chosen unit weight in the range of 90% to 95% of the loose unit weight. Mixtures designed in this range have a high probability of varying in and out of coarse aggregate interlock in the field with the tolerances generally allowed on the PCS. It is normal for an aggregate blend to consolidate more than the selected chosen unit weight due to the lubricating effect of asphalt binder. Also, each coarse aggregate typically contains some amount of fine material when the unit weights are determined, which causes both unit weights (loose and rodded) to be slightly heavier than they would have been, had this material been removed by sieving prior to the test. Therefore, a chosen unit weight as low as 95% of the loose unit weight can often be used and still result in some degree of coarse aggregate interlock. In summary, the amount of additional consolidation, if any, beyond the selected chosen unit weight depends on several factors: aggregate strength, shape, and texture; the amount of fine aggregate that exists in each coarse aggregate when the loose and rodded unit weight tests are performed; combined blend characteristics; relation of the selected chosen unit weight to the rodded unit weight of coarse aggregate; type of compactive effort applied (Marshall, Gyratory, etc.); and amount of compactive effort applied (75 versus 125 gyrations, 50 versus 75 blows, etc.). After selecting the desired

chosen unit weight of the coarse aggregate, the amount of fine aggregate required to fill the corresponding VCA is determined.

Rodded Unit Weight of Fine Aggregate

For dense-graded mixtures, the voids created by the coarse aggregate at the chosen unit weight are filled with an equal volume of fine aggregate at the rodded unit weight condition. The rodded unit weight is used to ensure the fine aggregate structure is at or near its maximum strength. A schematic of the rodded unit weight of fine aggregate is shown in Figure B.5. Rodded unit weight is determined on each fine aggregate stockpile as outlined in the rodding procedure in AASHTO T-19: “Unit Weight and Voids in Aggregate,” which leaves the aggregate in a compacted condition in the unit weight container [24]. The rodded unit weight (density in kg/m^3) is calculated by dividing the weight of the aggregate by the volume of the mold. In a dense-graded mixture, the rodded unit weight is always used to determine the appropriate amount of fine aggregate needed to fill the voids in the coarse aggregate at the chosen unit weight condition. A chosen unit weight is not selected. Note that the rodded unit weight is not determined for dust sized material, such as mineral filler (MF) or bag house fines.

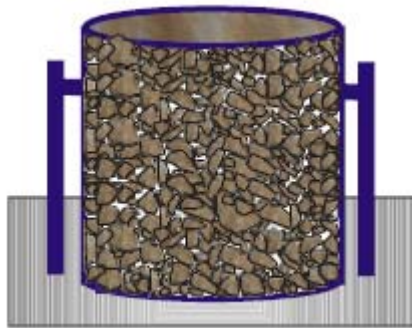


Figure B.5
Rodded unit weight of fine aggregate

Determining a Design Blend

The only additional information required other than that typically used in a dense-graded mix design is the corresponding unit weight for each coarse and fine aggregate [excluding MF, bag house fines, and recycled asphalt pavement (RAP)]. The following decisions are made by the designer and used to determine the individual aggregate percentages by weight and the resulting combined blend:

- Bulk specific gravity of each aggregate,
- Chosen unit weight of the coarse aggregates,
- Rodded unit weight of the fine aggregates,

- Blend by volume of the coarse aggregates totaling 100.0%,
- Blend by volume of fine aggregates totaling 100.0%, and
- Amount of –0.075-mm material desired in the combined blend, if MF or bag house fines are being used.

An example design is presented below, which provides the step-by-step calculations required to blend a set of aggregates by volume and determine the resulting combined blend by weight. The following steps are presented to provide a general sense of blending aggregates by volume.

- Pick a chosen unit weight for the coarse aggregates, kg/m³.
- Calculate the volume of voids in the coarse aggregates at the chosen unit weight.
- Determine the amount of fine aggregate to fill this volume using the fine aggregates rodded unit weight, kg/m³.
- Using the weight (density) in kg/m³ of each aggregate, determine the total weight and convert to individual aggregate blend percentages.
- Correct the coarse aggregates for the amount of fine aggregate they contain and the fine aggregates for the amount of coarse aggregate they contain, in order to maintain the desired blend by volume of coarse and fine aggregate.
- Determine the adjusted blend percentages of each aggregate by weight.
- If MF or bag house fines are to be used, adjust the fine aggregate percentages by the desired amount of fines to maintain the desired blend by volume of coarse and fine aggregate.

Determine the revised individual aggregate percentages by weight for use in calculating the combined blend.

Analysis of the Design Blend

After the combined gradation by weight is determined, the aggregate packing is analyzed further. The combined blend is broken down into three distinct portions, and each portion is evaluated individually. The coarse portion of the combined blend is from the largest particle to the PCS. These particles are considered the coarse aggregates of the blend. The fine aggregate is broken down and evaluated as two portions. To determine where to split the fine aggregate, the same 0.22 factor used on the entire gradation is applied to the PCS to determine a secondary control sieve (SCS). The SCS then becomes the break between coarse particles and fine particles. The fine particles are further evaluated by determining the tertiary control sieve (TCS), which is determined by multiplying the SCS by the 0.22 factor. A schematic of how the gradation is divided into the three portions is given in

Figure B.6. The analysis is done using ratios that evaluate packing within each of the three portions of the combined aggregate gradation. Three ratios are defined: coarse aggregate ratio (CA ratio), fine aggregate coarse ratio (F_{AC} ratio), and fine aggregate fine ratio (F_{AF} ratio). These ratios characterize packing of the aggregates. By changing gradation within each portion, modifications can be made to the volumetric properties, construction characteristics, or performance characteristics of the asphalt mixture.

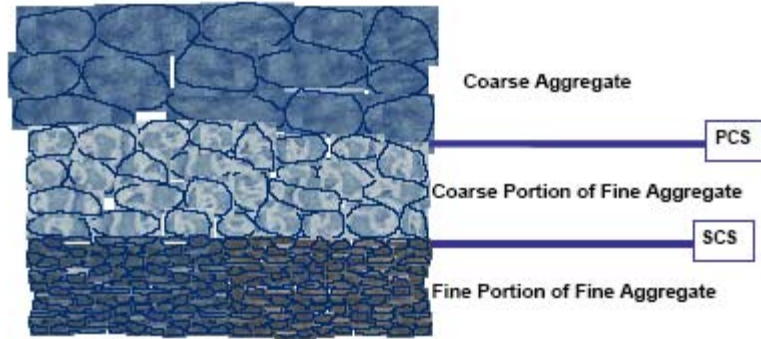


Figure B.6
Overview of the divisions in a continuous gradation

CA Ratio

The CA ratio is used to evaluate packing of the coarse portion of the aggregate gradation and to analyze the resulting void structure. Understanding the packing of coarse aggregate requires the introduction of the half sieve. The half sieve is defined as one half the NMPS. Particles smaller than the half sieve are called “interceptors.” Interceptors are too large to fit in the voids created by the larger coarse aggregate particles and hence spread them apart. The balance of these particles can be used to adjust the mixture’s volumetric properties. By changing the quantity of interceptors it is possible to change the VMA in the mixture to produce a balanced coarse aggregate structure. With a balanced aggregate structure the mixture should be easy to compact in the field and should adequately perform under load. The equation for the calculation of the coarse aggregate ratio is:

$$\text{CA Ratio} = (\% \text{Passing half sieve} - \% \text{Passing PCS}) / (100 - \% \text{Passing half sieve}) \quad (\text{B.2})$$

The packing of the coarse aggregate fraction, observed through the CA ratio, is a primary factor in the constructability of the mixture. As the CA ratio decreases (below ~1.0), compaction of the fine aggregate fraction increases because there are fewer interceptors to limit compaction of the larger coarse aggregate particles. Therefore, a mixture with a low CA ratio typically requires a stronger fine aggregate structure to meet the required volumetric properties. Also, a CA ratio below the corresponding range suggested in Table

B.1 could indicate a blend that may be prone to segregation. It is generally accepted that gap-graded mixes, which tend to have CA ratios below these suggested ranges, have a greater tendency to segregate than mixes that contain a more continuous gradation.

As the CA Ratio increases towards 1.0, VMA will increase. However, as this value approaches 1.0, the coarse aggregate fraction becomes “unbalanced” because the interceptor size aggregates are attempting to control the coarse aggregate skeleton. Although this blend may not be as prone to segregation, it contains such a large quantity of interceptors that the coarse aggregate fraction causes the portion above the PCS to be less continuous. The resulting mixture can be difficult to compact in the field and have a tendency to move under the rollers because it does not want to “lock up.” Generally, mixes with high CA Ratios have an S-shaped gradation curve in this area of the 0.45-power grading chart. Superpave mixtures of this type have developed a reputation for being difficult to compact.

Table B.1
Recommended ranges of aggregate ratios
NMPS, mm

	37.5	25.0	19.0	12.5	9.5	4.75
CA Ratio	0.80–0.95	0.70–0.85	0.60–0.75	0.50–0.65	0.40–0.55	0.30–0.45
FA _c Ratio	0.35–0.50	0.35–0.50	0.35–0.50	0.35–0.50	0.35–0.50	0.35–0.50
FA _f Ratio	0.35–0.50	0.35–0.50	0.35–0.50	0.35–0.50	0.35–0.50	0.35–0.50

As the CA Ratio exceeds a value of 1.0, the interceptor-sized particles begin to dominate the formation of the coarse aggregate skeleton. The coarse portion of the coarse aggregate is then considered “pluggers” as these aggregates do not control the aggregate skeleton, but rather float in a matrix of finer coarse aggregate particles.

Coarse Portion of Fine Aggregate

All of the fine aggregate (i.e., below the PCS) can be viewed as a blend by itself that contains a coarse and a fine portion and can be evaluated in a manner similar to the overall blend. The coarse portion of the fine aggregate creates voids that will be filled with the fine portion of the fine aggregate. As with the coarse aggregate, it is desired to fill these voids with the appropriate volume of the fine portion of the fine aggregate without overfilling the voids. The equation that describes the fine aggregate coarse ratio (FA_c) is given in as follows:

$$F_{AC} = \% \text{Passing SCS} / \% \text{Passing PCS} \tag{B.3}$$

where,
SCS = Secondary Control Sieve.

As this ratio increases, the fine aggregate (i.e., below the PCS) packs together tighter. This increase in packing is due to the increase in volume of the fine portion of fine aggregate. It is generally desirable to have this ratio less than 0.50, as higher values generally indicate an excessive amount of the fine portion of the fine aggregate is included in the mixture. A F_{AC} ratio higher than 0.50, which is created by an excessive amount of natural sand and/or an excessively fine natural sand should be avoided. This type of a blend normally shows a “hump” in the sand portion of the gradation curve of a 0.45 gradation chart, which is generally accepted as an indication of a potentially tender mixture.

If the F_{AC} ratio becomes lower than 0.35, the gradation is not uniform. These mixtures are generally gap-graded and have a “belly” in the 0.45-power grading chart, which can indicate instability and may lead to compaction problems.

Fine Portion of Fine Aggregate

The fine portion of the fine aggregate fills the voids created by the coarse portion of the fine aggregate. This ratio shows how the fine portion of the fine aggregate packs together. One more sieve is needed to calculate the F_{AF} , the Tertiary Control Sieve (TCS). The TCS is defined as the closest sieve to 0.22 times the SCS. The equation for the F_{AF} ratio is as follows:

$$F_{AF} = \% \text{Passing TCS} / \% \text{Passing SCS} \quad (\text{B.4})$$

The F_{AF} ratio is used to evaluate the packing characteristics of the smallest portion of the aggregate blend. Similar to the F_{AC} ratio, the value of the F_{AF} ratio should be less than 0.50 for typical dense-graded mixtures. VMA in the mixture will increase with a decrease in this ratio.

Summary of Ratios

- CA ratio: This ratio describes how the coarse aggregate particles pack together and, consequently, how these particles compact the fine aggregate portion of the aggregate blend that fills the voids created by the coarse aggregate.
- F_{AC} ratio: This ratio describes how the coarse portion of the fine aggregate packs together and, consequently, how these particles compact the material that fills the voids it creates.

- F_{AF} ratio: This ratio describes how the fine portion of the fine aggregate packs together. It also influences the voids that will remain in the overall fine aggregate portion of the blend because it represents the particles that fill the smallest voids created.

These ratios are valuable for evaluating and adjusting VMA. Once an initial trial gradation is evaluated in the laboratory, other gradations can be evaluated on paper to choose a second trial that will have an increased or decreased VMA as desired. When doing the paper analysis, the designer must remember that changes in particle shape, strength and texture must be considered as well. The ratios are calculated from the control sieves of an asphalt mixture, which are tied to the NMAAS.

Example Bailey Method Design Calculations

The calculations in Figure B.7 provide an example of a design using two coarse aggregates, one fine aggregate, and MF. This design uses aggregates of different specific gravity to show how aggregates are blended together by volume. The designer will need to collect information including:

- Stockpile gradation, and bulk specific gravity, and Loose and rodded unit weights (AASHTO T-19). In addition, the designer will make several decisions that will determine the stockpile splits. These items include:
 - Chosen unit weight as a percentage of the loose unit weight;
 - Desired percent passing 0.075-mm sieve;
 - Blend by volume of coarse aggregates; and
 - Blend by volume of fine aggregates.

Step 1

Determine the chosen unit of weight for each aggregate according to the loose unit weight for each coarse aggregate and the overall coarse aggregate chosen unit weight for the mixture. The chosen unit weight for the fine aggregates is simply the rodded weight of that aggregate.

Calculation

Multiply the loose unit weight percent for each coarse aggregate by the coarse aggregate chosen unit weight for the mixture.

Equation

Coarse aggregate chosen unit weight = loose unit weight * desired percent of loose unit weight

$$\text{CA \#1: Chosen unit weight} = 1426 \text{ kg/m}^3 \times 103\% = 1469 \text{ kg/m}^3 \quad (\text{B.5})$$

$$\text{CA \#2: Chosen unit weight} = 1400 \text{ kg/m}^3 \times 103\% = 1442 \text{ kg/m}^3 \quad (\text{B.6})$$

Step 2

Determine the unit weight contributed by each coarse aggregate according to the desired proportions (by volume) of coarse aggregate.

Calculation

Multiply the blend percentage of coarse aggregate by the chosen unit weight of each aggregate.

Material Grade	Coarse Aggregate Number			Fine Aggregate Number			Mineral Filler
	CA-1	CA-2	CA-3	FA-1	FA-2	FA-3	
	Coarse	Intermediate		Slag Sand			MF
				Design Value	Specification		
				CA Chosen Weight as % of Loose Weight	103	95 – 105	
				Desired % Pass 0.075 mm	4.5	3.5 – 6.0	
	Coarse Aggregate Blend by Volume			Fine Aggregate Blend by Volume			
	25.0	75.0		100.0			
	Above blending % must sum to 100		100.0	Above blending % must sum to 100		100.0	
	Combined Bulk Specific Gravity of All Aggregates			2.888	Total Volume of Coarse Aggregate	53.7	
					Total Volume of Fine Aggregate	46.3	
	Aggregate Properties						
	19.0	100.0	100.0		100.0		100.0
	12.5	94.0	100.0		100.0		100.0
	9.5	38.0	99.0		100.0		100.0
	4.75	3.0	30.0		99.0		100.0
	2.36	1.9	5.0		79.9		100.0
	1.18	1.8	2.5		48.8		100.0
	0.60	1.8	1.9		29.0		100.0
	0.30	1.8	1.4		14.2		100.0
	0.15	1.8	1.3		8.8		98.0
	0.075	1.7	1.2		3.0		90.0
	Bulk Spec. Gr.	2.702	2.898		3.162	3.162	2.808
	Apparent Gr.	2.812	2.812		3.600	3.600	2.808
	% Absorp.	1.452	1.502		3.844	3.844	
	Loose Weight kg/m ³	1426	1400				
	Rodded Weight kg/m ³	1808	1592		2167	2167	

Figure B.7
Example calculation information

Equation

Contribution = percent coarse aggregate * chosen unit weight

$$\text{CA \#1: Contribution} = 25\% \times 1469 \text{ kg/m}^3 = 367 \text{ kg/m}^3 \quad (\text{B.7})$$

$$\text{CA \#2: Contribution} = 75\% \times 1442 \text{ kg/m}^3 = 1081 \text{ kg/m}^3 \quad (\text{B.8})$$

Step 3

Determine the voids in each coarse aggregate according to its corresponding chosen unit weight and contribution by volume. Then sum the voids contributed by each coarse aggregate.

Calculation

First calculate one minus the chosen unit weight divided by the bulk specific gravity and density of water. Multiply the result by the percent of coarse aggregate blend. Then, sum the contribution of each coarse aggregate.

Equation

$$\text{Voids in coarse aggregate} = \left(1 - \frac{\text{chosen unit weight}}{G_{sb} \times 1000}\right) \times \text{Blend\%}$$

where, G_{sb} = bulk specific gravity.

$$\text{CA \#1: Voids in CA\#1} = \left(1 - \frac{1469}{2.702 \times 1000}\right) \times 25.0 = 11.4 \quad (\text{B.9})$$

$$\text{CA \#2: Voids in CA\#2} = \left(1 - \frac{1442}{2.698 \times 1000}\right) \times 75.0 = 34.9 \quad (\text{B.10})$$

$$\text{Total: Voids in CA\#1} + \text{Voids in CA\#2} = 11.4 + 34.9 = 46.3 \quad (\text{B.11})$$

Step 4

Determine the unit weight contributed by each fine aggregate according to the desired volume blend of fine aggregate. This is the unit weight that fills the voids in the coarse aggregate.

Calculation

Multiply the fine aggregate chosen unit weight by the volume percentage of this aggregate in the fine aggregate blend and multiply this by the total percentage of coarse aggregate voids from Eq. (B.11).

Equation

Contribution of each fine aggregate = fine aggregate chosen unit weight * % fine aggregate blend * % voids in coarse aggregate.

$$\text{FA \#1: Contribution} = 2167 \text{ kg/m}^3 \times 100\% \times 46.3\% = 1002 \text{ kg/m}^3 \quad (\text{B.12})$$

Note: If there is more than one fine aggregate the calculation is repeated for each fine aggregate.

Step 5

Determine the unit weight for the total aggregate blend.

Calculation

Sum the unit weight of each aggregate.

Equation

$$\text{Unit weight of blend} = (\text{B. 7}) + (\text{B. 8}) + (\text{B. 12}) \quad (\text{B.13})$$

$$\text{Unit weight of blend} = 367 \text{ kg/m}^3 + 1081 \text{ kg/m}^3 + 1002 \text{ kg/m}^3 = 2450 \text{ kg/m}^3 \quad (\text{B.14})$$

Step 6

Determine the initial blend percentage by weight of each aggregate.

Calculation

Divide the unit weight of each aggregate by the unit weight of the total aggregate blend.

Equation

Percent by weight = unit weight of aggregate/unit weight of blend

$$\text{CA \#1: \% by weight} = 367 \text{ kg/m}^3 / 2450 \text{ kg/m}^3 = 0.150 = 15.0\% \quad (\text{B.15})$$

$$\text{CA \#2: \% by weight} = 1081 \text{ kg/m}^3 / 2450 \text{ kg/m}^3 = 0.441 = 44.1\% \quad (\text{B.16})$$

$$\text{FA \#1: \% by weight} = 1002 \text{ kg/m}^3 / 2450 \text{ kg/m}^3 = 0.409 = 40.9\% \quad (\text{B.17})$$

These initial estimates of stockpile splits are based on the choice of how much coarse aggregate to have in the mixture. The initial estimates of stockpile splits will be adjusted to account for fine aggregate particles in the coarse aggregate stockpiles and coarse aggregate particles in the fine aggregate stockpiles.

Step 7

In a 12.5-mm NMPS mixture, the CA/FA break (PCS) is the 2.36-mm sieve.

Calculation

For the coarse aggregate stockpiles, determine the percent passing the 2.36-mm sieve.
For the fine aggregate stockpiles, determine the percent retained on the 2.36-mm sieve.

Equation

$$\text{CA \#1: \% fine aggregate} = 1.9\% \quad (\text{B.18})$$

$$\text{CA \#2: \% fine aggregate} = 5.0\% \quad (\text{B.29})$$

$$\text{FA \#1: \% coarse aggregate} = 100.0\% - 79.9\% = 20.1\% \quad (\text{B.20})$$

Step 8

Determine the fine aggregate in each coarse stockpile according to its percentage in the blend.

Calculation

For each coarse aggregate stockpile determine the percent passing the 2.36-mm sieve as a percentage of the total aggregate blend.

Equation

Percent fine aggregate in blend = Coarse stockpile percent of blend * percent fine aggregate in coarse stockpile.

$$\text{Percent fine aggregate in blend} = 15.0\% \times 1.9\% = 0.3\% \quad (\text{B.21})$$

$$\text{Percent fine aggregate in blend} = 44.1\% \times 5.0\% = 2.2\% \quad (\text{B.22})$$

Step 9

Sum the percent of fine aggregate particles in all the coarse aggregate stockpiles.

$$\text{All CAs: Percent fine aggregate in blend} = 0.3\% + 2.2\% = 2.5\% \quad (\text{B.23})$$

Step 10

Determine the coarse aggregate in each fine stockpile according to its percentage in the blend.

Calculation

For each fine aggregate stockpile determine the percent retained on the 2.36-mm sieve as a percentage of the total aggregate blend.

Equation

Percent coarse aggregate in blend = Stockpile percent of blend * percent coarse aggregate in fine stockpile.

$$\text{FA\#1: Percent coarse aggregate in blend} = 40.9\% \times 20.1\% = 8.2\% \quad (\text{B.24})$$

Step 11

Sum the percent of fine aggregate particles in all the coarse aggregate stockpiles.

$$\text{All FAs: Percent fine aggregate in blend} = 8.2\% \quad (\text{B.25})$$

Step 12

Correct the initial blend percentage of each coarse aggregate to account for the amount of fine aggregate it contains and coarse aggregate contributed by the fine aggregate stockpiles.

Equation

Adjusted stockpile percent in blend

$$= (\text{initial \%}) + (\text{FA in CA}) - \left(\frac{\text{initial \%} \times \text{Sum CA in FA}}{\text{Total \% of CA}} \right)$$

$$\text{CA\#1: Adjusted stockpile percent in blend} = (15.0\%) + (0.3\%) - \left(\frac{15.0\% \times 8.2\%}{15.0\% + 44.1\%} \right) = 13.2\% \quad (\text{B.26})$$

$$\text{CA\#2: Adjusted stockpile percent in blend} = (44.1\%) + (2.2\%) - \left(\frac{44.1\% \times 8.2\%}{15.0\% + 44.1\%} \right) = 40.2\% \quad (\text{B.27})$$

Step 13

Correct the initial blend percentage of each fine aggregate to account for the amount of coarse aggregate it contains and fine aggregate contributed by the coarse aggregate stockpiles.

Equation

$$\begin{aligned} &\text{Adjusted stockpile percent in blend} \\ &= (\text{initial}\%) + (\text{CA in FA}) - \left(\frac{\text{initital \%} \times \text{Sum FA in CA}}{\text{Total \% of FA}} \right) \end{aligned}$$

$$\begin{aligned} &\text{Adjusted stockpile percent in blend} \\ &= (40.9\%) + (8.2\%) - \left(\frac{40.9\% \times 2.5\%}{40.9\%} \right) = 46.7\% \end{aligned} \quad (\text{B.28})$$

The next steps will determine whether MF will be needed to bring the percent passing the 0.075-mm sieve to the desired level.

Step 14

Determine the amount of -0.075-mm material contributed by each aggregate using the adjusted stockpile percentages.

Calculation

Multiply the percent passing the 0.075-mm sieve for each aggregate by the adjusted blend percentage for each aggregate.

Equation

Percent contribution of 0.075-mm sieve for each stockpile = adjusted stockpile percent * percent passing 0.075-mm sieve for that stockpile.

$$\text{CA \#1: Percent contribution 0.075 mm} = 13.2\% \times 1.7\% = 0.2\% \quad (\text{B.29})$$

$$\text{CA \#2: Percent contribution 0.075 mm} = 40.2\% \times 1.2\% = 0.5\% \quad (\text{B.30})$$

$$\text{FA \#1: Percent contribution 0.075 mm} = 46.7\% \times 3.0\% = 1.4\% \quad (\text{B.31})$$

Step 15

Determine the amount of mineral filler required, if any, to bring the percent passing the 0.075-mm sieve to the desired level. For this mixture the desired amount of -0.075-mm material is 4.5%.

Equation

$$\text{Percent of MF} = \left(\frac{\% \text{ 0.075 mm desired} - \% \text{ 0.075 mm in blend}}{\% \text{ 0.075 mm in filter}} \right)$$

$$\text{MF Percent MF} = \left(\frac{4.5-2.1}{90\%} \right) = 2.7\% \quad (\text{B.32})$$

Step 16

Determine the final blend percentages of fine aggregate stockpiles by adding the percent MF to the fine aggregate. In this step the blend percentage of CA is not changed. The blend percentage of FA is adjusted to account for the MF.

Equation

$$\begin{aligned} &\text{Final blend percent for fine aggregate} \\ &= \text{Adjusted blend percent} - \left(\frac{\% \text{FA} \times \% \text{MF}}{\text{Total \%FA}} \right) \end{aligned}$$

$$\text{FA \#1: Final blend percent} = 46.7\% - \left(\frac{46.7\% \times 2.7\%}{46.7\%} \right) = 44.0 \quad (\text{B.34})$$

Results

The final blending percentages are summarized in Table B.2 below.

Table B.2
Final Blending Percentage

	Equation	Results (%)
CA #1	B.26	13.2
CA #2	B.27	40.2
FA #1	B.34	44.0
MF	B.32	2.7

APPENDIX C

Sample Calculations

SGC Locking Point

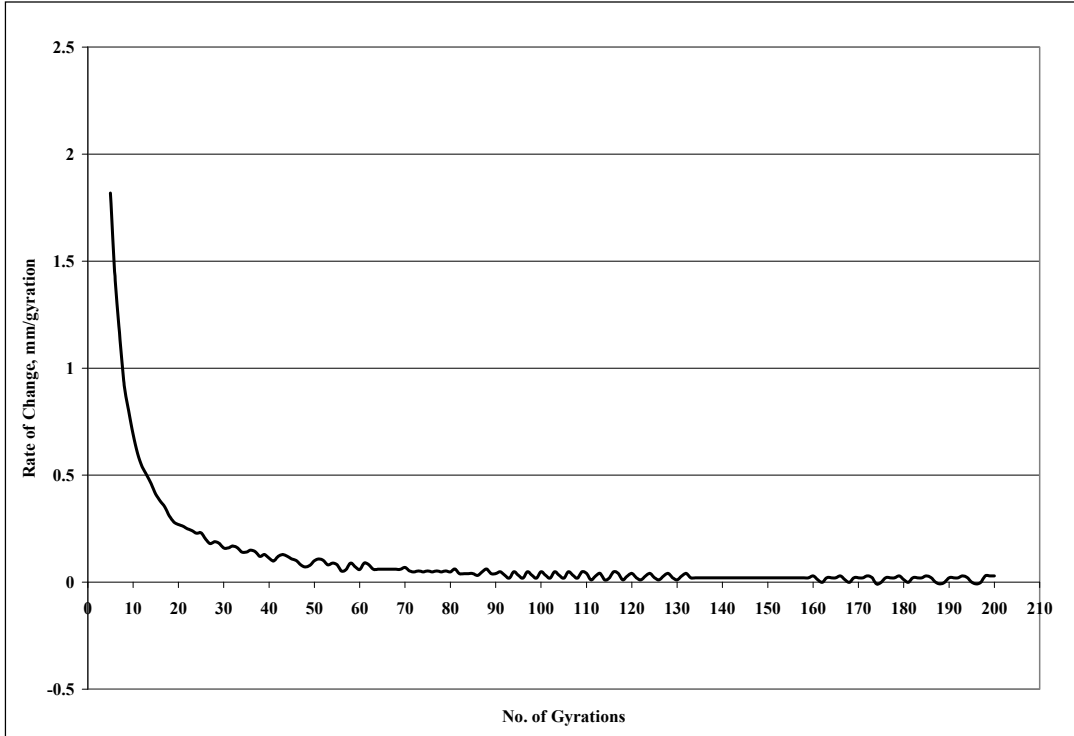


Figure C.1
Rate of change of height during SCG compaction

Sample Data

Table C.1
Example data set for SCG locking point determination

Number of Gyration	Rate of Change, mm/gyration	
61	0.07	
62	0.06	
63	0.08	
64	0.07	
65	0.06	
66	0.07	
67	0.07	
68	0.06	
69	0.06	
70	0.05	Locking Point
71	0.05	
72	0.05	
73	0.05	
74	0.05	

The SGC locking point is the number of gyrations after which the rate of change in height is equal to or less than 0.05 mm for three consecutive gyrations.

Pressure Distribution Analyzer (PDA)

Step 1: The device is inserted on top of the mixture.

Step 2: Approximately 4000 g of mix is used with the SGC mold of 150 mm in diameter

Step 3: The device is started using the testquip software prior to inserting it to the SGC mold.

Step 4: Once the device is started and inserted in the SGC mold, the standard compaction procedure is followed. It is very important to time either the start or the end of compaction using the computer clock. This allows for identifying the beginning of each gyration for data reduction as explained in the next point.

Step 5: The rate of data collection is one sample per 0.25 seconds. Since the SGC applies one gyration per 2 seconds, eight readings are obtained per gyration for both the load and the eccentricity. The average value of those eight readings is used for analysis.

Step 6: A total of 250 gyrations is recommended in order to ensure that mixture behavior under compaction load until N_{des} is captured. A higher number of gyrations can be explored although reduction in mix temperature might make the compaction process difficult and ultimately might damage the SGC.

PDA Locking Point

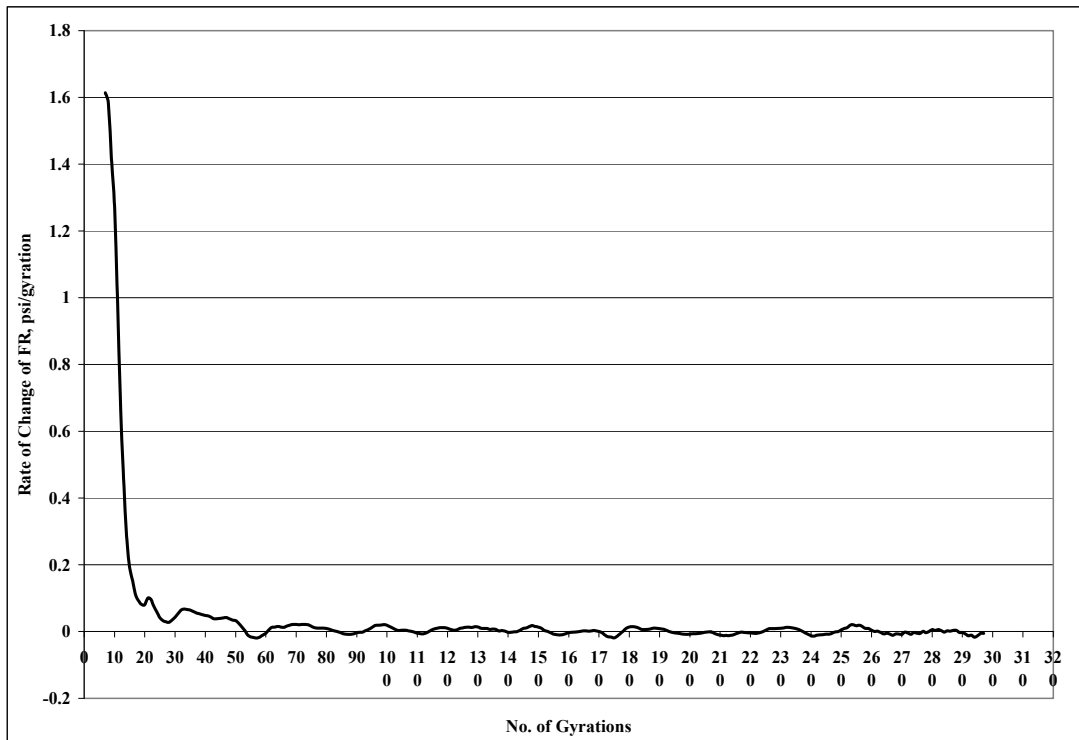


Figure C.2
Rate of change of frictional resistance during SCG compaction

Sample Data

Table C.2
Example data set for PDA locking point determination

No. of Gyration	Rate of change of FR	
36	0.05	
37	0.05	
38	0.05	
39	0.05	
40	0.05	
41	0.04	
42	0.03	
43	0.05	
44	0.05	
45	0.05	
46	0.04	
47	0.04	
48	0.03	
49	0.03	
50	0.03	
51	0.01	Locking Point

It is defined as the number of gyrations at which the rate of change of frictional resistance per gyration is less than 0.01

SGC Compaction Densification Index (CDI)

CDI is defined as the area under the SGC densification curve from N=1 to the SGC locking point.

SGC Traffic Densification Index (TDI)

TDI is the area under the SGC densification curve from the SGC locking point to N at 98% G_{mm} or the end of compaction (N=205 gyrations), whichever comes first.

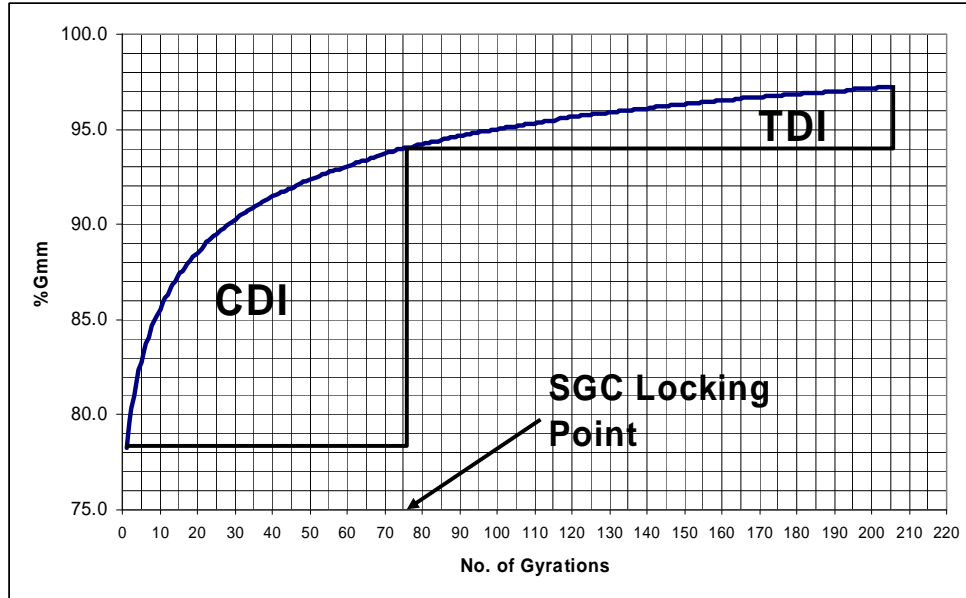


Figure C.3
SCG compaction indices definition

PDA Compaction Force Index (CFI)

CFI is the area under frictional resistance vs. No. of gyration curve from N=1 to the SGC locking point. It is analogous to the CDI.

PDA Traffic Force Index (TFI)

TFI is the area under frictional resistance vs. No. of gyration curve from the SGC locking point to N=205.

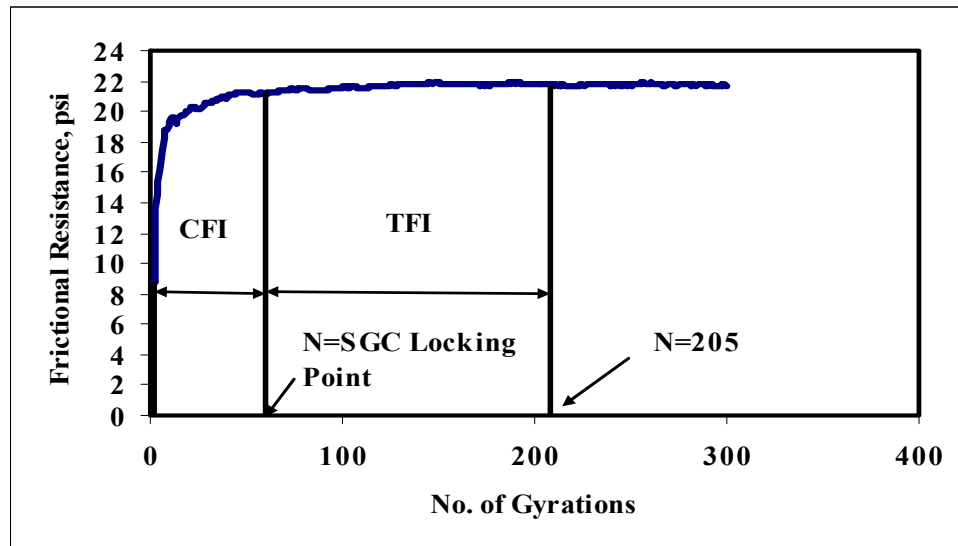


Figure C.4
PDA compaction indices definition

Indirect Tensile Strength

Table C.3
Indirect tensile strength test

Time	Length 1	Force 1	epsilon-h1	epsilon-v1	epsilon-h2	h total	strain	Stress	stress Mpa
Sec	in	lbf	in	in	in				
2.9	0.06358	6748.345	0.003398	-0.0231	0.013798	0.00859	0.44708	361.621	2.49

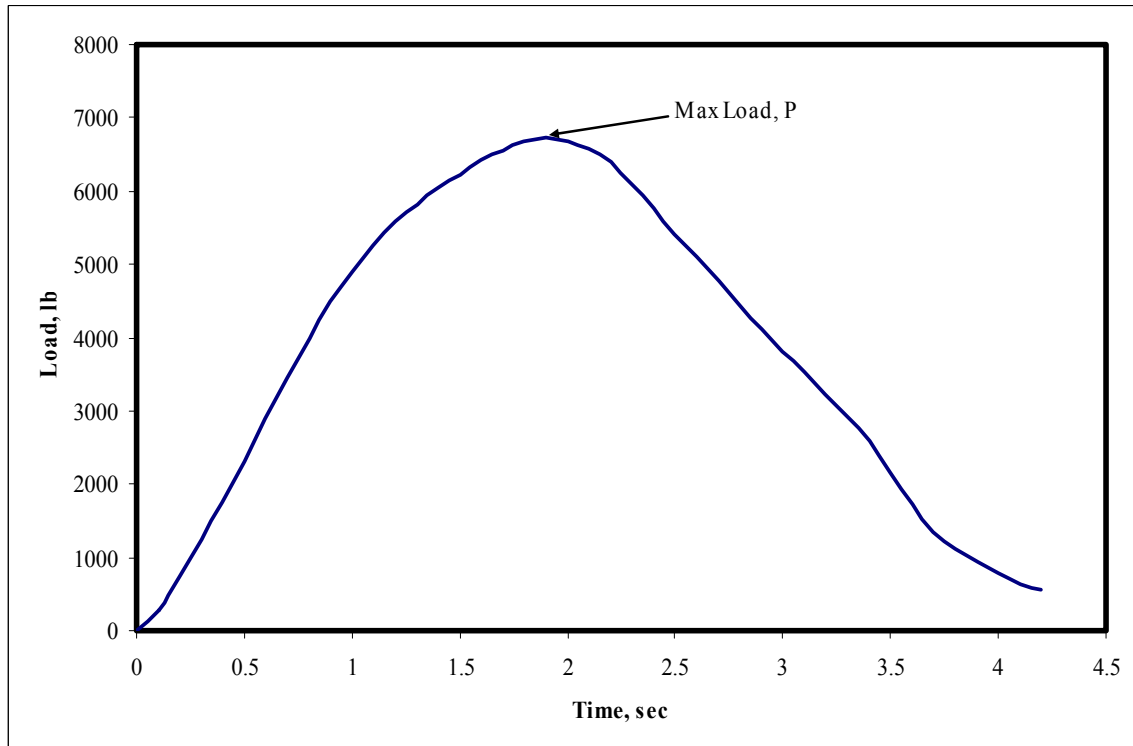


Figure C.5
Indirect tensile strength test

Indirect tensile strength and strain were computed as follows:

$$ITS = \frac{2P}{\pi DT} \quad (C.1)$$

$$\epsilon_t = 0.52H_t \quad (C.2)$$

where,

P = the peak load, lb

D = specimen diameter, in

T = specimen thickness, in

H_t = horizontal deformation at peak load, in

Semi-Circular Fracture Energy Test

The load and deformation were continuously recorded determined as follows:

$$J_c = -\left(\frac{1}{b}\right) \frac{dU}{da} \quad (C.3)$$

Table C.4 shows a typical set of data from the J_c test. From that table, the average J_c is calculated for every notch depth. Average J_c values are then plotted against notch depth and the slope of the line will be the fracture energy for the mixture in consideration, as shown in Figure C.6.

Table C.4
Average J_c for different notch depth

Notch Depth	Average J_c
1	1.14715
1.25	0.88481
1.5	0.50769

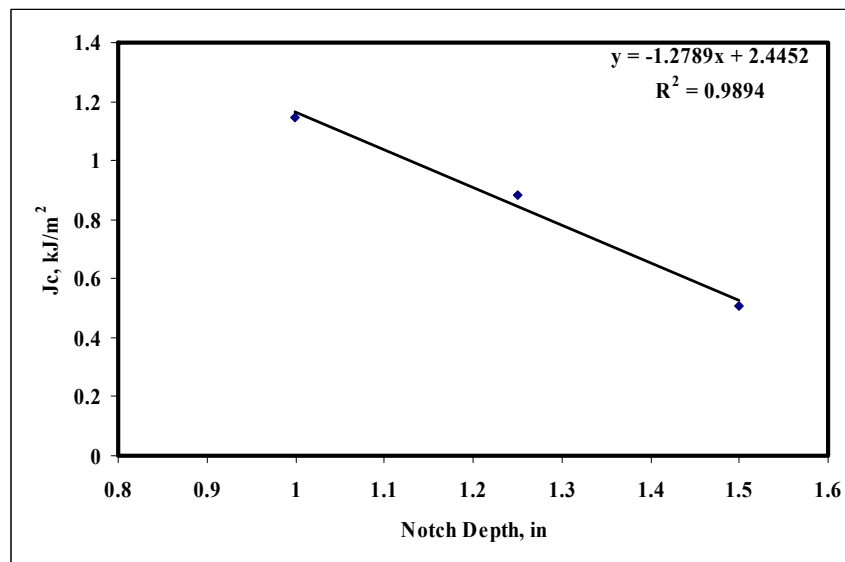


Figure C.6
Critical strain energy release rate vs. notch depth

Dissipated Creep Strain Energy (DCSE)

This property is obtained using data from two tests; resilient modulus (M_r) and indirect tensile strength test (ITS). The standard procedure for resilient modulus test is followed as practiced by the DOTD. A haversine load of 0.1 second duration is applied followed a 0.4 second rest period. The magnitude of the load is chosen so that no more than a 100 microstrain is induced to the specimens at the test temperature of 10°C. The Figure below shows typical output from the M_r test. The instantaneous horizontal deformation is

determined as the difference between the deformation at peak load and the deformation recorded at the end of the loading period (i.e. at time $t_{\text{peak}}+0.05$ seconds where t_{peak} is the time corresponding to the peak load). The total horizontal deformation is the difference between the deformation at peak load and the deformation at the beginning of the second cycle). Once Mr test is conducted, The sample is tested for its tensile strength at the same test temperature.

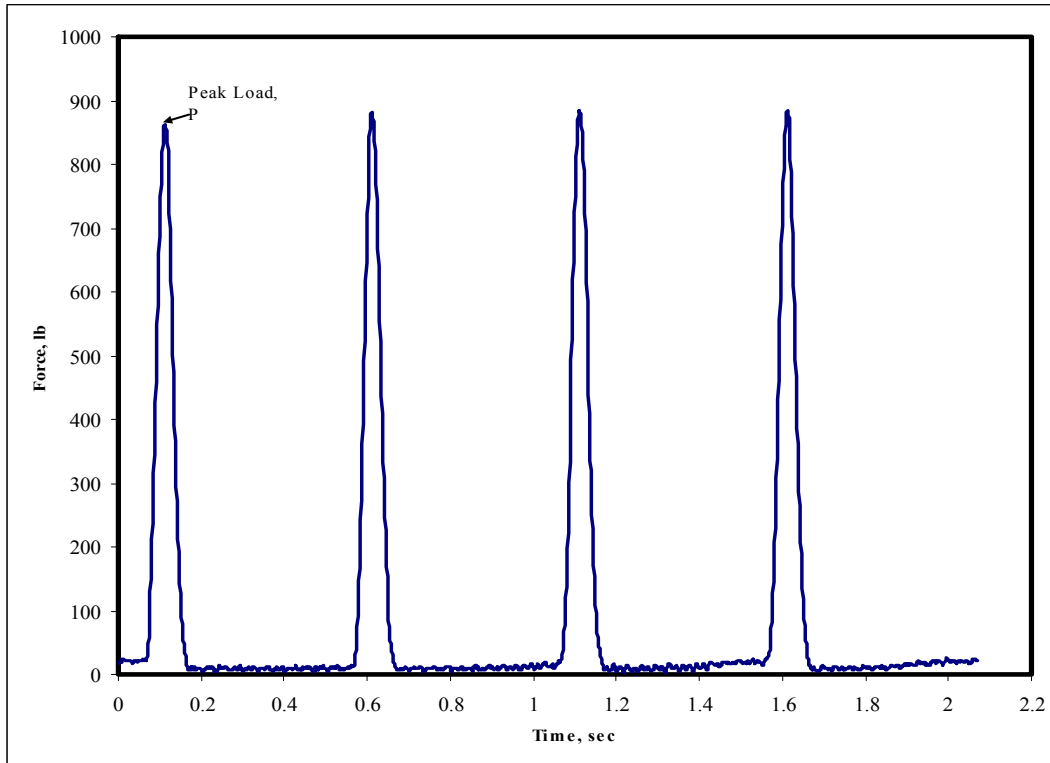


Figure C.7
Typical loading rate- dissipated creep strain energy

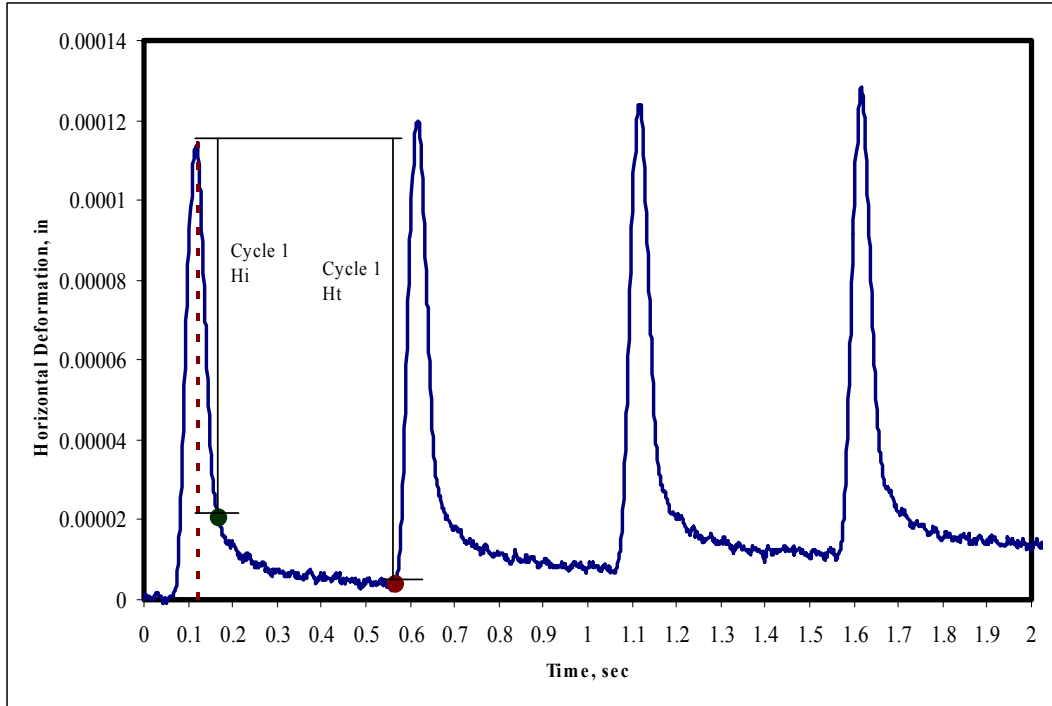


Figure C.8

....

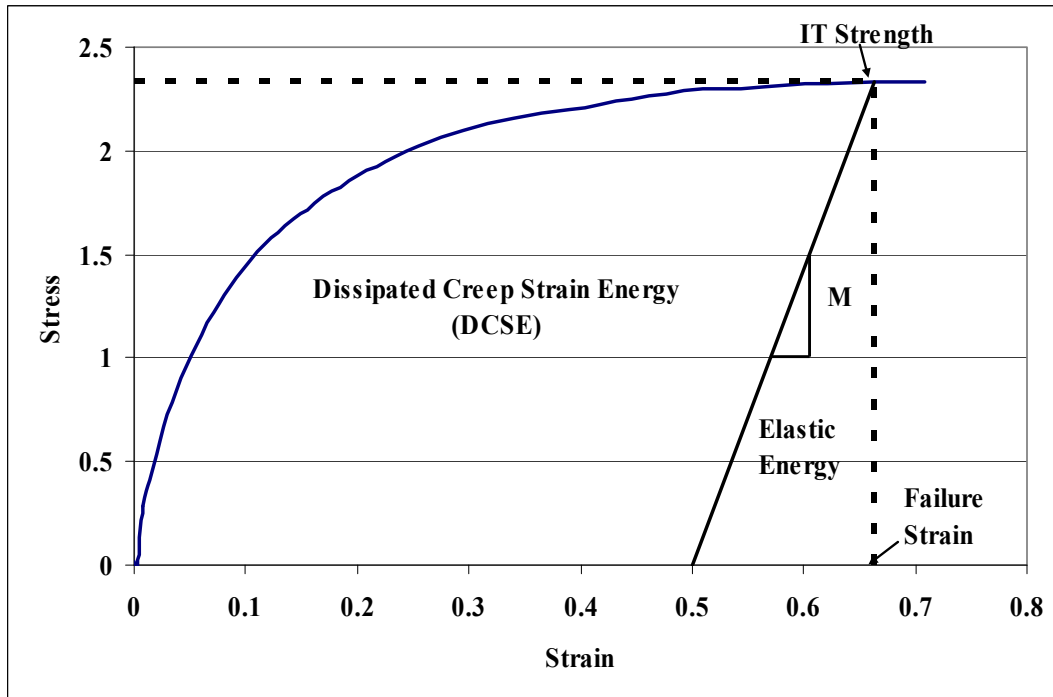


Figure C.9

Dissipated creep strain energy determination

DCSE is defined as the fracture energy, FE, minus the elastic energy, EE. The fracture energy is defined as the area under the stress-strain curve up to the point where the specimen begins to fracture. The elastic energy is the energy recovered after unloading the specimen. The failure strain (ϵ_f), tensile strength (S_t) and fracture energy are determined from the IT strength test. From the resilient modulus test, the resilient modulus (M_R) is obtained. The calculation of the DCSE was then determined as follows:

$$\epsilon_0 = (M_R * \epsilon_f - S_t) / M_R \quad (C.4)$$

$$EE = \frac{1}{2} S_t (\epsilon_f - \epsilon_0) \quad (C.5)$$

$$DCSE = FE - EE \quad (C.6)$$

Sample Data

Table C.4
Sample data computation- critical creep strain

					Calculated Parameters		
Mixture	Mr	Fracture Energy	ITS, Mpa	final strain, microns	initial strain, microns	Elastic Energy	DCSE- kJ/m ³
GRF-1/2"	19.4	1.5	2.8	5700	5699.86	0.20	1.3

$$\text{initial strain} = \frac{(\text{Mr} * \text{final strain}) - \text{ITS}}{\text{Mr}}$$

$$\text{Elastic Energy} = \frac{1}{2} * \text{ITS} * (\text{Final strain} - \text{initial strain})$$

$$\text{DCSE} = \text{Fracture Energy} - \text{Elastic Energy}$$

APPENDIX D

Recommended Design Approach

The research presented herein suggests that suitable mixes can be developed with dense aggregate structures using the Bailey Method of aggregate gradation that provides good resistance to permanent deformation while still maintaining adequate level of durability. The research also recognizes the limitation of setting strict empirical criteria for mixtures volumetrics that might narrow the options of the design engineer to be more innovative and develop mixtures that are well performing yet economical. Figure D.1 presents a recommended design algorithm for asphalt mixtures based on the results of this research study. The suggested design approach has the following advantages:

- Utilizes an analytical aggregate blending method that provides a rational and systematic approach to designing aggregate structures instead of the conventional trial and error procedure.
- Acknowledges the fact that every asphalt mixture is unique in its composition and response to compaction loads during construction. The procedure calls for using the concept of locking point that defines a unique compaction level for every mixture in consideration. It provides a predictive equation to estimate the locking point based on some aggregate characteristics.
- Bypasses the controversial empirical design step in the current Superpave design system; mixtures volumetrics requirements that have been the basis for acceptance/rejection of mixtures based only on failing to meet one or more volumetric parameters that are in most cases indirectly calculated from other laboratory test procedures that have high level of subjectivity.
- Checks the mixtures against two important pavement distresses; rutting and fatigue cracking using engineering properties determined from laboratory mechanistic tests that are relatively fast and simple to perform.

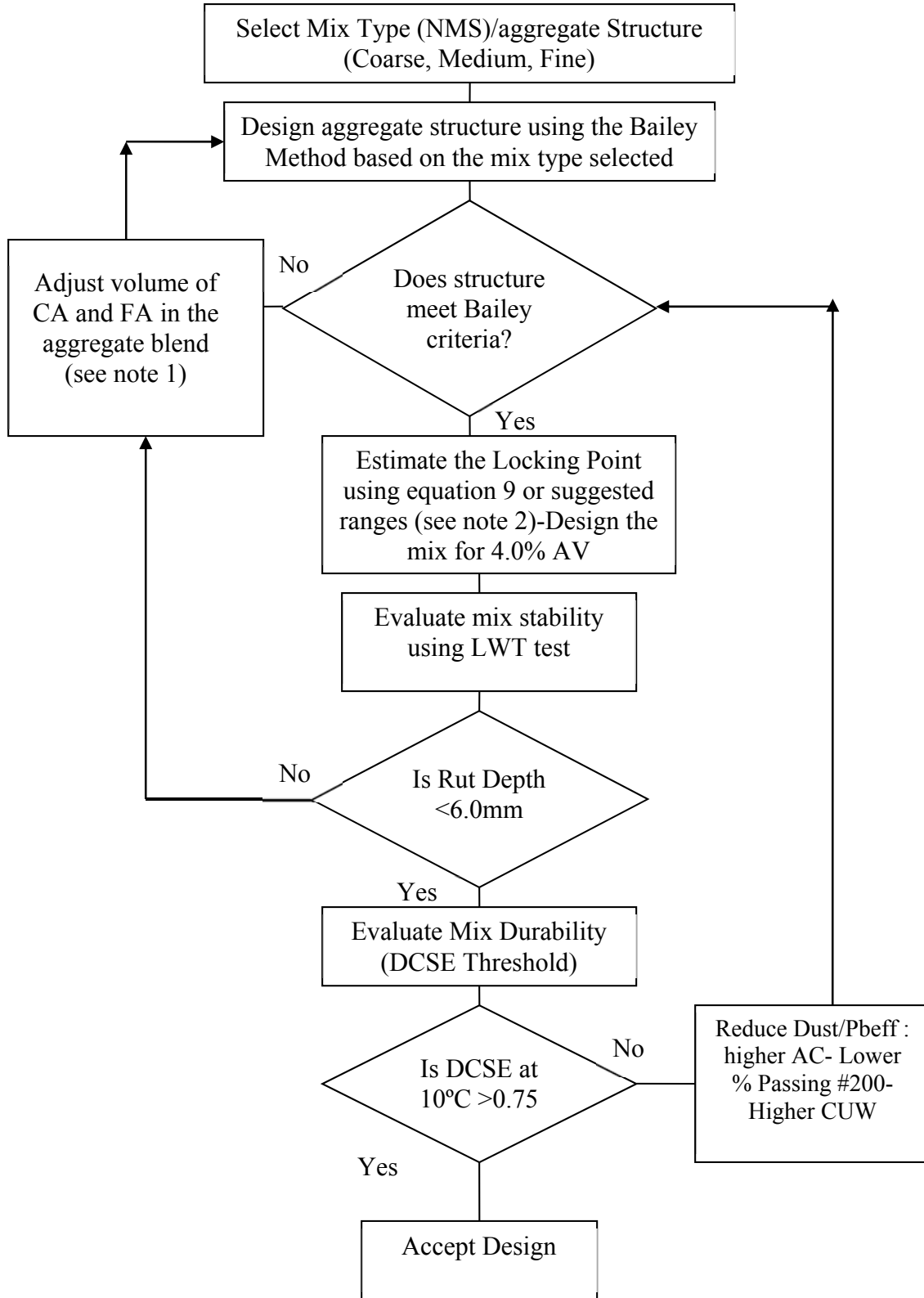


Figure D.1
Recommended design methodology

Note 1: If changing volume of coarse and fine aggregates in the mix does not improve the gradation, aggregate stockpiles from different sources that might have different surface characteristics may allow the designer to meet the Bailey criteria.

Note 2: The ranges are those obtained from this research for the different types and gradation of aggregates. If the specimen height during compaction is monitored by the operator, the locking point can be identified instantaneously as the specimen is being densified and the compaction process can be then terminated. This will eliminate the need to estimate the locking point although it is highly recommended to get a rough estimate before the start of the compaction process.

Note 3 : Please note that changing the Dust/ P_{beff} ratio by changing the amount of fines passing the #200 sieve or by using a different CUW requires re-evaluating the blend using the Bailey ratios.

Note 4: List of Abbreviations used in the design flow chart:

CUW = Chosen Unit Weight

DCSE = Dynamic Creep Strain Energy

P_{beff} = Effective asphalt Content